CHARLES UNIVERSITY IN PRAGUE

FACULTY OF PHARMACY IN HRADEC KRÁLOVÉ

DEPARTMENT OF INORGANIC AND ORGANIC CHEMISTRY

UNIVERSITY OF MONTPELLIER

FACULTY OF PHARMACY

INSTITUTE OF BIOMOLECULES MAX MOUSSERON

Synthesis of Bioactive Lipids

Synthesis of lipophenolic derivatives of hydroxytyrosol, phloroglucinol and resveratrol

DIPLOMA THESIS

Supervisor: Dr. Céline Crauste

Advisor: Assoc. Prof. PharmDr. Kateřina Vávrová, Ph.D.

Montpellier 2016 Tereza Pavlíčková

DECLARATION

„Hereby, I declare that this paper is my own work. All the literature and other sources of information I used in this work are mentioned in the list of literature and properly cited throughout the work. This work has not been used to gain equal or different degree. “

Tereza Pavlíčková

ACKNOWLEDGEMENT

Here, I would like to thank all the members of the team of the Bioactive Lipids of IBMM, particularly Dr. Thierry Durand for inviting me to his laboratory and providing me this priceless experience, prof. Joseph Vercauteren for having me in his team and Dr. Céline Crauste for her kind and thorough supervision and endless patience. Special thanks also belong to Mélissa Rosell for all her advice and cheerful spirit. I am eternally grateful once again to prof. Joseph Vercauteren and Simon Cassegrain who did not hesitate to invest their time and computational skills and recovered a significant part of my work that I had accidentally deleted. Last but not least, I would like to thank my Czech advisor, assoc. prof. PharmDr. Kateřina Vávrová, Ph.D., for having fired up my passion in organic chemistry and for her long-term overall support. Thank you.

This work was carried out in the frame of Erasmus+ program.

ABSTRAKT

Univerzita Karlova v Praze

Farmaceutická fakulta v Hradci Králové, Katedra anorganické a organické chemie

Université de Montpellier

Faculté de Pharmacie

Institut des Biomolécules Max Mousseron, UMR5247 CNRS ENSCM, UM

Kandidát: Tereza Pavlíčková

Vedoucí diplomové práce: Doc. PharmDr. Kateřina Vávrová, PhD.

Školitel: Dr. Céline Crauste

Název diplomové práce: Syntéza lipofenolů

Lipofenoly jsou deriváty (poly)fenolů obsahující lipidovou funkční skupinu, které jsou zde navrženy s cílem získat lipofilní antioxidanty.

První část práce je zaměřena na lipofenoly olivového oleje. Tři nové lipofenolické sloučeniny, deriváty hydroxytyrosolu (nejhojnější fenolický derivát olivového oleje) a tří různých nenasycených mastných kyselin byly připraveny ve dvou krocích, v dobrém výtěžku a vysoké čistotě. Tyto produkty budou využity jako standardy pro stanovení jejich přítomnosti v extra panenském olivovém oleji (EVOO) a ve vzorcích jater potkanů krmených EVOO pro zjištění případné *in vivo* metabolizace.

Druhá část práce je zaměřená na lipofenoly jakožto potenciálně účinné antioxidační a anti-karbonylová činidla v retinálních onemocněních, kde jsou tyto faktory součástí patofyziologie. Napojení (poly)fenolů na specifickou lipofilní mastnou kyselinu může zvýšit jejich biodostupnost, potenciálně umožnit vektorizaci do cílové retinální tkáně a přinést synergický efekt obou funkčních skupin. Lipofenoly dříve připravené v rámci skupiny vykazovaly slibné výsledky in vitro prosti oxidačnímu a karbonylovému stresu. [1] Dva nové deriváty resveratrolu byly připraveny v pěti krocích, v gramových množstvích. Produkty budou využity k in vitro experimentům za účelem objasnění významu dokosahexaenové kyseliny (DHA; C22:6, *n*-3) v lipofenolech z předchozích výsledků.

Konečně, ke zvýšení antioxidačních vlastností lipofenolických derivátů floroglucinolu, byla otestována šestikroková syntéza pro spojení DHA a alkyl-floroglucinolu přes nový typ linkeru.

ABSTRACT

Charles University in Prague

Faculty of Pharmacy in Hradec Králové, Department of inorganic and organic chemistry

University of Montpellier

Faculty of Pharmacy

Institute of Biomolecules Max Mousseron, UMR5247 CNRS ENSCM, UM

Candidate: Tereza Pavlíčková

Advisor: Assoc. prof. PharmDr. Kateřina Vávrová, Ph.D.

Supervisor: Dr. Céline Crauste

Title: Synthesis of lipophenolic derivatives of hydroxytyrosol, resveratrol and phloroglucinol

Lipophenols are conjugates of (poly)phenolic derivatives with a lipid moiety that are designed here to access lipophilic antioxidants.

First part of this work targets olive oil lipophenols. Three new lipophenolic compounds, conjugates of hydroxytyrosol (most abundant olive oil phenol derivative) and three different unsaturated fatty acids were synthesized in two steps, in good yield and high purity. These products will be used as standards for determination of their presence in extra virgin olive oil (EVOO) and in liver samples of rats being fed by EVOO to examine possible *in vivo* metabolization.

Second part of the work targets lipophenols as potential antioxidant and anti-carbonyl-stress agents in retinal diseases, where those factors are involved in the physiopathology. (Poly)phenols linkage to specific lipophilic FAs can increase their bioavailability, potentially enable vectorization to the target retina tissue and bring synergic effect of both moieties. Lipophenolic conjugates previously synthesized within the team showed promising results *in vitro* against oxidative and carbonyl stress. [1] Two new conjugates of resveratrol were synthesized in five steps, in gram amounts. Products will be used for *in vitro* experiments to investigate the effect and the importance of the docosahexaenoic acid (DHA; C22:6, *n*-3) part in previously obtained lipophenols.

Finally, to increase antioxidant properties of phloroglucinol lipophenolic derivatives, a promising six-step pathway was tested to link the DHA and the alkyl-phloroglucinol moities through a new kind of linker.

LIST OF CONTENTS

LIST OF FIGURES

LIST OF SCHEMES

LIST OF TABLES

AIM OF WORK

Lipophenols are conjugates of (poly)phenolic derivatives with a lipid moiety. Aim of my work was to synthesize five new lipophenolic compounds (Fig. 1) designed as lipophilic antioxidants.

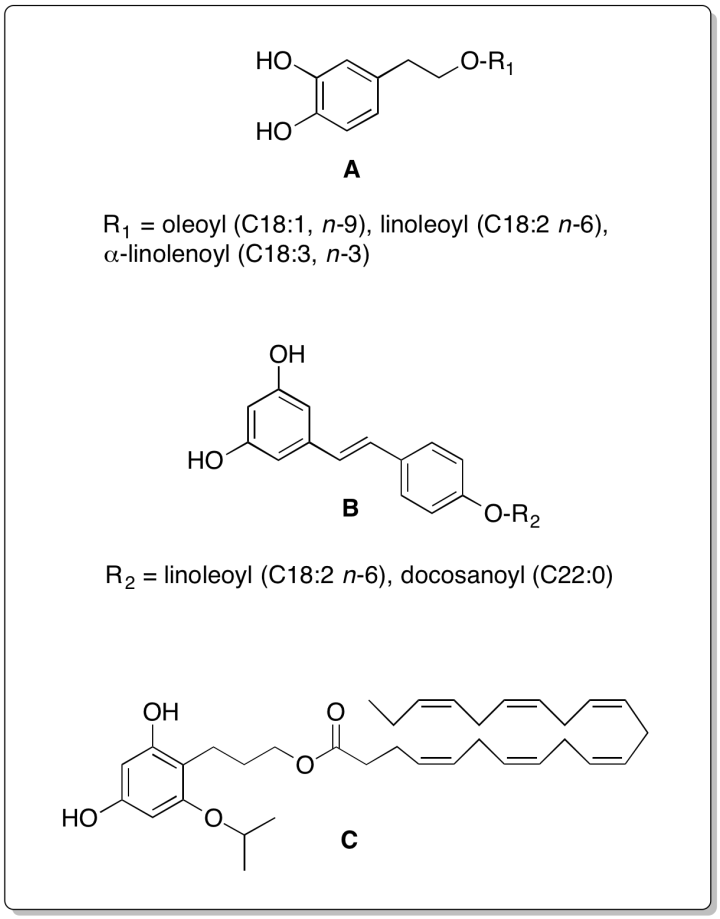

*Figure 1: Target lipophenolic derivatives of hydroxytyrosol (**A**), resveratrol (**B**) and phloroglucinol (**C**).*

This work is divided in two parts: part A which targets lipophenols of olive oil (Fig. 1, series **A**) and part B devoted to lipophenols as antioxidants and anti-carbonyl-stress agents in retinal diseases (Fig. 1, series **B** and **C**).

A. OLIVE OIL LIPOPHENOLS

A.1 INTRODUCTION

Olive oil is a fatty oil obtained by cold expression or other suitable mechanical means from the ripe drupes of *Olea europaea* L. (virgin olive oil) or by refining of crude olive oil (refined olive oil). [2] Extra virgin olive oil (EVOO) is an important constituent of diet in the Mediterranean area and it has many health benefits attributed to its consumption, especially in preventing cardiovascular and metabolic diseases. Various studies proved its benefit in decreasing the cardiovascular risk factors [3] as well as the cardiovascular mortality [4] and revealed its ability to improve the overall antioxidant status. [5]

Several chemical components of olive oil, such as polyunsaturated fatty acids (PUFAs), particularly α-linolenic acid (ALA; C18:3, *n*-3) [6, 7] but also mono-unsaturated oleic acid (OA) and phenolic compounds (hydroxytyrosol) [8, 9] are known to contribute to this effect.

In this part, we work on the synthesis of lipophenolic derivatives, conjugates of hydroxytyrosol and fatty acids (FAs) present in olive oil to investigate the existence of those compounds either in EVOO or after in vivo metabolization in animals fed by EVOO.

A.2 THEORETICAL BACKGROUND

A.2.1 Chemical composition of olive oil

Generally, olive oil can be divided in a saponifiable or glycerol fraction comprising glycerol esters (triglyceride) with various FAs, mainly OA, and non-saponifiable or non-glycerol fraction which includes tocopherols, steroid alcohols and various aromatic hydrocarbon compounds such as polyphenols.
In this work, only FAs and phenolic compounds contents are further discussed.

A.2.1.1 Fatty acids

The European Pharmacopoeia specifies the percentages of various FAs in total FAs fraction (both free and triglyceride bound FAs) of virgin olive oil.
Palmitic acid (C16:0) is the most abundant saturated fatty acid (SFA) present in olive oil saponifiable fraction. Its content may reach up to 20% of total FAs fraction. Other minor SFAs present are stearic (C18:0), margaric (C17:0), arachidic (C20:0), behenic (C22:0) and lignoceric acid (C24:0). [2]
OA (C18:1, *n*-9), a mono-unsaturated fatty acid (MUFA), is the most abundant of all the FAs in olive oil with a content ratio of 55-83%. OA is less prone to oxidative degradation so olive oils high in its content are usually more stable. [10] Other MUFAs such as palmitoleic (C16:1, *n*-7), margaroleic (C17:1, *n*-8) or gadoleic (C20:1, *n*-9) acid are only present in small proportions. [2]
Among PUFAs, only linoleic acid (LA, C18:2 *n*-6; 2.5-21%) and ALA (C18:3 *n*-3; < 1%) are to be found in considerable amounts. [2]
The actual content of different FAs may vary within the range regarding the variety and cultivar of *Olea europea* trees and also the origin and site of plantation. [10-13]
FAs in the form of triacylglycerides of various composition were proven the most distinctive feature among different *O. europea* L. cultivars. [12]

A.2.1.2 Phenolic compounds

Among (poly)phenolic compounds[1] [14], hydroxytyrosol and tyrosol are the most abundant molecules in EVOO. They can be present in a free form or they can form complex phenols when esterified by another phenolic acid moiety such as elenolic acid. In this kind of molecules (secoiridoids; Fig. 2), they can be further glycosylated to create even more complex structures. [15]

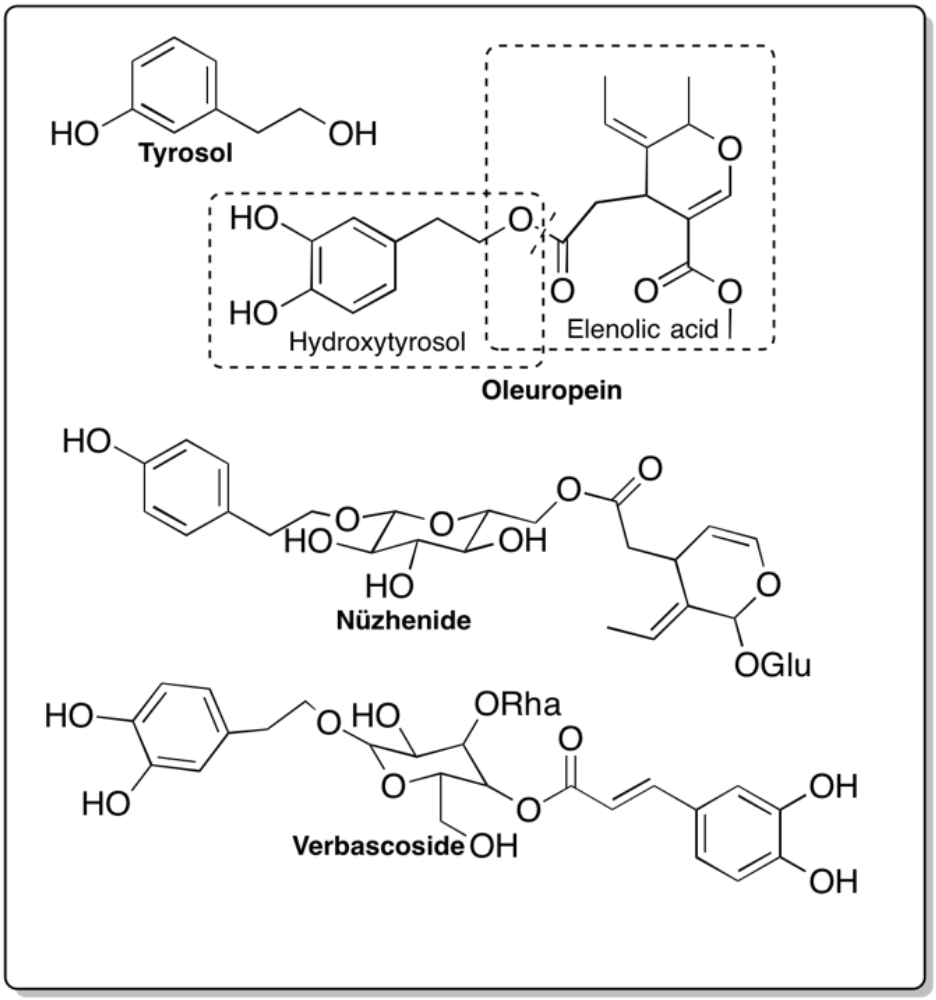

Figure 2: Examples of olive oil polyphenols. Glu – glucose, Rha – rhamnose.

Free hydroxytyrosol is mainly present in the waste after cold mechanical extraction of the virgin olive oil from the fruit; in the olive oil, it occurs mainly in an esterified form even though the rate changes during the shelf time because of the ester hydrolysis.

[1] *According to some definitions (Haslan, 1994), the term "polyphenols" refers to water-soluble plant phenolics with molecular mass from 500 to 3000-4000 Da containing 5-7 aromatic rings and 12-16 phenolic hydroxyls per 1000 Da of molecular mass. In this work, term "polyphenols" includes phenolic compounds defined by biosynthesis in the chapter „Polyphenols".*

Other polyphenols present in olive oil are flavonoids (glucosides of quercetin, luteolin) and lignans (pinoresinol and acetoxypinoresinol). [16]

Among oils, the amount of polyphenols that can be found in olive oil is unique. The content, which is 200–500 mg/kg on the average, shows a huge variability from 50 to 1000 mg/kg depending on the cultivar, period of harvest, the extraction process and other environmental and climatic factors. Some of the polyphenols (demethyloleuropein) may be considered varietal markers, others (elenolic acid glucoside and hydroxytyrosol) indicators of ripeness of the fruit. [10, 17-19]

A.2.2 Health benefits of olive oil

Olive oil is an important constituent of Mediterranean diet and its consumption is believed to lead to various health benefits, particularly in cardiovascular diseases and cancer prevention. The beneficial effects are due to a synergic activity of two key components of olive oil: particular FAs content (high MUFA/SFA ratio) and number of phenolic compounds. It is executed by an ensemble of different mechanisms including direct antioxidant effect and interaction with enzymes, ensuing anti-atherosclerotic and anti-cancerous activity among many.

A.2.2.1 Fatty acids

PUFAs as well as MUFAs are known for their ability to decrease plasma low-density lipoprotein (LDL) cholesterol levels and increase high-density lipoprotein (HDL) cholesterol levels on the other hand. [20, 21] High LDL and low HDL cholesterol levels are the main risk factors of atherosclerosis. Atherogenicity of LDL cholesterol is caused by its oxidation. The susceptibility of LDL towards peroxidation varies with many intrinsic (level of antioxidants) and extrinsic factors, one of them is the amount of highly oxidizable PUFAs in the lipoprotein particle. The mono-unsaturated fatty acids (MUFAs) such as OA can be incorporated in the LDL particle after ingestion, decrease the overall rate of unsaturation and positively affect its resistance against peroxidation. [21] The hypothesis was proven in clinical studies. [20] Considering the high content of OA in olive oil, this can be one of the explanations of the phenomenon of reduced cardiovascular risk in the Mediterranean area.

A.2.2.2 Phenolic compounds

A.2.2.2.1 Anti-atherosclerotic activity

Probably the most significant health benefit of olive oil phenols lies in their effect in prevention of atherosclerosis and coronary heart disease as the major complication of atherosclerosis. However, as mentioned earlier, only oxidized LDL cholesterol is atherogenic. Main mechanism of action of phenolic compounds including oleuropein and hydroxytyrosol is thus the inhibition of oxidation of LDL-cholesterol by direct trapping of free radicals. This was proven in various *in vitro* studies. [22, 23] Besides direct trapping of free radicals, phenolic compounds inhibit 3-hydroxy-3-methylglutaryl-coenzyme A reductase (*in vitro*) and platelet aggregation via interaction with thromboxane. Hydroxytyrosol has shown an anti-platelet activity comparable to that of acetylsalicylic acid used worldwide in secondary prevention of coronary heart disease. [24]

As inflammation plays a key role in the pathology of atherosclerosis, anti-inflammatory effect of olive oil phenols is another important factor in the cardiovascular disease prevention. The main mechanism involved in this process is the inhibitory activity of olive oil phenols on cyclo- and lipooxygenase resulting in a reduced formation of pro-inflammatory cytokines. [24]

A.2.2.2.2 Prevention of cancer

ROS can play a major role in cancer development by attacking the DNA molecules. This is one of the mechanisms of action of antioxidants such as simple phenolic compounds (tyrosol and hydroxytyrosol). In addition, more complex olive oil polyphenols such as lignans or secoiridoids can inhibit xanthine oxidase causing a decrease of ROS levels. Lignans can act specifically through their hormonal (anti-estrogen) effect. Another suggested anti-cancerous and anti-inflammatory mechanism is by inhibition of VEGF-induced angiogenesis. [25]

A.3 AIM OF WORK

Aim of this part of work was to synthesize lipophenolic conjugates of hydroxytyrosol linked to three unsaturated FAs (Fig. 3), namely OA (C18:1, *n*–9), LA (C18:2, *n*–6) and ALA (C18:3, *n*–3).

All of the above-mentioned compounds are naturally present in a free form and also in the form of a triglyceride (FAs) or glycoside conjugate (hydroxytyrosol) in olive oil. However, presence of their mutual ester conjugates has never been determined. Our synthesized conjugates should thus act as HPLC standards to find out if those lipophenols could exist naturally in olive oil or could be formed *in vivo* after ingestion and metabolization.

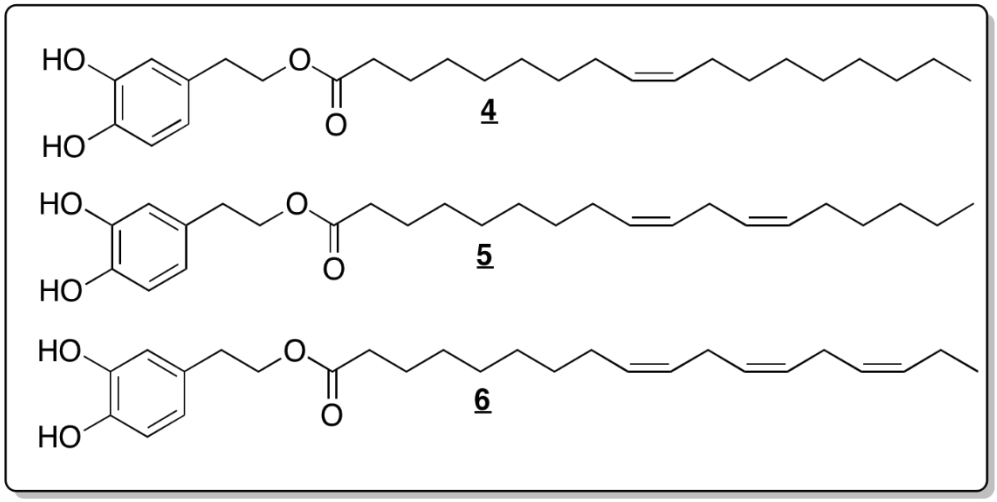

*Figure 3: Structures of hydroxytyrosol-OA (**4**), hydroxytyrosol-LA (**5**) and hydroxytyrosol-ALA (**6**).*

A.4 RESULTS AND DISCUSSION

Two-step synthetic strategy was developed to obtain compounds **4**, **5** and **6** (Scheme 1). In the first step, the commercially available 2-(3,4-dimethoxyphenyl)ethan-1-ol is linked to the FA using dicyclohexylcarbodiimide (DCC) as a coupling agent in the presence of catalytic amount of 4-dimethylaminopyridine (DMAP). The resulting esters were then deprotected by combination of BCl_3 and tetrabutylammonium iodide.

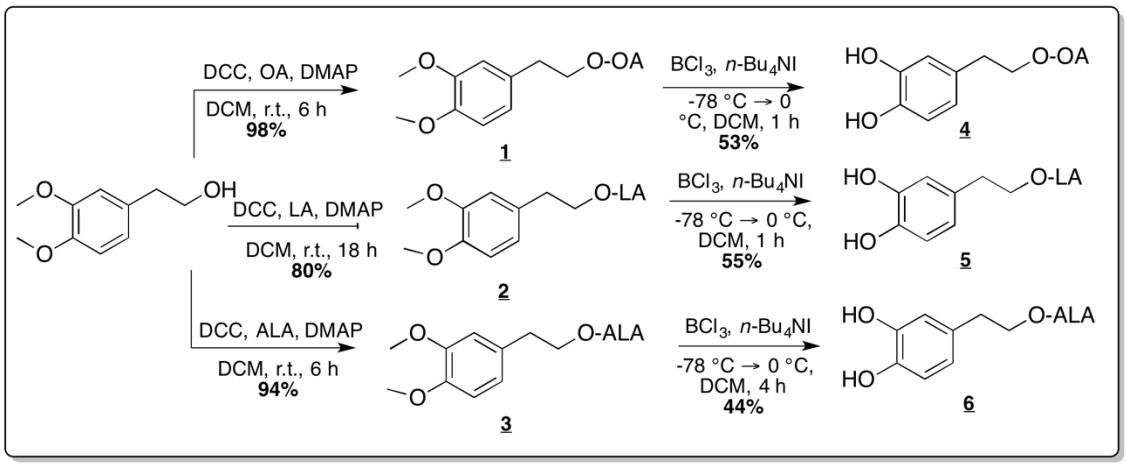

Scheme 1: Synthesis of hydroxytyrosol-FA conjugates.

Compounds **1**, **2** and **3** were obtained in very good to excellent yields. In all three cases, 1.1 eq. of DCC, 1.1 eq. of the corresponding FA and 0.1 eq. of DMAP were added to protected hydroxytyrosol and the reaction was carefully monitored by thin-layer chromatography (TLC). The starting material still appeared on TLC after a couple of hours in case of compounds **1** and **3**, further 0.5 eq. and 0.05 eq. of DCC and DMAP, respectively, were thus added.

The first attempt of the second step – deprotection of methyl groups – was carried out on LA conjugate **2**. According to Brooks et al., [26] BCl_3 in combination with *n*-Bu_4NI can serve as effective and mild agent to cleave primary alkyl aryl ethers and there were some successful reactions executed in our laboratory using this reagent. The mild deprotection using BCl_3 was selected compared to the stronger Lewis acid BBr_3 because of the instability of PUFAs. Because of the presence of an ester group, a potential Lewis base site able to form a complex with BCl_3, more equivalents of this reagent than usual should be required to result in successful deprotection. Therefore, 5 eq. of BCl_3 and *n*-Bu_4NI were introduced into the reaction at -78 °C, the reaction was then slowly brought to 0 °C and terminated after 3 hours. Unfortunately, the obtained product was highly degraded at the level of double bond (bis-allylic protons almost disappeared in the ^1H NMR spectra).

Few more experiments were performed to optimize the eq. of BCl_3/*n*-Bu_4NI (Tab. 1). and the reaction time on the compound **2**. Around 3 eq. of BCl_3 and *n*-Bu_4NI were needed to access acceptable yield (78% after purification on silicagel column, Tab. 1, Entry 3). Optimized conditions were applied to compounds **1** and **3**, adapting them to the course of reaction (Tab. 1).

Table 1 : Deprotection reactions. Influence of reaction time and reagents equivalents.

Entry	Starting mat.	Starting amount	Eq. of BCl_3/*n*-Bu_4NI, time	Mass obtained	Yield Purification on silicagel	Yield Purification on C18 preparative HPLC
1	**2**	300 mg	5 eq., 3h	200 mg	0%	0%
2	**2**	150 mg	2.5 eq., 2.5 h	77 mg	55%	Not purified
3	**2**	150 mg	3 eq., 1 h	111 mg	78%	55%
4	**1**	500 mg	3 eq., 1 h	354 mg	76%	53%
5	**3**	170 mg	3.5 eq., 4.5 h	100 mg	63%	44%

Compounds were obtained in a fair purity according to ^1H NMR and good yields after purification on silicagel chromatography. Yet, after UPLC analysis, some minor by-products were found in a proportion of more then 10% in each of the synthesized lipophenolic compounds. Since the intention of the synthesized hydroxytyrosol-FA lipophenols was to serve as HPLC standards, the purity of the products was essential. The compounds were thus further purified by preparative HPLC using C18 preparative column (16 mL/min, H_2O/ACN, 20/80 to 0/100, detection UV 220 nm), which resulted in compounds **4**, **5** and **6** in high purity (Fig. 4-8).

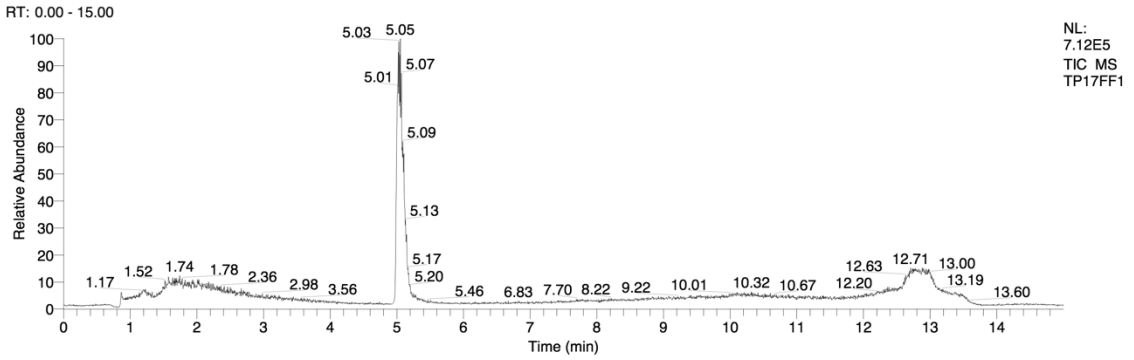

*Figure 4: Total ion count (TIC) chromatogram of compound **4**.*

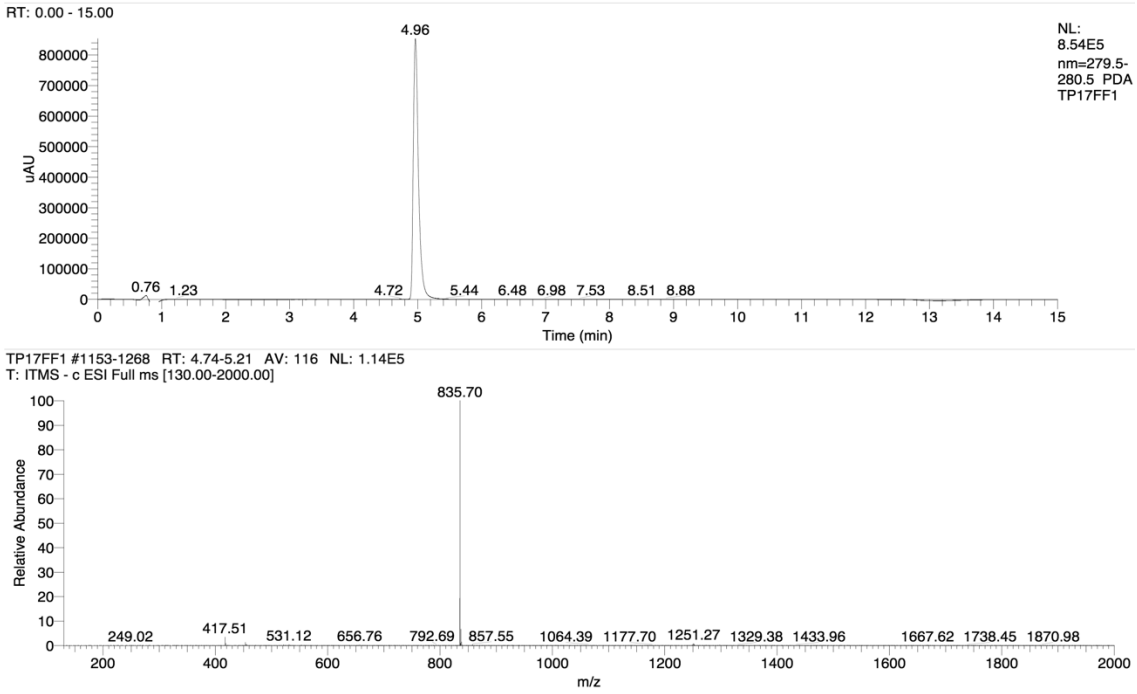

*Figure 5: UPLC/UV chromatogram (top) and UPLC/MS spectrum of compound **4**.*

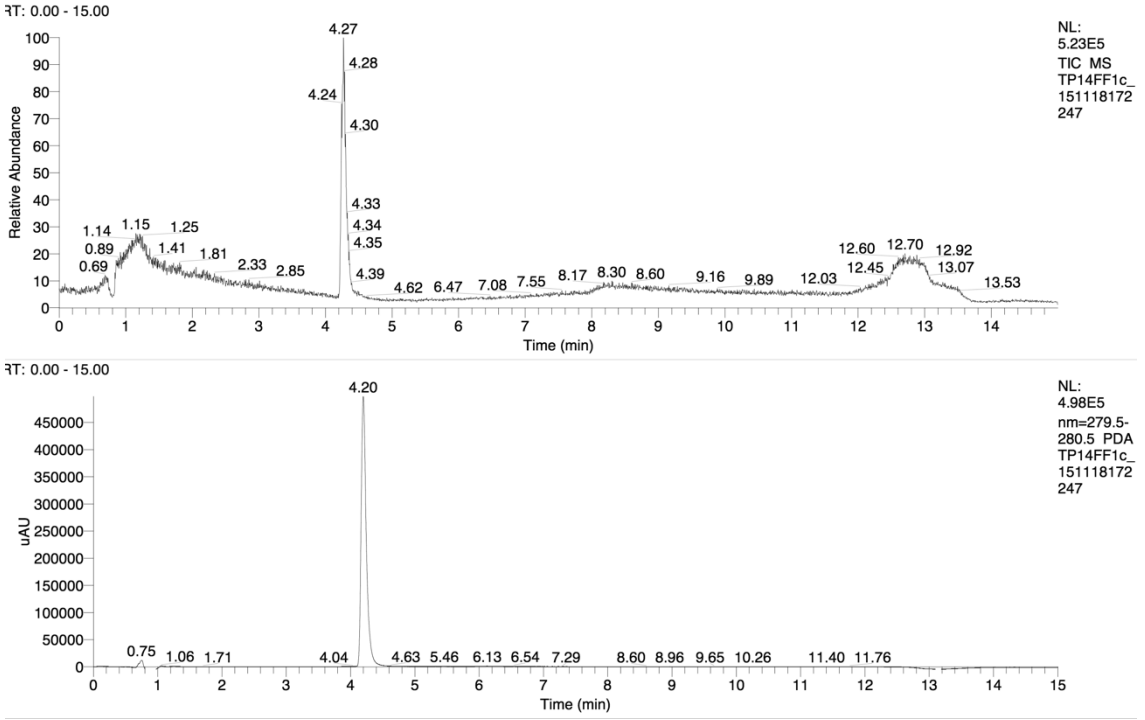

*Figure 6: TIC chromatogram (top) and UPLC/UV chromatogram (bottom) of compound **5**.*

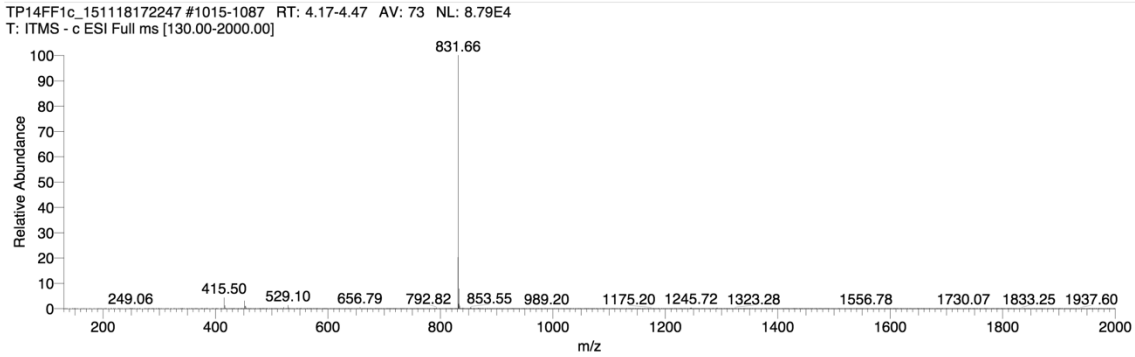

*Figure 7: UPLC/MS spectrum of compound **5**.*

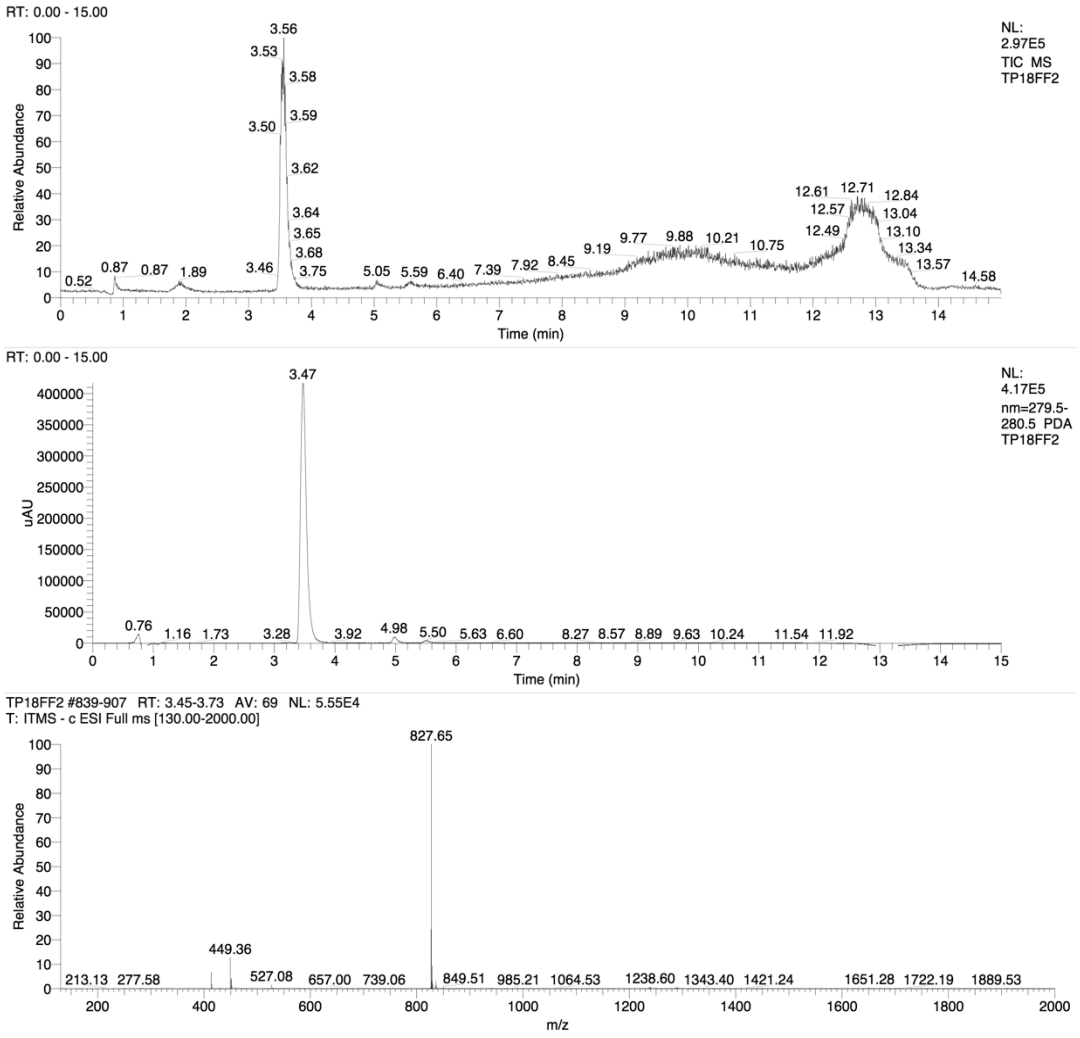

*Figure 8: TIC (top), UPLC/UV (middle) chromatogram, UPLC/MS spectrum (bottom) of compound **6**.*

The impurities were isolated in all three cases and after in-depth analysis of the ^{1}H, ^{13}C and 2D spectra, possible structure of the side product was proposed during the synthesis of compound **4**.

This impurity was derived from the double bond and implied iodine addition to the double bond. This assumption was based on the ^{1}H NMR chemical shift of CH signal which was only present in the impurity (Fig. 9) and was attributed to the original double chain site. Since the number of different side products in the isolated fraction of impurity (regarding the number of CH_3 triplets in the ^{1}H NMR spectra) correlated with the number of double bonds in the FA chain, the OA-derived side product **4b** was the easiest to identify because of the relative simplicity of the structure. Extrapolation of this result to other analyzed spectra led us to conclude that a formation of a mixture of similar halogenated by-productss may also have occurred during the synthesis of **5** and **6**.

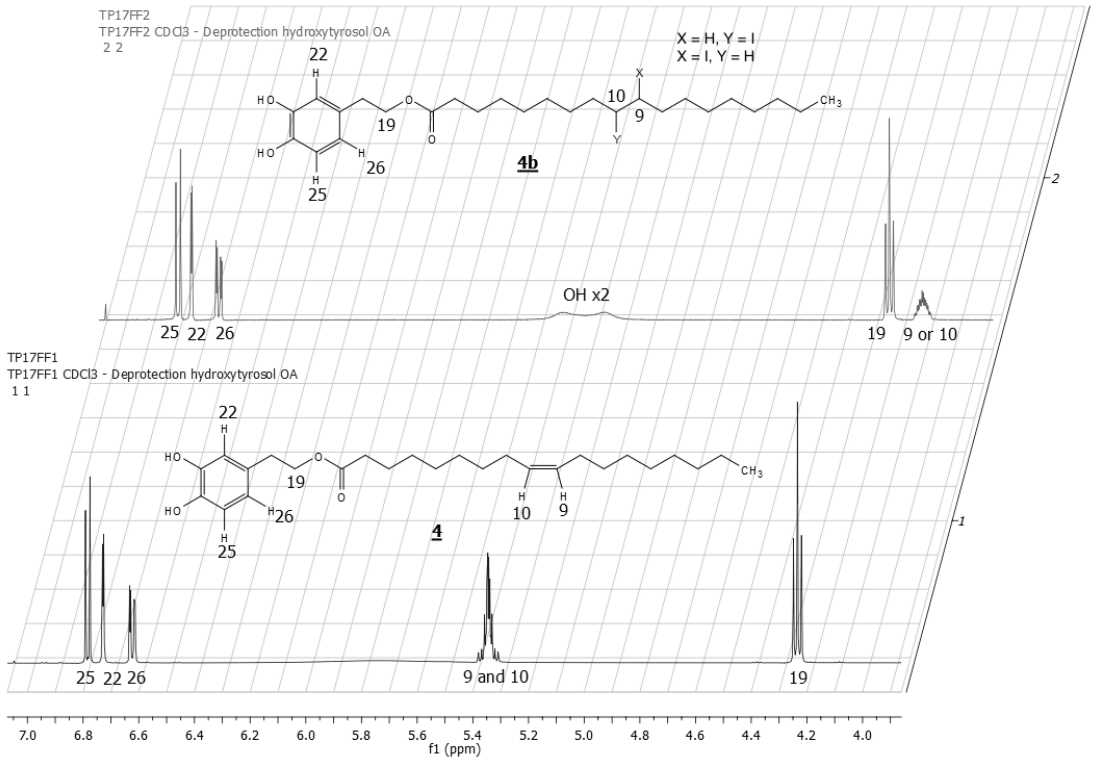

*Figure 9: Part of ^{1}H NMR spectra of **4** and **4b** with assignments.*

A.5 CONCLUSION AND PERSPECTIVES

Effective two-step synthesis was developed to gain compound **4**, **5** and **6** in 52%, 44% and 41% respective overall yields. Cleavage of the methoxy bond was fairly optimized but the double bonds in the FA moiety still showed to be prone to be attacked by iodine.
A preparative HPLC method was developed to purify the final compounds; as it was applicable and successful in all three cases, it can be applied to other hydroxytyrosol-FA conjugates that might be later synthesized.
Eventually, the three new lipophenols were obtained in high purity.
In the future, some further reactions should be executed trying a different deprotecting agent, possibly BBr_3 which is more potent but does not demand the presence of the *n*-Bu_4NI. It was successfully used to deprotect methyl groups on resveratrol conjugate linked to ALA. [27]
The synthesized products will be quantified in EVOO and in liver samples of rats being fed EVOO using HPLC-MS detection. This work will be performed in collaboration with Pr. Jetty Chung-Yung Lee of the University of Hong Kong.
In addition, those derivatives, particularly hydroxytyrosol-ALA (**6**) could serve as nutritional supplements for their antioxidant capacity and as a source of *n*–3 PUFAs. We believe those lipophenolic conjugates could be more stable and less prone to oxidation then a mixture of free hydroxytyrosol and ALA.

B. LIPOPHENOLS AS ANTIOXIDANTS AND ANTI-CARBONYL-STRESS AGENTS IN RETINAL DISEASES

B.1 INTRODUCTION

Retinal pathologies are a major issue in many developed countries. Age-related macular degeneration (AMD) is a leading cause of blindness in people over 60 [28], it also has a gene-related juvenile form (Stargardt disease). In both forms, oxidative and carbonyl stress play a major role and cause transformation of all-*trans*-retinal (A*t*R, a carbonyl stressor that accumulates abnormally in photoreceptors) in toxic bis-retinoid derivatives that accumulate in retinal pigment epithelium (RPE). The result is degeneration and death of RPE cells causing the death of photoreceptors and progressive vision loss. [29-31]

Polyphenols are generally potent antioxidants and some of them, such as phloroglucinol, monomer of phlorotannin from brown algae, are also capable to trap reactive carbonyl species (RCS) such as 4-hydroxynonenal. [32, 33] Their major drawback is their low bioavailability and ability to cross the blood-retina barrier and penetrate to nervous tissues like the retina.

Lipophenols are conjugates of polyphenols and a lipid moiety (in this case FA moiety) and they are designed here as dual lipophilic scavengers of both reactive oxygen species (ROS) and RCS.

The linkage of polyphenols to FAs may increase their penetration to the retina not only by increasing lipophilicity and thus the bioavailability, but, because some PUFAs – namely docosahexaenoic acid (DHA, C22:6, *n*-3) and eicosapentaenoic acid (EPA, C20:5, *n*-3) – are highly present in the photoreceptor membranes. [34] Since those two FAs are essential for humans, which means they are absorbed mainly from nutrition, [35, 36] such lipid parts may act as a vector to carry the polyphenol molecule effectively to the retinal tissue.

Moreover, since consumption of PUFAs, especially DHA, showed some promise in the treatment of retinal diseases in some clinical trials, [37] the lipid moiety might bring some therapeutic activity to the molecule by itself and the final effect of a conjugate molecule can be significantly higher than in a simple one.

Lastly, the polyphenol moiety can provide its antioxidant effects to the FA moiety and vice versa. This type of molecule is subsequently less prone to undergo auto-oxidation or

to be attacked by radicals, that could lead to the formation of toxic electrophilic aldehydes (carbonyl stress).

A series of lipophenolic compounds, conjugates of phloroglucinol and PUFAs had previously been synthesized within the team and their protective effect against carbonyl stress was tested on the ARPE-19 lines (human retinal pigment epithelium cell lines) exposed to toxic concentrations of A*t*R. This study highlighted the importance of an alkyl-resorcinol pattern on the phenolic backbone for the trapping reactions of carbonyl stressors. Phloroglucinol analogues linked to DHA and LA have been shown to protect effectively ARPE-19 cells from carbonyl stress. [1]

B.2 THEORETICAL BACKGROUND

To clarify the objectives of the work, this part will include chapters about oxidative and carbonyl stress, their implication in the pathophysiology of retina diseases such as macular degeneration, current possibilities of AMD treatment and at last, some interesting properties of plant polyphenols to fight against both carbonyl and oxidative stress.

B.2.1 Oxidative and carbonyl stress

B.2.1.1 Oxidative stress

Oxidative stress is defined as a disturbance in the balance between the production of ROS (free radicals) and antioxidant defenses, which may lead to tissue injury. [38]

Body's natural antioxidant defense comprise enzymes such as superoxide dismutase, glutathione peroxidase and catalases and exogenous molecules like tocoferol, β-carotene or coenzyme Q. When this defense is impaired or overloaded, which happens in certain diseases (e.g. state of severe injury or various chronic diseases), cell and tissue damage may be induced and we talk about oxidative stress, [38] that can also lead to carbonyl stress regarding the substrate of the oxidation.

Free radical is any atom or molecule containing unpaired electron, but in physiological conditions, hydroxyl radical •OH, superoxide radical-anion $\bullet O_2^-$, nitric oxide radical •NO and peroxynitrite anion $ONOO^-$ are produced by several biochemical processes. They can then react with other radical species to form a covalent bond, but since most of the biomolecules present in the human body are nonradicals, they would rather react with them to form undesirable products and new reactive R• radicals. Any macromolecules can become target of the free radical reactions, mostly lipids and nucleic acids, but proteins and carbohydrates are not an exception.

To illustrate lipid peroxidation, the Scheme 2 [39] shows the effect of free radicals of PUFAs formed during lipid peroxidation process. ROS such as the hydroxyl radical can attack the PUFA side chain and abstract a methylene hydrogen atom (Scheme 2, **A**). Then, molecular rearrangement occurs to result in a more stable conjugated diene (Scheme 2, **B**), which reacts with oxygen to form a peroxyl radical (Scheme 2, **C**). This radical can abstract further hydrogen atom from another lipid molecule and induce a chain reaction (Scheme 2, **D)**; at this point, antioxidant defense should react otherwise the reaction continues until the substrate is consumed. [39] The formed lipid peroxide can be

decomposed to further reactive components, e.g. when transition metal or metal complexes are present to catalyze the reaction (Scheme 2, **E**, **F**).[40]

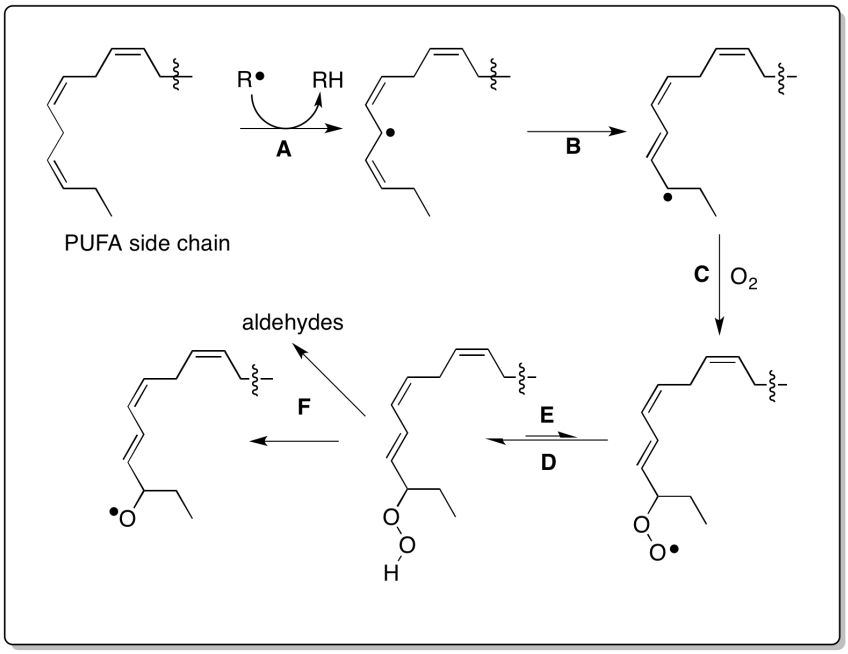

Scheme 2: PUFA side chain peroxidation. (Gutteridge et al., 1995)

One of the species resulting from this process can be small reactive electrophilic aldehydes that will be the starting point of carbonyl stress, able to react with nucleophilic part of DNA or protein.

Hydroxyl radical attack on guanine base (Scheme 3) is an example of DNA degradation by ROS. After the initial attack, resulted radical can undergo an oxidation, a reduction or a ring opening reaction. Product of the oxidation is relatively stable whereas other two products are further stabilized by a ring opening reaction or a reduction. [41]

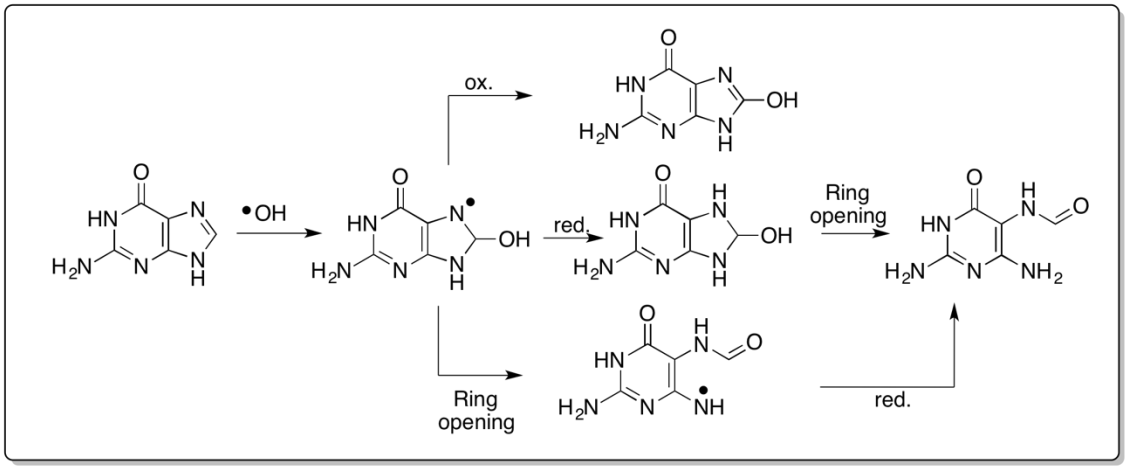

Scheme 3: Suggested mechanism of hydroxyl radical attack of guanine. (Nimse et al., 2015)

B.2.1.2 Carbonyl stress

When exposed to oxidative stress, some physiological molecules like lipids or carbohydrates may produce RCS – small molecules of aldehyde or ketone character, which are highly electrophilic and may by attacked by nucleophilic centers of macromolecules such as proteins and DNA and cause irreversible damage within the cells.

Reactive alpha-dicarbonyl compounds such as methylglyoxal, glyoxal, glucosone and 3-deoxyglucosone are the main products of oxidative auto-degradation of sugars, nominally glucose (Scheme 4). [42] This process is part of the formation of the advanced glycation end products, irreversible adducts such as cross-linked proteins, as observed in diabetes mellitus, but also Alzheimer's disease, ageing and other chronic diseases. Methylglyoxal was proven to attack DNA and cause reproductive toxicity. [43]

Endogenous reactive aldehydes that accumulate abnormally within the cells are also considered carbonyl stressors.

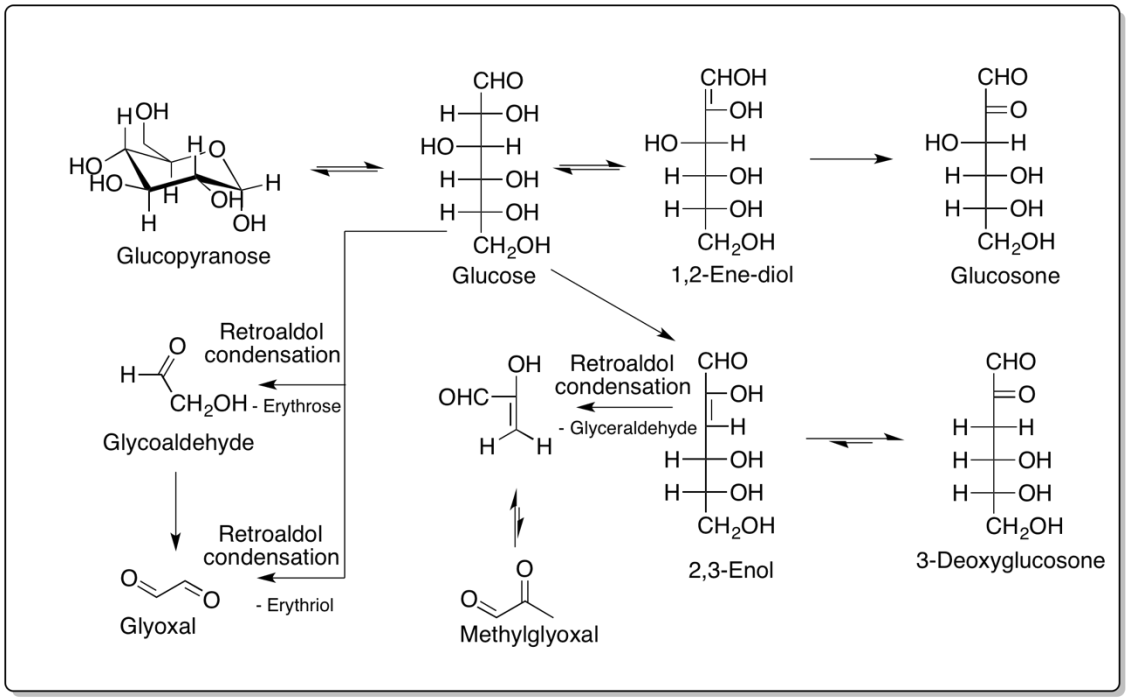

Scheme 4: RCS formation during the oxidative degradation of glucose. (Thornalley et al., 1999)

B.2.2 Macular degeneration

B.2.2.1 Introduction

Macular degeneration is the leading cause of blindness in the developed world and it represents a major public health issue. Macular degeneration can either affect the elderly, mostly people over 60 (AMD), or it can be gene-related (juvenile form such as the Stargardt disease). Up to date preventive treatment includes lifestyle modification and food supplementation with antioxidants and *n*-3 PUFAs. Specific treatment is only available for the late form of AMD, the neovascular form (wet form) which comprises only 20% of cases and the other, more common dry form (early stage of the pathology) is yet untreatable. Therefore, there is constant seek and growing need for an effective cure.

B.2.2.2 Pathophysiology

AMD affects the central part of the retina, the macula. It is considered a multifactorial disease, however, oxidative and carbonyl stress are the key factors in the beginning of the pathophysiology.

The retina consists of four layers of cells (Fig. 10): innermost ganglion cells covered by a nerve fibre, bipolar neurons, photoreceptor cells and the RPE which sits on the Bruch's membrane, providing barrier between the retina and external choriocapillaries and choroid vessels. In the macula, neuronal cells are displaced to maximize the light exposure of the photoreceptors; in its central part, the fovea, there are photoreceptors only. [29]

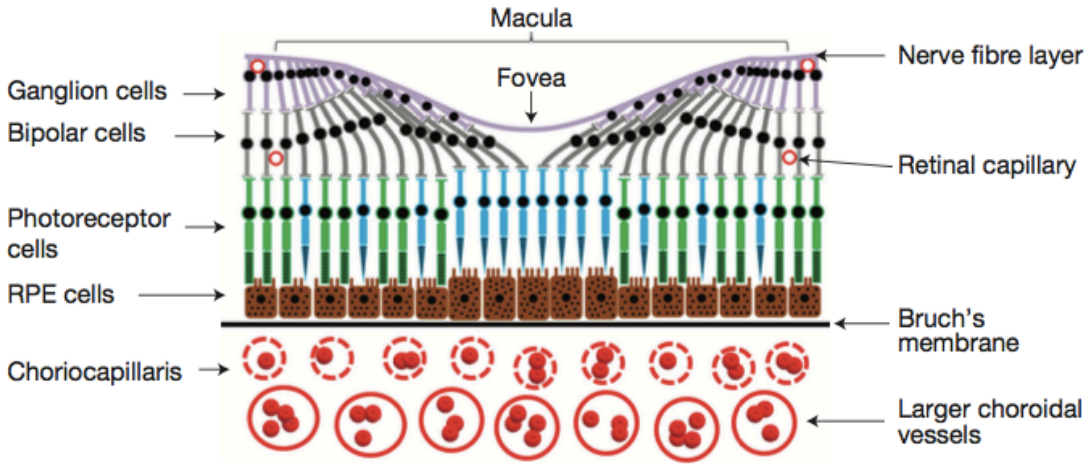

Figure 10: Structure of the healthy retina. (Khandhadia et al., 2010)

Due to this extreme light exposure, the retina is under constant influence of photo-oxidative stress. In a healthy tissue, this is compensated by increased levels of natural antioxidants.

In macular degeneration, RPE cells excessively accumulate lipofuscin, a fluorescence pigment containing toxic substances, that can cause direct cellular damage or indirect toxicity by producing ROS and RCS. One of the key components of lipofuscin is *N*-retinylidene-*N*-retinylethanolamine (called A2E), a by-products of a visual cycle in the photoreceptor cells. [29] It results from A*t*R which should normally be reduced to form retinol. Instead, A*t*R accumulates in the photoreceptors due to aging or due to a genetic modification. Two molecules of A*t*R (considered as carbonyl stressor) react with phosphatidyl ethanolamine to form the toxic bis-retinoid conjugate A2E (Scheme 5). [44, 45]

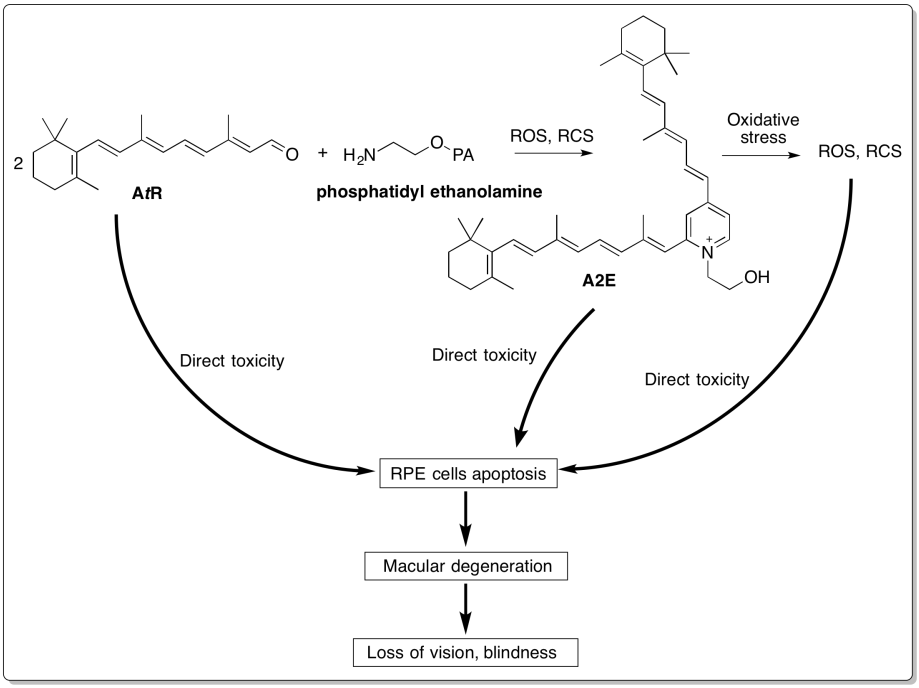

Scheme 5: Formation of A2E and impact of the process on RPE cells. (Crauste et al., 2014)

In Stargardt disease, this is caused by mutation of ABCR gene. This gene encodes a retina-specific protein which functions as an ATP-flippase, transporting A*t*R adducts out of the photoreceptor inner segment to the RPE. While doing so, it cleaves the bond between A*t*R and phosphatidyl ethanolamine and the A*t*R is reduced to retinol. When there is a mutation in ABCR gene A*t*R accumulates in photoreceptor, which under carbonyl and oxidative stress leads to A2E biosynthesis.

A2E stays in the inner segments [46] and after daily phagocytosis process of photoreceptor cells accumulates in the RPE. [44] The phagocytosis itself also leads to

ROS production. [29] A*t*R may damage the retina via direct toxicity due to production of ROS as well. [47]

Histological changes include formation of drusen (yellow deposits of proteins and lipids usually between RPE and Bruch's membrane), both atrophy and hypertrophy of the RPE cells and choroidal vessels atrophy, leading to bleeding.

This process of macular degeneration is manifestated clinically as a progressive loss of central vision. [29]

B.2.2.3 Treatment

Up to date, there is no effective cure for macular degeneration. The current available treatment targets prevention or it can delay its progression.

B.2.2.3.1 Food supplementation

Valuable clinical data come from a multicenter, double-blind, prospective, controlled Age-related disease study (AREDS) carried out by the National Eye Institute of the National Institutes of Health. This study investigated the effect of high and low doses of zinc and copper and some antioxidant vitamins on the development and progression of AMD. This stage showed significant benefit of a zinc and copper-enriched diet, which increased with addition of antioxidant vitamins. [28]

In the second part of this study (AREDS2), effect of *n*-3 PUFAs (DHA, EPA) and carotenoid antioxidants (lutein, zeaxanthin) on AMD progression in comparison with AREDS formulation were investigated. Even though both might have some benefits in the development of advanced AMD in people at moderate to high risk for progression (risk was reduced by 10% for lutein/zeaxanthin, 3% for DHA/EPA, 11% for lutein/zeaxanthin + DHA/EPA) and in progression to moderate vision loss (risk reduced by 5% for lutein/zeaxanthin, 4% for DHA/EPA, 6% for lutein/zeaxanthin + DHA/EPA), the results from AREDS2 remain nonsignificant. [48, 49] In two other studies (Blue Mountain Eye study and Alienor study), supplementation by long-chain PUFAs decreased the risk of AMD. [50] In a recent pilot study, daily intake of long-chain PUFAs improved visual acuity in 100% of patients with dry AMD. [51]

B.2.2.3.2 Lifestyle changes

Lifestyle changes can play a role especially in prevention of AMD. Smoking is known for increasing the overall oxidative stress and depressing the natural antioxidant defense, contributing thus significantly to the risk of progression of the disease. [52] Three out of four studies on severe alcohol consumption showed a positive correlation with the

development of late AMD. Other suggested lifestyle modification is physical activity, although without any direct evidence. [28]

B.2.2.3.3 Targeted therapy

For the more severe wet (neovascular) form of the AMD, intravitreal application of vascular endothelial growth factor (VEGF) inhibitors such as pegaptanib (Macugen), ranibizumab (Lucentis), aflibercept (Eyelea) or bevacizumab (Avastin, off label use) are indicated. However, the wet form most probably rises as a result of a long, less pronounced process of dry macular degeneration. [53]

B.2.2.3.4 Future approaches

Future approaches to AMD treatment, some of them in clinical trials, target some of the factors in the AMD pathophysiology.

AMD drusen have shown some similarity to plaques found in Alzheimer's disease. Therefore, anti-β-amyloid antibodies might reduce drusen formation and some of them are in clinical trials [54] as well as glatiramer acetate, which successfully reduced drusen formation in mice. [55] Studies with various anti-inflammatory agents such as anti-complement antibodies, corticosteroids or tacrolimus are also ongoing. Other drugs aim to reduce retinal oxidative stress and the accumulation of toxic by-products of the visual cycle. Those drugs are in phase II clinical or preclinical studies, but represent some promising possibilities. Agents aiming to improve choroidal perfusion showed no significant results so far. [28]

Gene therapy might be an attractive therapeutic alternative, particularly for Stargardt disease and other gene-related forms of macular degeneration.

B.2.3 Polyphenols

B.2.3.1 Introduction

Natural polyphenols are a vast group of plant secondary metabolites. They are abundant in human nutrition such as fruit, vegetables and cereals and they possess pleiotropic biological effects beneficial to human health, although some of the mechanisms of action are not fully understood. Among them, they possess interesting antioxidant and anti-carbonyl-stress properties interesting in retinal pathologies.

According to the purely chemical definition, polyphenols are compounds bearing several hydroxyl groups on an aromatic ring. However, this definition would comprise some alkaloids as well as some aromatic terpenoids, which are not considered polyphenols. To define plant polyphenols more specifically, those are phenolic compounds resulting from one of two metabolic pathways: shikimic acid pathway or acetic acid pathway. [56]

Naturally, they are present in the form of conjugates (esters, glycosides, or polymers) most commonly linked to sugars (poly- or monosaccharides; polyphenolic part is then called the aglycone) but linkage to carboxylic acids, amines or lipids is also possible. This linkage may be through the hydroxyl moiety in the majority of cases, or less commonly by a direct bond to the aromatic ring. [57]

B.2.3.2 Classification

Based on the biosynthesis of the aromatic ring, so called aromagenesis, polyphenols can be classified in three major classes. [56]

B.2.3.2.1 Shikimates – polyphenols of the shikimic acid pathway

Cinnamic acids (Scheme 6), phenolic acids of the C6-C3 (phenylpropane) pattern, are the first group of polyphenols in the shikimic acid pathway.

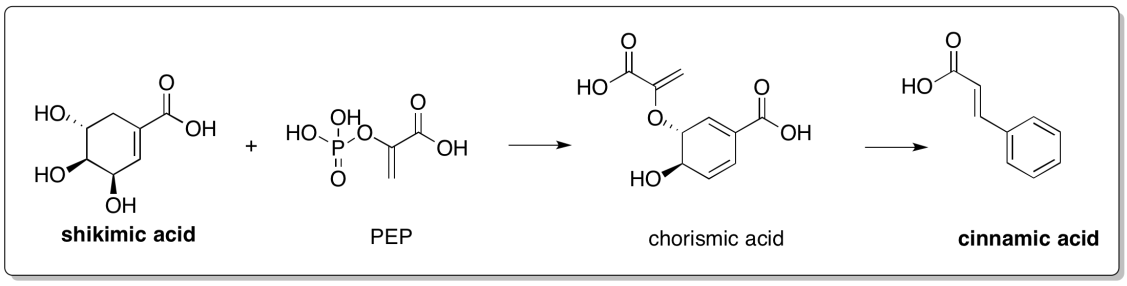

Scheme 6: Biosynthesis of cinnamic acid from shikimic acid and phosphoenolpyruvic acid (PEP)

Chlorogenic and caffeic acid (Fig. 11) are examples of cinnamic acid polyphenols. Caffeic acid is released from its conjugate form chlorogenic acid after microbial hydrolysis in the colon. [58]

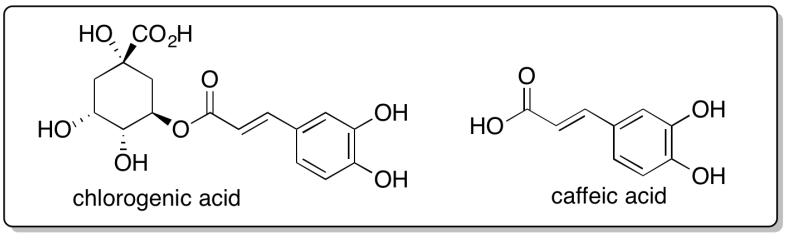

Figure 11: Structures of chlorogenic and caffeic acid.

Coumarines (benzo-α-pyrones; Scheme 7) are lactones derived from cinnamic acids.

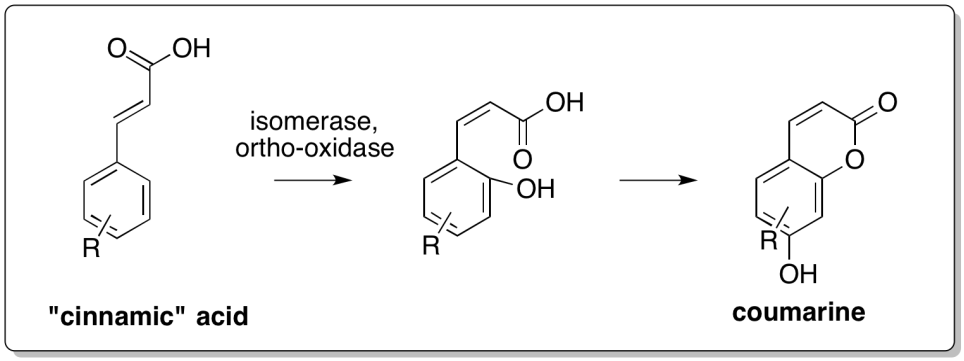

Scheme 7: Biosynthesis of coumarines from cinnamic acids.

Lignans (Scheme 8) are products of radical dimerization of cinnamates.

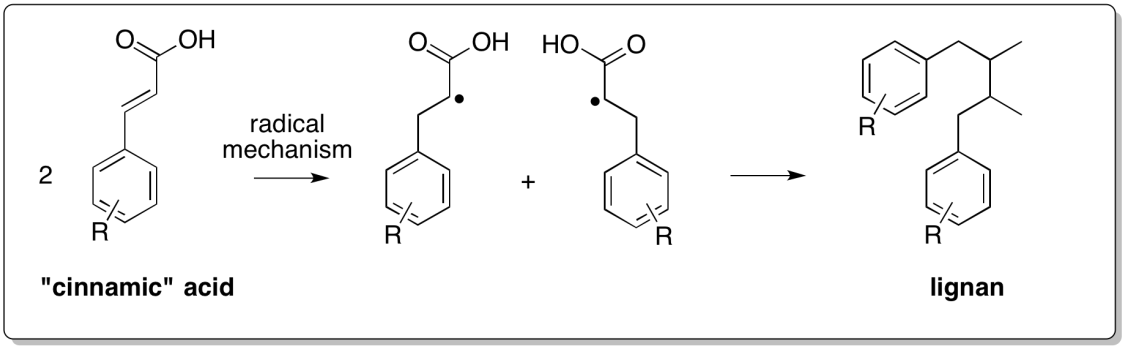

Scheme 8: Biosynthesis of lignans from cinnamic acids.

Hydroxybenzoic acids (Scheme 9), phenolic acids of the C6-C1 pattern, can be described as oxidative products of cinnamic acids degradation.

Simple phenols (C6 pattern; Scheme 9) result from (hydroxy)benzoic acids decarboxylation.

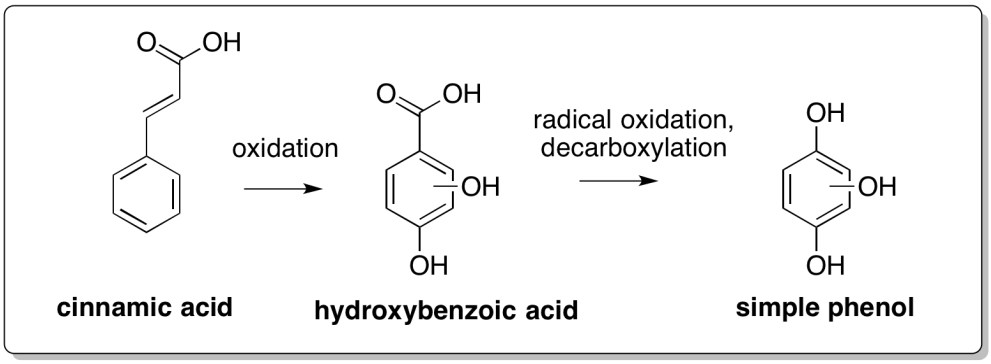

Scheme 9: Biosynthesis of hydroxybenzoic acids and simple phenols from cinnamic acids.

B.2.3.2.2 Polyacetates – polyphenols of the acetic acid pathway

Key intermediate in the biogenesis of acetic acid pathway polyphenols is, similarly to FAs or terpenoids, acetyl coenzyme A (acetyl-CoA). [56]

Aldol condensation of polyacetates leads to 2,4-dihydroxy-6-alkylbenzoic acids – so called **orsellinic acids** (Scheme 10).

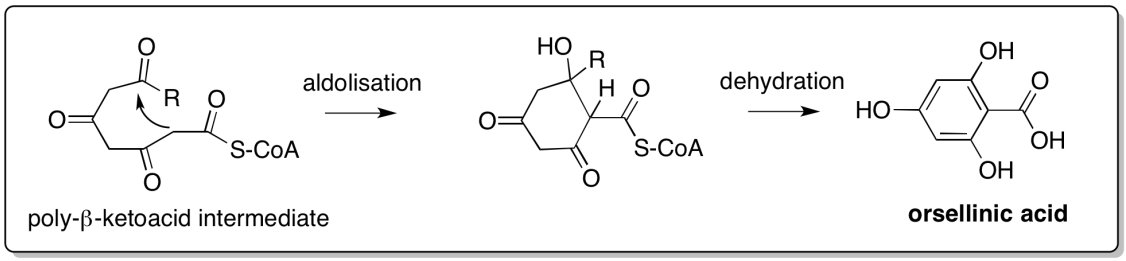

Scheme 10 : Biosynthesis of orsellinic acids from polyacetate intermediate.

In contrast, Claisen condensation followed by enolization provides 1-acyl-2,4,6-trihydroxybenzenes – acylated **phloroglucinols** (phloroacetophenones; Scheme 11).

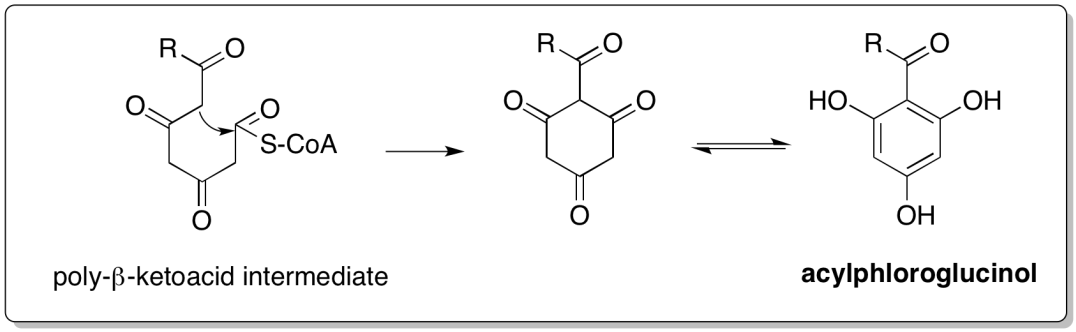

Scheme 11: Biosynthesis and tautomeric forms of acylphloroglucinol.

When the Claisen condensation is followed by heterocyclization, it provides to benzo-γ-pyrones, **isocoumarines** (Fig. 12).

Quinones (Fig. 12) are also products of the acetic acid pathway where they are formed via aldolic polycondensations.

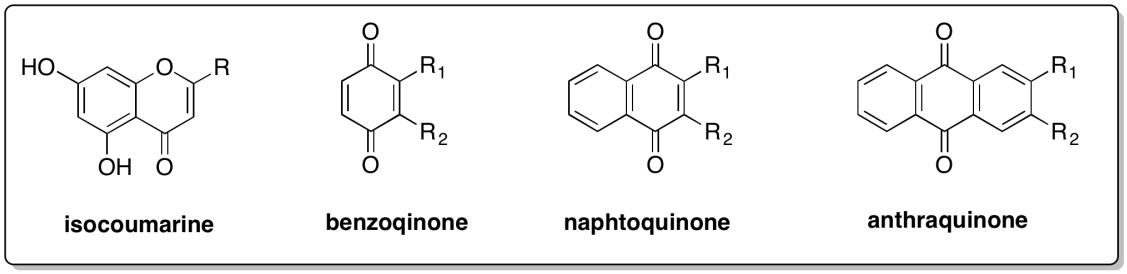

Figure 12: Structure of isocoumarines and different structural types of quinones.

B.2.3.2.3 Mixed polyphenols – combination of the shikimic and acetic acid pathway

Flavonoids (Fig. 13) are compounds of C6-C3-C6 backbone and they result from condensation from activated cinnamates (shikimic acid pathway) with triacetates (acetic acid pathway).

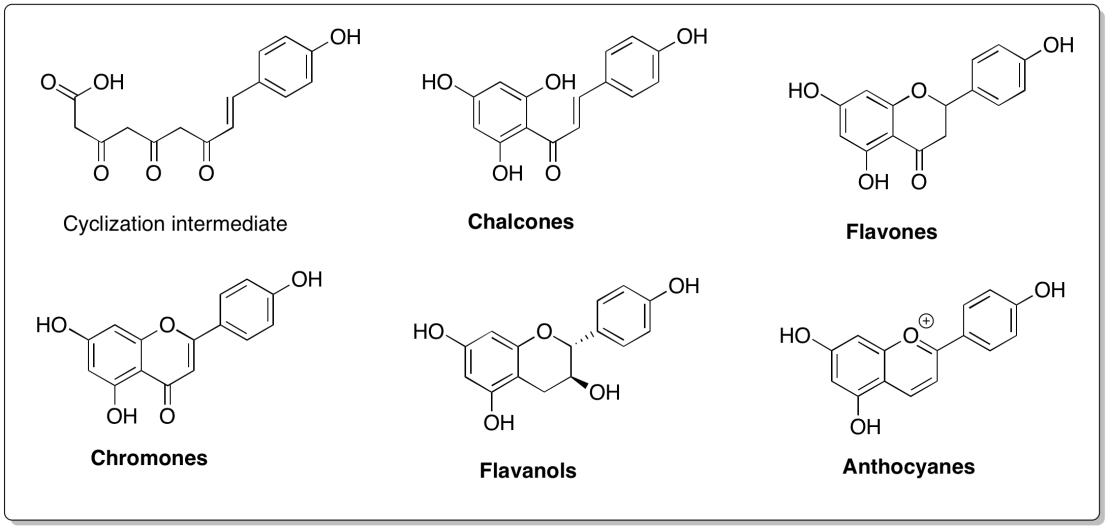

Figure 13: Different structural types of flavonoids.

Subsequent Claisen-like cyclization leads to first group of flavonoids – chalcones. Those can undergo Michael-like cyclization to provide flavones. By reduction of flavones, either antocyanes or flavanols (condensed tannins) can be achieved. On the other hand, chromones (flavonoids in the strict sense) are products of flavones oxidation. [59]

Stilbenoids, compounds of C6-C2-C6 pattern, are formed from the same cyclization intermediate as flavonoids by an aldol condensation. Further dehydration and decarboxylation leads to stilbenoid backbone found in resveratrol (Fig. 14). [59]

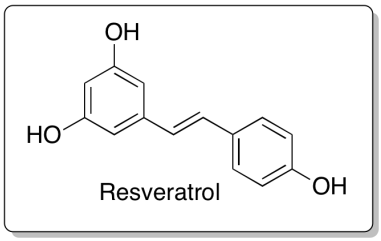

Figure 14: Stilbenoid derivative resveratrol

B.2.3.3 Pharmacokinetic properties: ADME

Considering the significant biological potential of polyphenols, their relatively low BAV and ability to penetrate to tissues may be their major drawback. Thus, their effect within the human body does not solely depend on the quantity present in nutrition or their intrinsic activity but also on the quantity absorbed after intake, their metabolization and the activity of their metabolites.

B.2.3.3.1 Absorption

Not unlike their chemical structure, the site and mode of absorption of polyphenols is not uniform. The absorption is also highly influenced by their glycosylation – in some cases, only the free aglycone is readily absorbed whereas in others glycosylation has been shown to facilitate the absorption. [60] Linkage to atypical sugar moieties may require specific microbial enzymes for cleavage so that kind of polyphenol must reach the colon before it can be absorbed in the aglycone form. [58] Several transporters such as Na^+-dependent saturable carrier [61] or sodium/glucose cotransporter 1 [60] may be involved in the absorption.

B.2.3.3.2 Distribution

In the bloodstream, the polyphenols and their metabolites are barely present in the free form. Their protein-binding rate varies with their structure but it is generally high, reaching from around 35% for benzoic acid derivatives up to 100% in flavonoids. [62] The antioxidant capacity may stay preserved in the albumin-bound form, the free form may be required to allow them to implement some specific effects. [63]

Due to the high albumin binding rate and also the hydrophilicity of the polyphenols, their partioning between aqueous and the lipid phase is highly in favor of the aqueous phase.

Their ability to bind to cellular membranes is realized via hydrogen bond formed between hydroxyl groups and the polar heads of phospholipids. This may explain the aptitude of polyphenols to preserve cell membranes integrity. [64]

Penetration of polyphenols to tissues is hard to determine because of the large number of possible metabolites. Moreover, the tissue metabolites may differ considerably from the circulating ones as a consequence of an intracellular metabolism. [63] Studies in humans are scarce but in mice, accumulation of polyphenols and their metabolites was observed mainly in blood and the tubular digestive tract and metabolic organs such as the liver. [65]

B.2.3.3.3 Metabolism and excretion

Polyphenols are highly metabolized according to their structure, in particular the number of hydroxyls. Conjugative phase of their metabolism is similar to other xenobiotics of their character and includes methylation, sulfation and glucuronidation.

Catechol-*O*-methyl transferase and family of enzymes uridine diphosphate-glucuronosyltransferases UGT1A are both located in the enterocytes, resulting the two reactions to happen shortly after absorption in the small intestine. [66] Mainly glucuronidation is responsible for the first-pass metabolism of polyphenols. [63] Efflux transporters such as P-glycoprotein are also involved in this process, secreting significant amount of glucuronidated conjugates back to the intestinal lumen and decreasing bioavailability. [67]

Polyphenols are excreted by both urinary and biliary pathways, according to the polyphenol structure. Generally, large, extensively conjugated molecules follow the biliary route more likely whereas smaller molecules such as monosulfates are more likely to be eliminated by urine. [63]

B.2.3.4 Biological activity

Natural polyphenols have pleiotropic biological effects. Among them, antioxidant and anti-carbonyl activity play a major role in the potential treatment of retinal diseases.

B.2.3.4.1 Antioxidant activity

Plant polyphenols, regardless their large variability of structure, are generally potent antioxidants. One of the mechanism involved in this activity is a direct scavenging of ROS. In this case, a good antioxidant should prevent or delay the radical-mediated oxidation or auto-oxidation of the substrate and should form a stable radical after the scavenging reaction. Stability of the formed phenoxyl radical and thus the polyphenol's

antioxidant capacity is highly dependent on its chemical structure. Generally, conjugation with double bonds stabilizes the radical through resonance; an example proved in experimental conditions is quercetin and (+)-catechin (Fig. 15). Quercetin, which has an identical number and positions of hydroxyl groups as (+)-catechin, showed better antioxidant capacity due to the 2,3-double bond in the C ring and the 4-oxo function. [68]

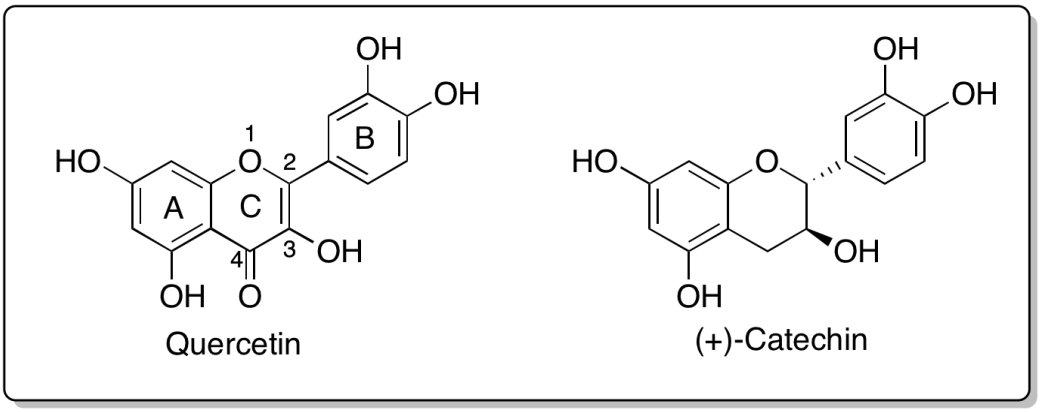

Figure 15: Structures of flavonoids quercetin and (+)-catechin.

The radical can also be stabilized by intramolecular hydrogen bonding or further oxidation reaction; as a result, there are many structure-activity relationship factors to be considered. Generally, flavonoids are probably the most powerful antioxidants among plant polyphenols, epicatechin gallate, epigallocatechin gallate and quercetin being the lead molecules according to some studies. [69] Moreover, their antioxidant capacity differs regarding the environment (aqueous or lipidic).

Consumption of polyphenols showed effectivity in the prevention of some diseases involving oxidative stress in their etiopathogenesis such as the Alzheimer's disease [70] or AMD. [71]

Some authors suppose that direct radical scavenging mechanism cannot explain the antioxidant effect of polyphenols *in vivo*, even though it is proved *in vitro*, arguing that polyphenols can never reach the intracellular concentration to effectively trap significant proportion of the ROS. They suggest that a different mechanism including enzyme induction is predominant in the living systems.

Nuclear factor erythroid 2-related factor 2 (Nrf2) is a transcription factor which binds to electrophile response element (EpRE), initiating natural antioxidant response (Scheme 12). This pathway thus plays a key role in reaction to various oxidative stimuli. [72]

In cytosol, Nrf2 binds to Kelch-like ECH-associated protein 1 (Keap1) which not simply prevents the translocation of Nrf2 to the nucleus but initiates its rapid degradation by the 26 S proteasome by assisting in Nrf2 ubiquitinylation. Keap1 can be deactivated by alkylation of its critical cysteine groups by electrophiles, prolonging the lifetime of Nrf2. Nrf2 can subsequently be phosphorylated, translocated to the nucleus and initiating the transcription of EpRE sequence. [73]

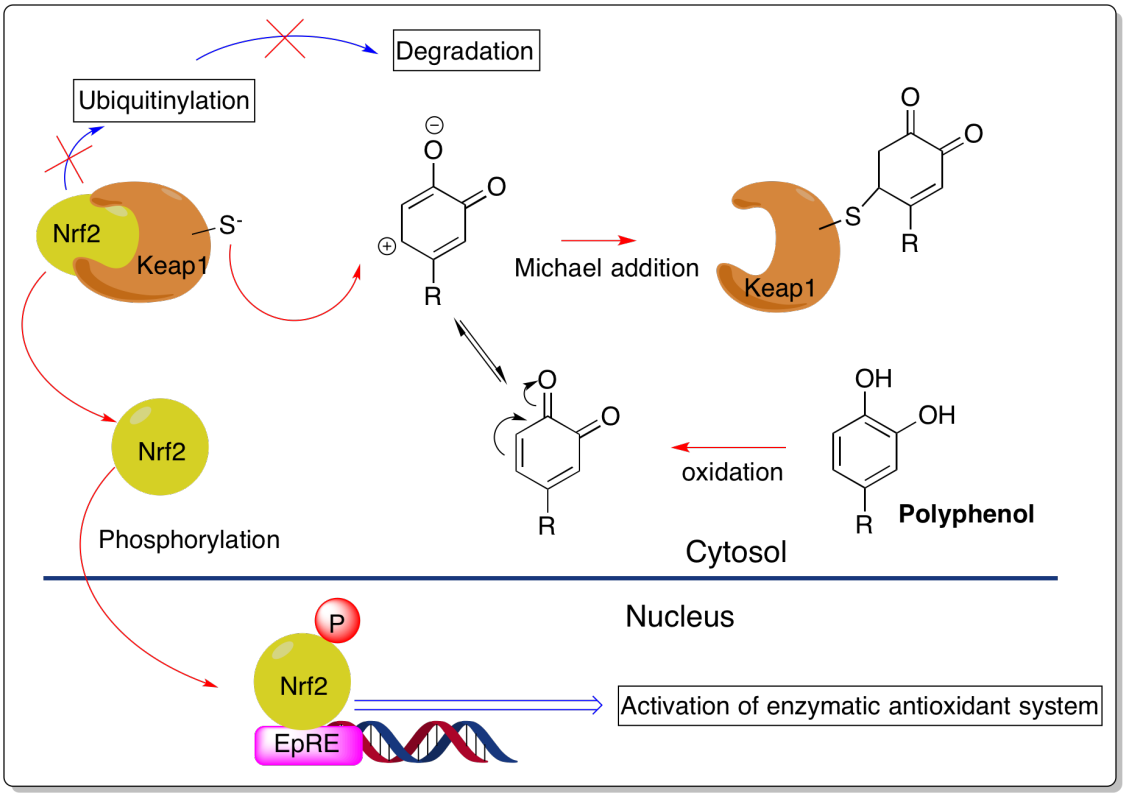

Scheme 12: Nrf-EpRE signaling pathway may be triggered by deactivation of Keap1 by oxidized polyphenols. (Forman et al., 2014)

It is suggested that quinone-like electrophiles may realize this alkylation. Those quinones may rise from the ROS scavenging process. The Nrf2-EpRE signaling pathway is triggered by small nontoxic concentrations of electrophiles which would explain the ability of polyphenols to act as antioxidants *in vivo*. [73]

B.2.3.4.2 Anti-carbonyl activity

Many polyphenols, in addition to their antioxidant potential, have shown the ability to trap and quench the RCS and hence reduce the carbonyl stress and the followed cellular and tissue damage. This capability to trap RCS was proven for tea flavonoid polyphenols *in vitro* by Chih-Yu Lo et al. (Scheme 13). [74] Recently, more structure-activity relationship studies were carried out by the same team for the trapping reactions of methylglyoxal by phenols and phenolic acids. Results obtained by both *in vitro* and *in silico* revealed the influence of relative negative charge on the aromatic carbons. [75] Those results are very valuable for the design of potentially promising molecules in medicinal chemistry screening.

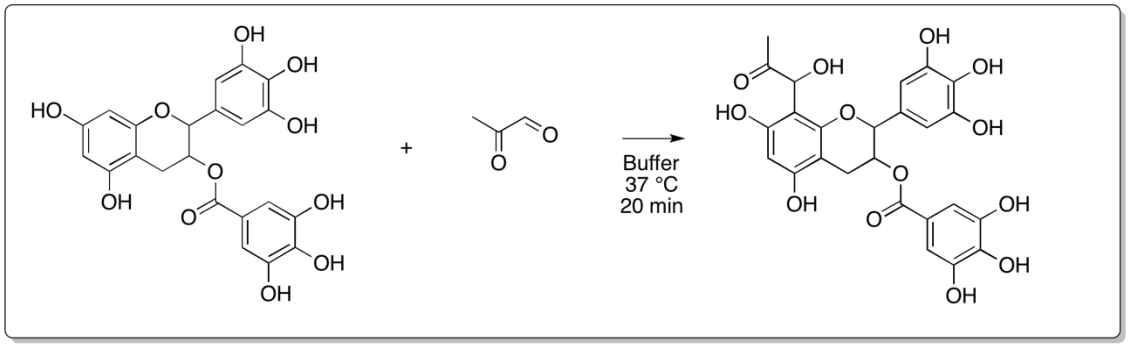

Scheme 13: In vitro trapping reaction of methylglyoxal by (–)-epigallocatechin gallate in simulated physiological conditions. (Lo et al., 2006)

In a recent study within our group, mechanism of trapping reactions of A*t*R by phloroglucinol was suggested. This study emphasized the importance of resorcinol pattern for a successful scavenging activity, suggesting a formation of chromene compound which structure was confirmed by NMR and mass spectrometry (Scheme 14). [1]

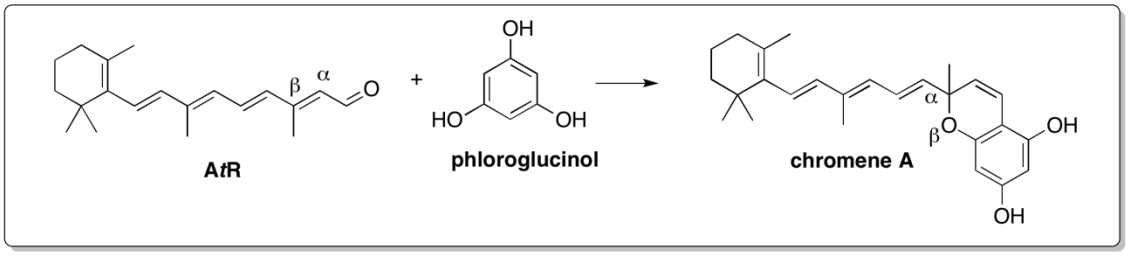

Scheme 14: Phloroglucinol traps AtR forming chromene A in flask experiments. (Crauste et al., 2014)

As polyphenols present capacity to reduce both oxidative and carbonyl stress, they have been investigated to reduce those toxic mechanisms involved in the biosynthesis and toxicity of A2E in retinal pathologies. Two following parts of the manuscript will present the synthesis of lipophenolic compounds designed to increases lipophilicity and bioavailability of active phenolic residue.

B.3 SYNTHESIS OF RESVERATROL-FA LIPOPHENOLS

B.3.1 Introduction and aim of work

Resveratrol is a polyphenol naturally present in grapes and it has, among other properties, very interesting antioxidant potential. [76-78] Being a vinyl analogue of phloroglucinol, resveratrol also has the resorcinol framework within its structure, which is necessary for trapping reactions of A*t*R.

Resveratrol-FA analogues will be synthesized and evaluated for their antioxidant and anti-carbonyl stress potency in ARPE-19 cell lines. Resveratrol-DHA and resveratrol-ALA had already been synthesized in the team [1]. The aim of my work was to synthesize two other lipophenolic conjugates (Fig. 16) to examine further the role of the PUFA part in the observed activity. Resveratrol-LA (**12**) would enable us to compare the effect of different PUFA moiety and resveratrol-DA (**13**; conjugate of resveratrol and saturated docosanoic acid, C22:0) could prove the benefit of unsaturation.

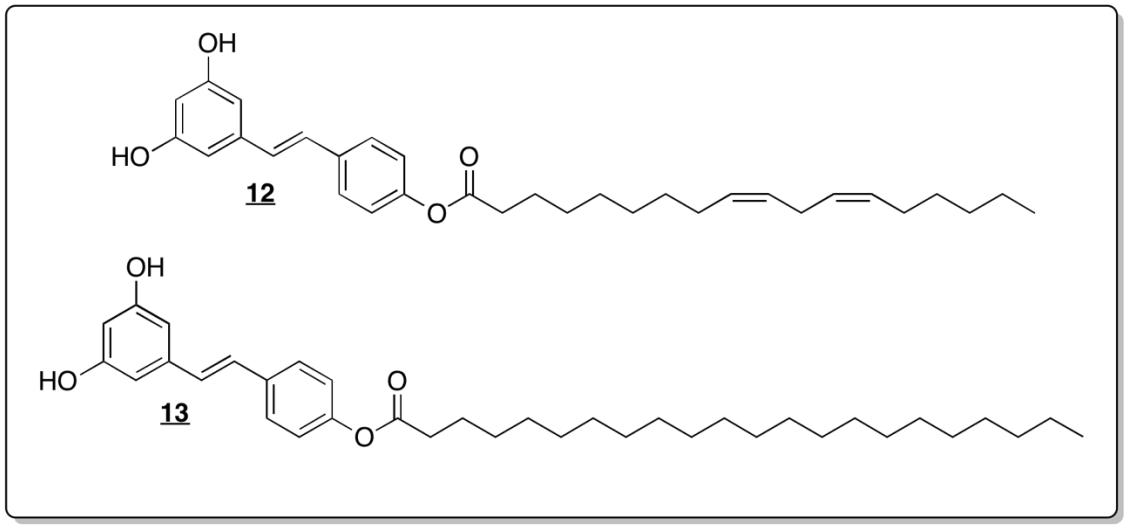

*Figure 16: Target lipophenolic molecules: resveratrol-LA (**12**) and resveratrol-DA (**13**).*

B.3.2 Results and discussion

An effective synthetic pathway starting from resveratrol to synthesize resveratrol-FA conjugates had been developed formerly by our group (Scheme 15). [1]

Both target molecules **12** and **13** can be obtained in two steps from intermediate **9** by linkage to a corresponding FA and deprotection. Compound **9** is approached by deprotection of 4′-O-acetyl group and protection of acetylated resveratrol **7** by triisopropylsilyl (TIPS) groups. Finally, intermediate **7** could be obtained via regioselective acetylation of resveratrol using lipase immobilized on acrylic resin (CALB).

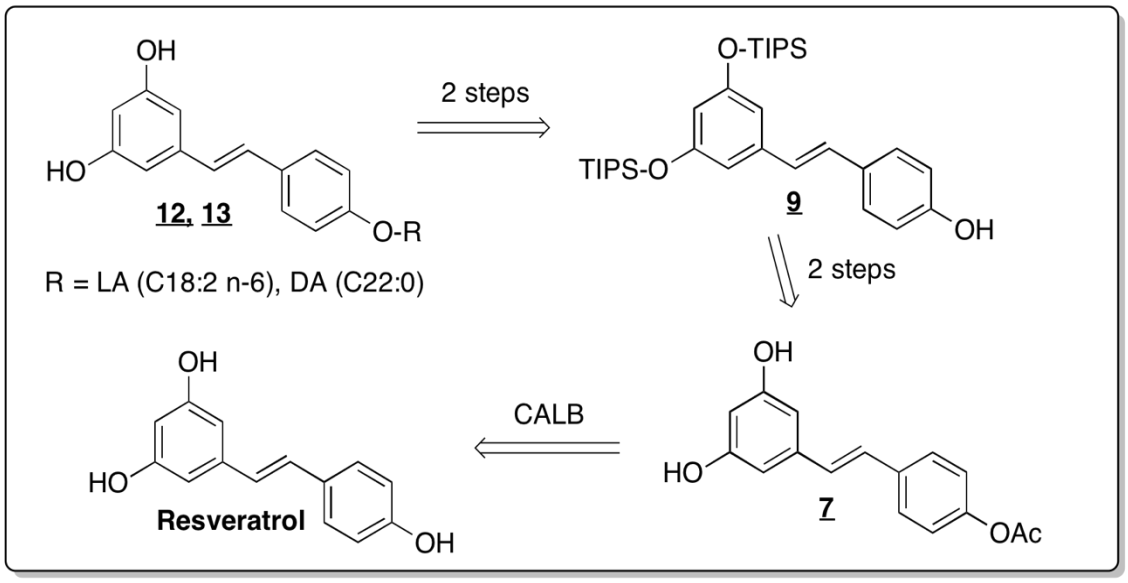

*Scheme 15: Synthetic strategy to access resveratrol-FA conjugates using a common intermediate **9**.*

This strategy was applied to synthesize two new conjugates in large scale (Scheme 16 and Scheme 17).

In the first step, CALB was used to introduce acetyl group region-selectively at the resveratrol C4′-OH position (Scheme 16). [79] One of the biggest advantages of this recyclable enzyme is the easy work-up of the reaction, performed by simple filtration of the resin and washing it with multiple solvents.

This reaction was carried out four times with different yields dependent mostly on the previous utilization of the enzyme (Tab. 2). Those experiments proved that using the recycled enzyme, regardless the conditions of the previous use, the yield of acetylation drops to about 50% compared to 85% in the first enzyme employment. Using the CALB enzyme immobilized on a different type of solid phase (Immobead) resulted in no product at all. A degradation (*cis*-isomerization of the acyclic double bond) of the starting

material was also observed when using Immobead, possibly due to slight overheating and excessive light exposure of the reaction during several days.

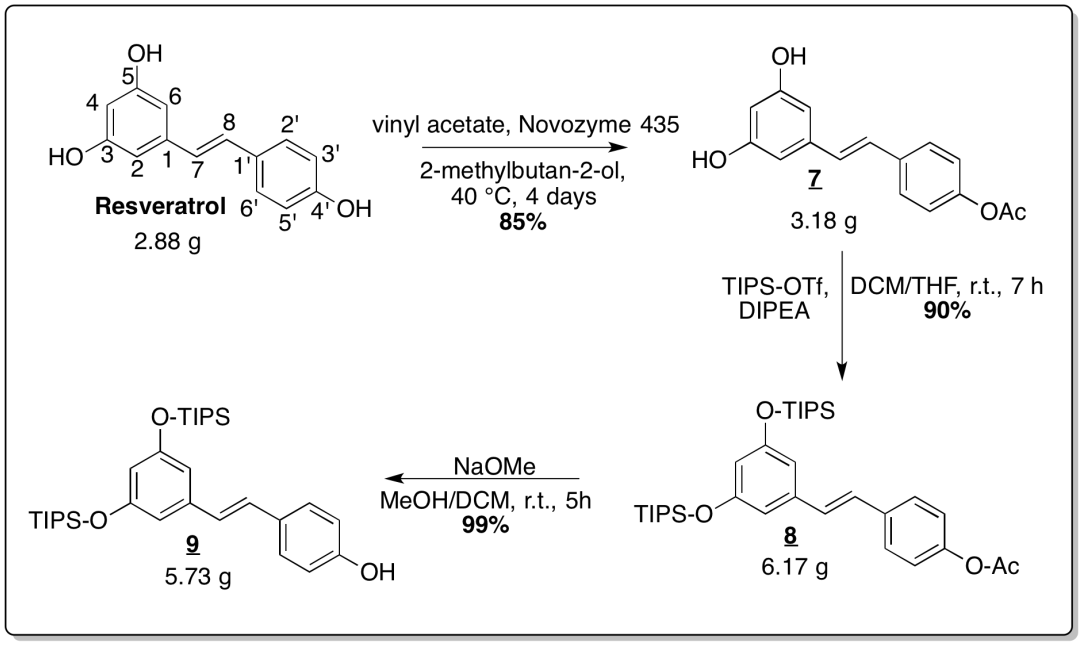

Scheme 16: Synthesis of resveratrol-FA conjugates until the common intermediate ***9***.

After acetylation at the 4´-O position, hydroxyl groups at 3 and 5 positions of compound **7** were protected by TIPS groups using TIPS-OTf and *N,N*-diisopropylethylamine (DIPEA) as a base. Reaction lasted 7 hours to obtain compound **8** in a very good yield. Based on the mass of the product obtained and its ^{1}H NMR, some excessive amount of TIPS-OH was present in the product; this impurity was purified two reaction steps later, when the desired molecule was more hydrophilic, hence corrected yields calculated from ^{1}H NMR are mentioned for the compounds **8** to **10**. The acetyl group of compound **8** was deprotected with MeONa in anhydrous methanol; this reaction was almost quantitative and resulted resveratrol-diTIPS (**9**) in an excellent yield of 99%.

Table 2: Influence of solid phase and previous utilization of enzyme on the enzymatic acetylation yields.

Entry	CALB solid phase, usage	Starting amount	Mass obtained	Yield
1	Acrylic resin, new	2.88 g	2.89 g	85%
2	Acrylic resin, used in 2-methylbutan-2-ol	2.88 g	1.61 g	47 %
3	Acrylic resin, used twice in THF	500 mg	280 mg	49%
4	Immobead, new	500 mg	No product + degradation	0%

This compound (**9**) served as a common intermediate to obtain protected conjugates **10** and **11** (Scheme 17). Both esterifications were initiated with 1.2 eq. of FA, 1.5 eq. of DCC and 0.5 eq. of DMAP. The reactions were carried out in dry dichloromethane (DCM) but a small amount of dry dimethylformamide (DMF) was added in case of compound **11** to dissolve the poorly soluble DA entirely. Due to the absence of double bond in DA molecule, its lower solubility and reactivity, additional DCC (1.5 eq.) and DMAP (0.5 eq.) were added after 4 hours. Eventually, the yield (76 %) was not significantly lower than in synthesis of compound **10** (82%) which was terminated after 3 hours without addition of more reagent equivalents.

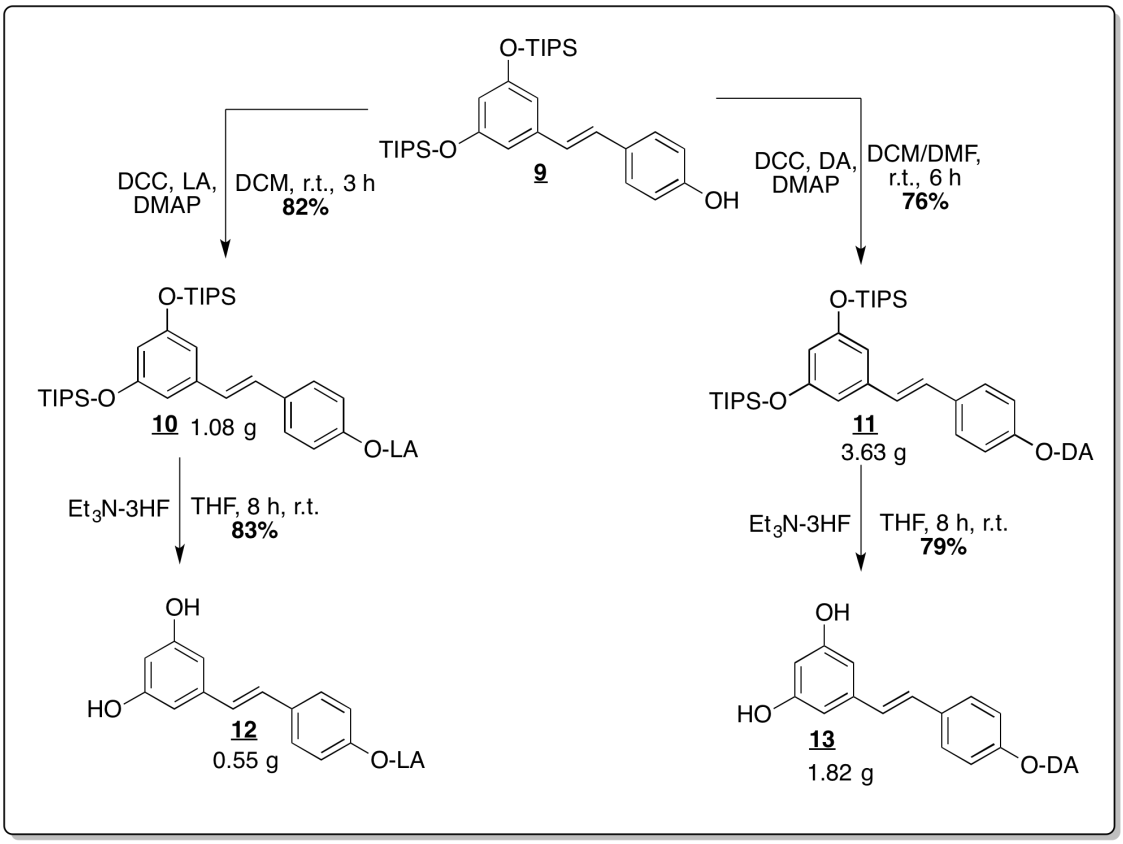

*Scheme 17: Synthesis of resveratrol-FA from the common intermediate **9**.*

Final deprotection of OH groups by Et_3N-3HF in dry tetrahydrofuran (THF) yielded compounds **12** (83%) and **13** (79%). A small proportion (up to 17%) of mono-deprotected compounds was also isolated in both cases.

B.3.3 Conclusion and perspectives

Previously developed synthetic pathway was successfully applied to synthesize resveratrol-LA and resveratrol-DA conjugates in 52% and 45% of overall yields, respectively, in five steps. More than 1 g of final products were obtained. The yields as well as obtained amounts exceeded those previously published for resveratrol-DHA [1] and they proved robustness of this strategy to synthesize various resveratrol-FA conjugates even in large amounts. Products will be used for biological experiments.

B.4 SYNTHESIS OF ALKYL-PHLOROGLUCINOL LIPOPHENOL

B.4.1 Introduction and aim of work

Phloroglucinol (benzene-1,3,5-triol) is a polyphenol present is some type of brown algae in a free form or in the form of phlorotannins; [80] it can be obtained from other natural polyphenols by alkali hydrolysis. [81]

Phloroglucinol occurs in two equilibrated tautomeric forms but many intermediate resonance structures were observed. Enolate form of phloroglucinol monoanion explains its interesting reactivity as a nucleophile which results in its anti-carbonyl activity (Scheme 18). [82]

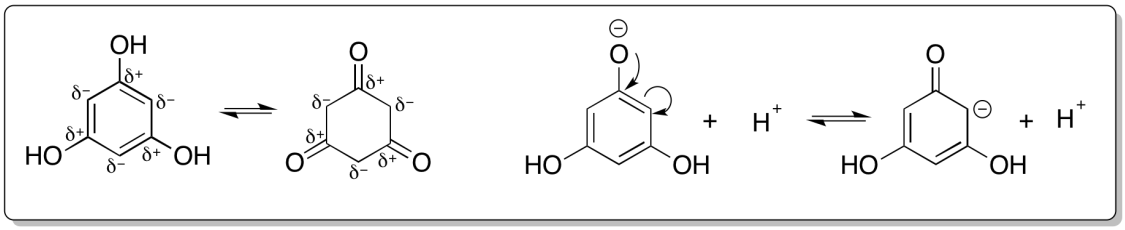

Scheme 18: Tautomeric forms of phloroglucinol and its mono-anion.

Thanks to the number of hydroxyl groups, phloroglucinol also has antioxidant activity. Previous structure-activity relationship studies in our group highlighted a lead molecule (Fig. 17) which showed a considerable anti-carbonyl activity in ARPE-19 cell lines.

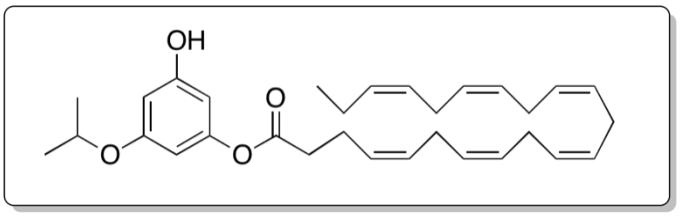

Figure 17: Lead molecule from previous studies

Unfortunately, the antioxidant properties of the lead molecule that could enhance the overall therapeutic effect in retinal diseases were rather poor. For this reason, to fight both types of stress involved in the pathophysiology of macular degeneration, a new molecule was designed (Fig. 18). In this lipophenolic conjugate, DHA is attached to the aromatic ring by a short linker to preserve two free aromatic hydroxyl functions and thus improve the antioxidant properties of the phloroglucinol moiety.

The aim of this part of my work was to synthesize this molecule.

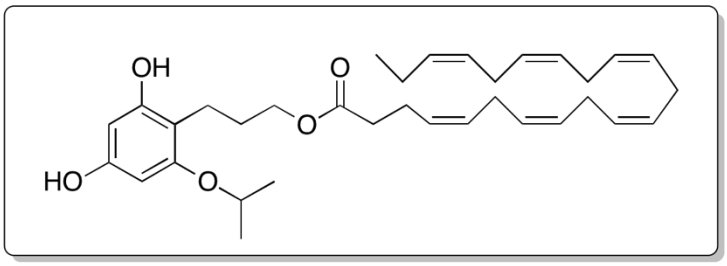

Figure 18: Target molecule – new phloroglucinol-DHA lipophenolic conjugate.

B.4.2 Results and discussion

B.4.2.1 Synthetic strategy A

First, a six-step synthetic pathway starting with phloroglucinol protected by methyl groups in all three phenolic positions (1,3,5-trimethoxybenzene) was designed (Scheme 19).

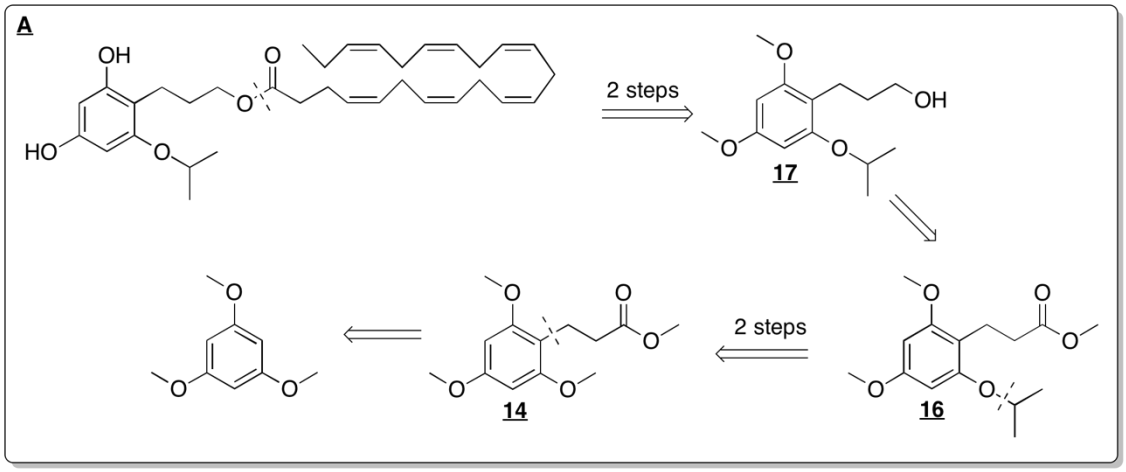

*Scheme 19: Synthetic strategy **A** – retrosynthetic analysis.*

Our target molecule is obtained from **17** by a coupling reaction with DHA and selective deprotection of the methyl groups. Compound **17** is approached via ester bond reduction from intermediate **16**, which is achieved by mono-deprotection and isopropylation of compound **14**. Finally, compound **14** is approached from commercially available 1,3,5-trimethoxybenzene.

This strategy was suggested after several ineffective attempts, previously performed in the team, to synthesize **16** in two steps from commercially available 3,5-dimethoxyphenol, in order to avoid the difficult mono-deprotection of one hydroxyl of trimethoxybenzene ester derivative (Scheme 20). Because of the asymmetry of the alkylated phloroglucinol, an inseparable mixture of two regioisomers was obtained after

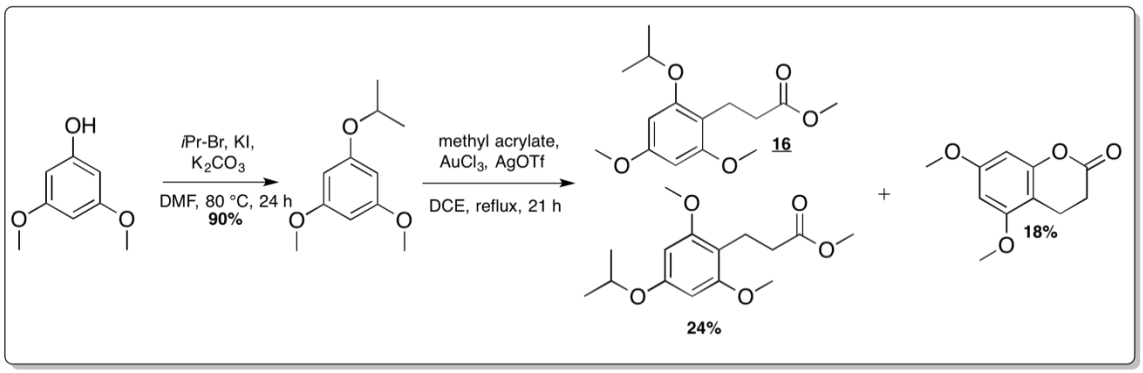

*Scheme 20: First, failed strategy to achieve **16**.*

gold-catalyzed addition of methyl acrylate. A significant amount of a third by-product (lactone) was also formed. This first strategy was thus abandoned.

In the first step of the new strategy, methyl acrylate was linked to the aromatic ring of 1,3,5-trimethoxybenzene in the presence of $AuCl_3$ and Ag-OTf as a co-catalyst (Scheme 21). [83, 84] This reaction was carried out in dichloroethane (DCE) to enable heating up to 84 °C and lasted three days. It provided stable yield of 64% of compound **14** when repeated twice.

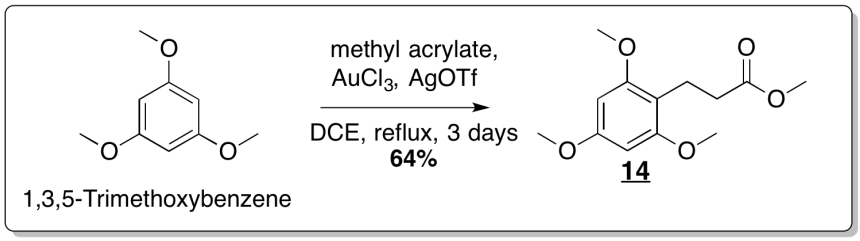

Scheme 21: $AuCl_3$-catalyzed addition of methyl acrylate to 1,3,5-trimethoxybenzene.

Subsequent mono-deprotection of methyl group by BCl_3 emerged as the major drawback of this synthetic strategy (Scheme 22). The reaction is not regioselective and both products **15a** and **15b** were formed in various rates, yielding **15a** in slightly higher yields then **15b** in most of the cases.

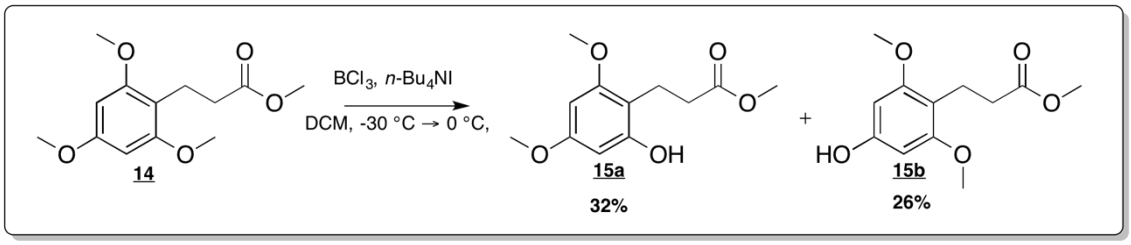

*Scheme 22: Deprotection of **14** by BCl_3/n-Bu_4NI.*

There was also a small quantity of di-deprotected product isolated from the reaction mixture.

Some preliminary attempts focused mainly on the number of equivalents (eq.) of BCl_3/*n*-Bu_4NI and the reaction temperature had been done previously in the laboratory and the starting conditions had thus been established. Several more attempts based on change of reaction time and the number of eq. of BCl_3/*n*-Bu_4NI were performed to optimize the conditions (Tab. 3). Conditions were optimized on 2 eq. of BCl_3/*n*-Bu_4NI and reaction time 1 h with the best yield of 32% of compound **15a** acquired. Products **15a** and **15b** were easily separable by column chromatography.

*Table 3: Optimization of deprotection of **14**.*

Entry	Starting amount	Eq. of BCl_3/*n*-Bu_4NI, time	Mass obtained (15a/15b)	Yield of (15/15b)
1	100 mg	2eq., 3h	23 mg/17 mg	25%/19%
2	100 mg	2eq., 1h	28 mg/16 mg	30%/18%
3	500 mg	2 eq., 1h	151 mg/123 mg	32%/26%
4	1000 mg	2 eq., 1h	235 mg/234 mg	25%/25%

Another deprotecting agent BBr_3 (stronger Lewis acid) was also tested to investigate if better results can be achieved (Scheme 23). [85] This reagent is available in the form of 1M solution in DCM, as well as BCl_3, which enables a drop-by-drop addition via syringe; manipulation with BBr_3 is therefore analogous to BCl_3. One preliminary reaction was performed on the compound **14** when 2×0.5 eq. of BBr_3 were added at -78 °C and -50 °C, respectively, and no product was observed on the TLC. Subsequently, 2 more eq. were added and the reaction was slowly brought to room temperature. Even though the reaction was shortly terminated (1 h after the last BBr_3 addition), the product **15a** was not isolated.

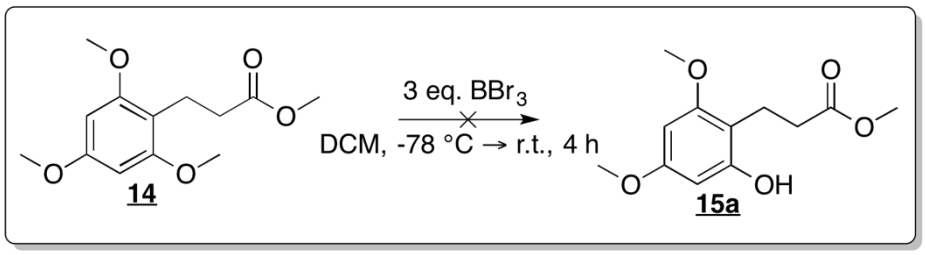

*Scheme 23: Deprotection of **14** by BBr_3.*

Instead of mono-deprotected product **15a**, a mixture of di-deprotected and fully deprotected compound was obtained. Possible explanation is the formation of a complex of BBr_3 with the ester bond which would consume the initial 1 eq. of BBr_3, further addition of 2 eq. would thus result in fast deprotection of all hydroxyl groups. Deprotection may also have continued after quenching of the reaction with water and during evaporation. To optimize the deprotection reaction, following reaction was carried out on a test compound, 1,3,5-trimethoxybenzene, in order to set up basic starting conditions (Scheme 24). BBr_3 (0.5 eq.) was added at -50 °C, reaction was stirred 3.5 h at 0 °C for 4 h. Then the reaction was brought to r.t. and quenched by water.

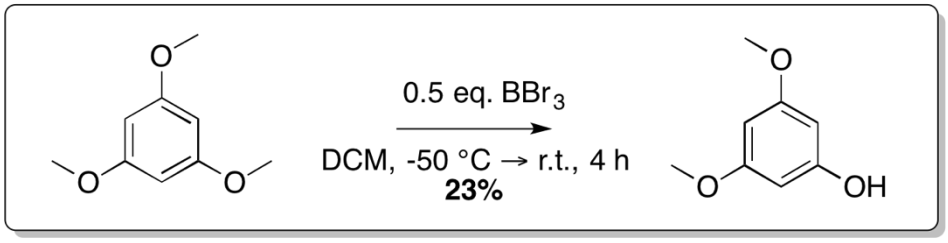

Scheme 24: BBr_3 deprotection reaction.

Under these conditions, 23% yield of mono-deprotected product was obtained. This yield was not acceptable considering the fact that it would represent a mixture of the two regioisomers in case of **15a** and **15b**. This deprotection conditions using BBr_3 seemed to be less efficient than BCl_3/*n*-Bu_4NI.

Amount of product **15a** was sufficient to proceed to the next reaction step, the isopropylation of aromatic hydroxyl by 2-iodopropane generated in situ from 2-bromopropane and KI in the presence of K_2CO_3 as a base (Scheme 20). Unfortunately, only 37% yield of compound **16** was obtained.

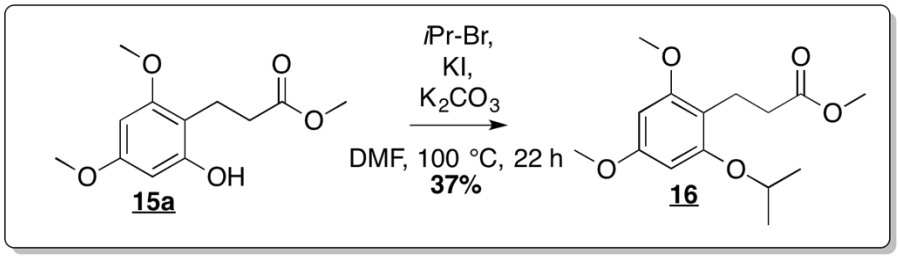

*Scheme 25: Isopropylation of **15**.*

In spite of the significant quantity (around 30%) of the starting material isolated during purification, formation of a C-alkylated side product (5%) was observed. Two more attempts using this strategy were done on the symmetric isomer compound **15b** changing the number of reagents equivalents and the course of addition and also the reaction time and temperature (Tab. 4) but the yield was not improved. The reactivity of the desired product towards C-alkylation appeared to be higher than the one of the starting material, so the reaction had to be stopped before the conversion of the starting material **15a/15b** was significant.

Table 4: Isopropylation reactions.

Entry	Starting mat.	Starting amount	Eq. of iP-Br, KI, K_2CO_3	Reaction time and temperature	Mass obtained	Yield
1	**15a**	109 mg	5 eq., added at once	15 h at 80 °C, 7 h at 100 °C	47 mg	37%
2	**15b**	100 mg	1.5 eq., added at once	6 h at 100 °C	32 mg	27%
3	**15b**	100 mg	5 eq., added gradually	40 h at 100 °C	44 mg	37%

Different isopropylation reaction using propan-2-ol saturated with gaseous HCl (*i*PrOH/HCl) was suggested, accepting the risk of highly probable trans-esterification which would not necessarily compromise the following reaction steps, and one reaction was performed on the test compound **15b** (Scheme 26).

However, the desired *O*-alkylation did not occur at all in this case despite the 5 equivalents of reagent and significant reaction time (22 h) and we only identified the trans-esterified product in ^{1}H NMR of crude product.

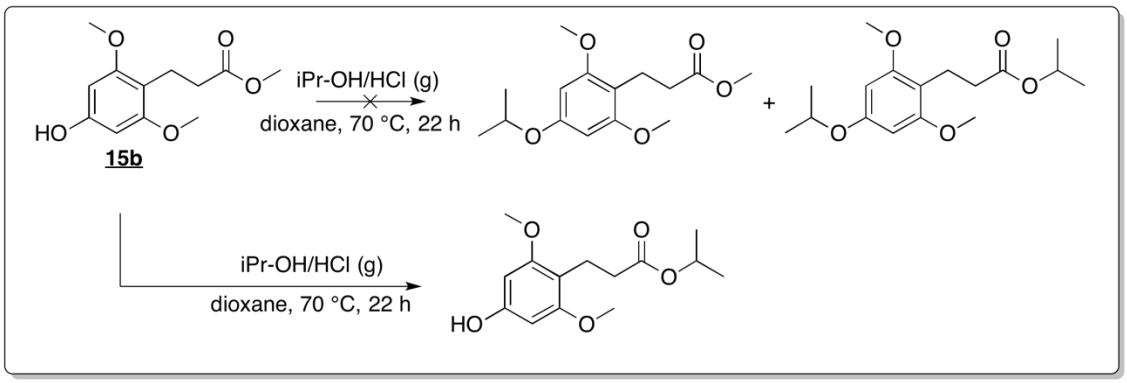

*Scheme 26: Isopropylation of **15b** with iPr-OH/HCl (g)*

Despite a low quantity of our product, compound **16** was brought to the following step, reduction of ester by $LiAlH_4$ (Scheme 27), which resulted in the corresponding alcohol **17** in almost quantitative yield and good purity to be introduced to the next reaction step without purification.

Because of the instability and high price of DHA, selective methyl deprotection was tested before linking the DHA to intermediate **17** (Scheme 27). Unfortunately, after an attempt of deprotection of 42 mg of compound **17** by mild BCl_3/(n-Bu)$_4$NI, an

undefinable mixture of compounds with various degree and site of deprotection was isolated from the reaction. This type of deprotection represented a significant obstacle throughout all the work and requires definitely further attention and optimization. Despite above mentioned facts, secondary alkoxy (isopropyloxy) bond was clearly not cleaved using $BCl_3/(n\text{-}Bu)_4NI$ which is in accordance with the literature. [26]

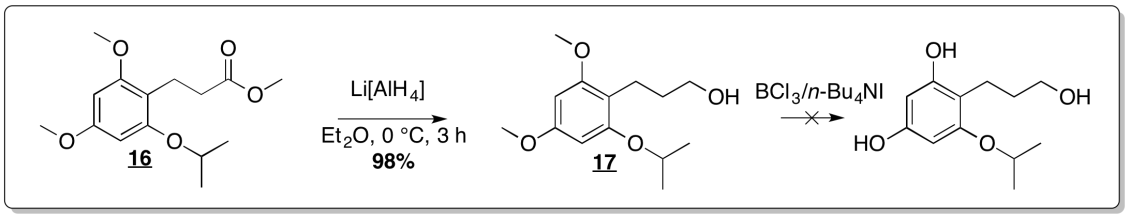

*Scheme 27: Synthesis of **17** by reduction of ester bond with a complex hydride $Li[AlH_4]$ and unsuccessful deprotection.*

*B.4.2.2 Synthetic strategy **B***

Seeing that there are many considerable drawbacks in the first strategy, an alternative pathway to obtain the desired product was suggested (Scheme 28).

In this second strategy, DHA is linked to side chain hydroxyl group. This alcohol is achieved in two steps from intermediate **20** by hydrogenation of double bond and reduction of ester. The α,β-unsaturated ester **20** is approached by a Wittig reaction between aromatic aldehyde **19** and methyl(triphenylphosphoranylidene) acetate.

Finally, aldehyde **19** is gained by aromatic formylation and isopropylation using phloroglucinol as a commercial starting compound.

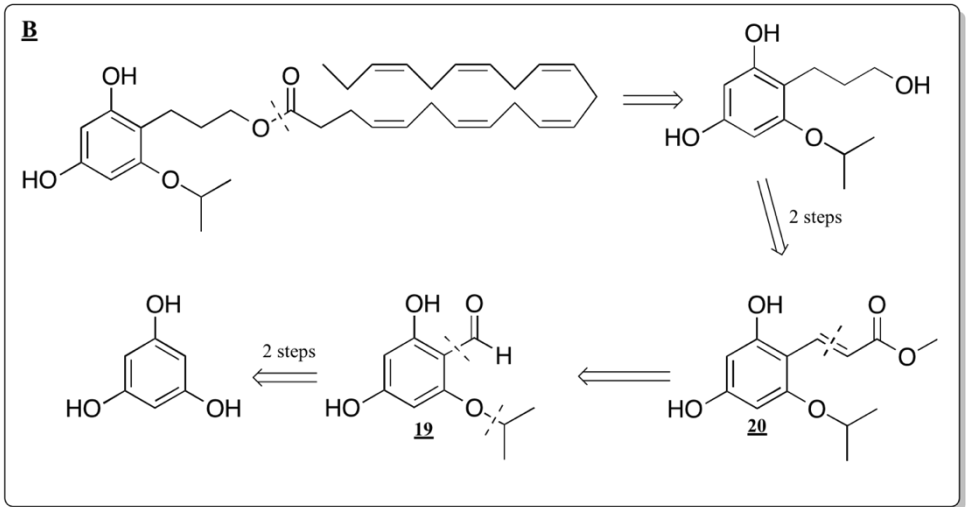

*Scheme 28: Synthetic strategy **B**.*

First, phloroglucinol was reacted with with *i*Pr-OH/HCl (Scheme 29). Only traces of product **18** were observed after first two additions of *i*Pr-OH/HCl, possibly because of the lower quality of the reagent, which was prepared several months ago. After

evaporation of the reaction mixture, fresh *i*Pr-OH/HCl was prepared and the reaction was re-launched using this new reagent achieving **18** in an acceptable yield of 28%.

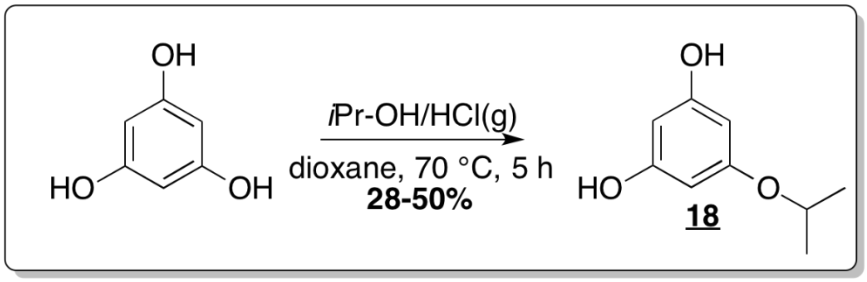

Scheme 29: Isopropylation of phloroglucinol.

This isopropylation had been previously done in our laboratory; it is scalable up to 10 g of starting material and yields up to 50% had been achieved.

The compound **18** was then formylated using triethyl orthoformate in the presence of boron trifluoride diethyl etherate (Scheme 30). Chiba et al. [86] applied these conditions on diisopropylated phloroglucinol, reported good yield and isolated only one regioisomer. One reaction was thus executed with 1.5 eq. of triethyl orthoformate and 3 mL of boron trifluoride diethyl etherate per 100 mg of **18**. Unfortunately, after purification on column, 49% of product was isolated representing a mixture of position isomer aldehydes **19a** and **19b** in proportion 6:4.

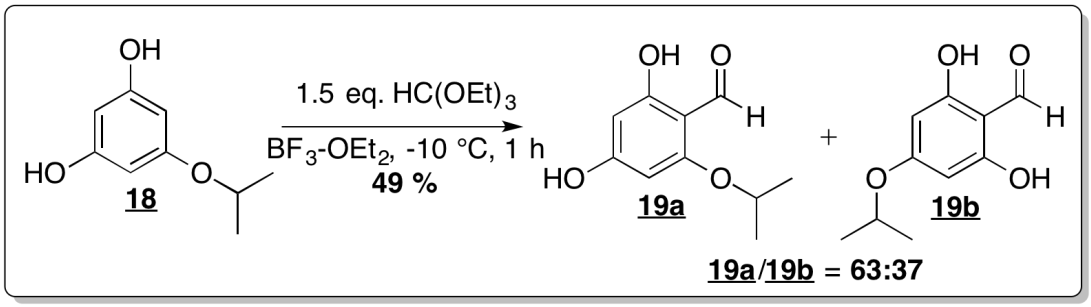

*Scheme 30: Formylation of **18** by triethyl orthoformate.*

Also, different conditions of formylation were suggested. [87] In this new reaction (Scheme 31), $Zn(CN)_2$ was reacted with compound **18** in the presence of HCl (g) and catalytic amount of Lewis acid $ZnCl_2$. Resulted imine was hydrolyzed and then purified on silica gel column to achieve crude product in a yield of 63% and a 8:2 ratio of **19a** and **19b**, separable by recrystallization from toluene (29% of **19a**).

This step was repeated in a larger scale (600 mg of **18** compared to 200 mg in the first attempt). The crude yield as well as the ratio of two aldehydes in the crude product and,

subsequently, the yield of **19a** were less favorable. However, these conditions of formylation might reach considerably better results once the purification is optimized.

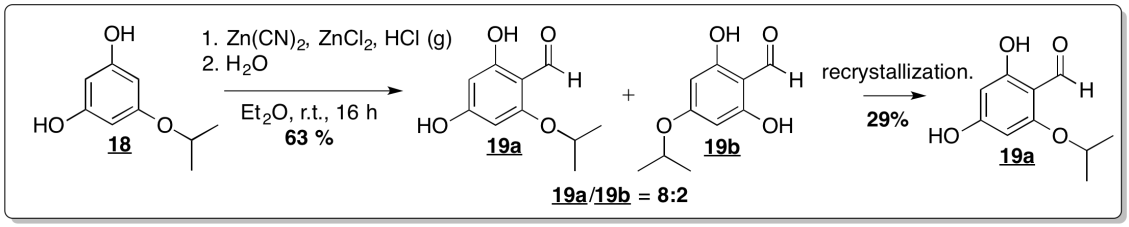

*Scheme 31: Formylation of **18** using $Zn(CN)_2$ (Gattermann reaction).*

A Wittig reaction between **19** and 1.5 eq. of methyl (triphenylphosphoranylidene)acetate [88] (Scheme 32) was first tried on the mixture of **19a** and **19b** obtained in the previous formylation reaction, assuming that the products could be more easily separated. After stirring at r.t., no starting material was observed after 50 min but only symmetric product **20b** was isolated (18%).

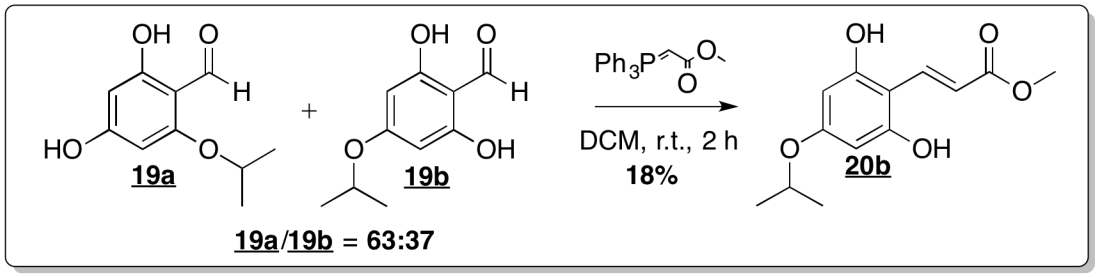

*Scheme 32: First attempt of Wittig reaction starting from a mixture of **19a/19b**.*

Second attempt was carried out on the aldehyde **19a** (containing less than 7% of isomer **19b**; Scheme 33). This time, reaction was stirred overnight to achieve acceptable yield of 51% of **20b** after two purifications. Even though the reactivity of the isomer **19b** appeared to be higher, compounds **20a** and **20b** were quite easily separable on column similarly to products **15a** and **15b**. To increase the overall yield of this strategy, it may thus be possible to perform the Wittig reaction directly on the mixture of **19a/19b,** that would enable us to avoid the recrystallization step of **19a** that led to a product loss. Reaction was not further optimized due to my limited time in the laboratory.

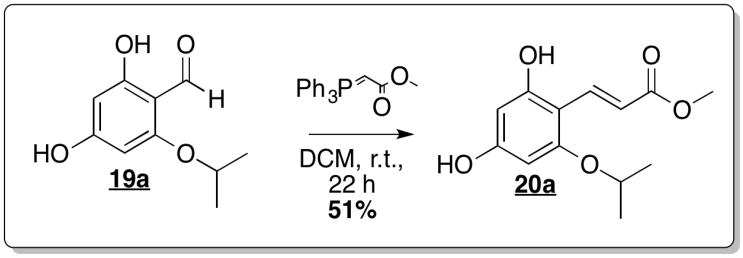

*Scheme 33: Second attempt of Wittig reaction starting from aldehyde **19a**.*

B.4.3 Conclusions and perspectives

Two different strategies to achieve new phloroglucinol-DHA based lipophenolic conjugate were suggested and tested in this part of work.

In the strategy **A**, both methyl mono-deprotection and isopropylation steps present major downsides. In spite of all the efforts of their optimization, overall yield drops to 8% after only three reaction steps which is unacceptable, given the fact that one more methyl deprotection would be needed. Even though some more reaction of the deprotection with BBr_3 could be done, this strategy was eventually abandoned.

The pathway **B** bypasses the deprotection steps which is its main advantage. The reactions are generally uncomplicated to perform and do not result in many by-productss in significant amounts. Even though the overall yield achieved so far in the first three steps is not outstanding, it is necessary to keep on mind that these are only the initial results, especially in the third step (synthesis of **20a**). Overall, this pathway promises to give better results after some more optimization.

EXPERIMENTAL PART

In this part, the experimental procedures are described for all the compounds synthesized as well as their analysis by TLC, NMR and UPLC.

General methods

To perform reactions, solvents such as DCM and THF were dried using PuriFlash system. In small quantities (15 mL and less), dry solvents on molecular sieve (Sigma-Aldrich) were used. Technical quality solvents (≥98%, Sigma-Aldrich or Merck) were used in case of dioxane, 2-methylbutan-2-ol, isopropanol, DCE. For column chromatography, technical quality solvents (≥98%, Sigma-Aldrich or Merck) were used in all cases.

The TLCs were carried out on silica gel TLC plates F_{254} (Merck).

Four different TLC visualizing agents were used: UV light (λ = 254 nm), anisaldehyde (solution of 1 mL of *p*-anisaldehyde and 1 mL of 97% sulphuric acid in 100 mL of glacial acetic acid, stored in freezer), $KMnO_4$ (solution of 3 g of $KMnO_4$ and 10 g of K_2CO_3 in 300 mL of H_2O) and phosphomolybdic acid (PMA; 10 g of PMA in 100 mL of EtOH).

NMR spectra were measured at room temperature on a 500 MHz Bruker instrument. Chemical shifts are given as ppm, taking the signal of tetramethylsilane (0 ppm) as internal reference.

All UPLC analyses were performed on Thermo Fisher Scientific™ device (Accela™ autosampler, Accela 1250 pump, Accela photodiode array detector) combined with Thermo Fisher Scientific LCQ™ Deca XP Max mass spectrometer with an EASY-Spray™ ion source. Waters Acquity UPLC® Ethylene Bridged Hybrid C18 Column 1.7 μm (2.1 mm×50 mm) was used for all analyses.

All the silica gel column chromatography were performed using SDS 60 AC 35-70 μm silica gel.

Purifications of compounds **4**, **5** and **6** by preparative HPLC were carried out on a Shimadzu instrument, using column Atlantis Prep OBD™ 10 μm (19×250 mm).

Synthesis of hydroxytyrosol-FA conjugates

(9*Z*)-3,4-dimethoxyphenethyl octadec-9-enoate (1)

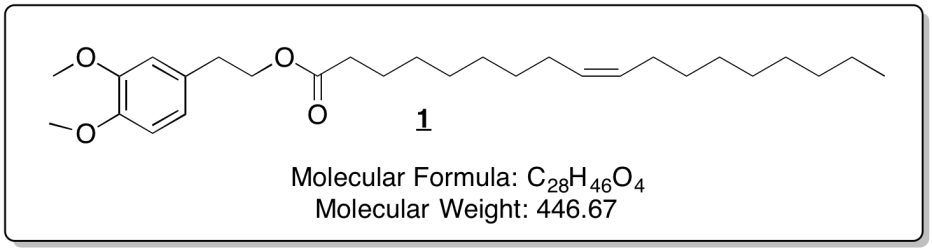

1

Molecular Formula: $C_{28}H_{46}O_4$
Molecular Weight: 446.67

Oleic acid (OA; 853 mg, 3.02 mmol) and commercially available 2-(3,4-dimethoxyphenyl)ethanol (500 mg, 2.75 mmol) were dissolved in dry DCM (40 mL) under argon. DCC (623 mg, 3.02 mmol) and DMAP (33 mg, 0.28 mmol) were added; white precipitate was observed immediately. The reaction was stirred at r.t. and monitored by TLC (pentane/EtOAc 8:2, visualized by UV 254 nm and anisaldehyde). After 3 h, further DCC (316 mg, 1.51 mmol) and DMAP (17 mg, 0.14 mmol) were added to drive the reaction to completion. Reaction was terminated after 6 hours of reaction time.

The reaction was cooled down to 4 °C to increase the amount of white *N*,*N*′-dicyclohexylurea (DCU) precipitate, which was then removed by filtration on frit, using only small amount of cold DCM to rinse the precipitate. The filtrate was extracted with H_2O (2×25 mL) and brine (25 mL); organic layers were combined, dried over $MgSO_4$, filtered and evaporated to obtain crude material (2.00 g).

Crude product was purified on silica gel column using 200 mL of silica and pentane/EtOAc (95:5 to 93:7) to obtain 1.20 g (98%) of compound **1** (colorless oil).

R_f (pentane/EtOAc 8:2) 0.7.

^{1}H NMR (500 MHz, $CDCl_3$) δ 6.80 (d, J = 8.1 Hz, 1H, CH Ar), 6.76 (dd, J = 8.0, 2.0 Hz, 1H, CH Ar), 6.74 (d, J = 1.9 Hz, 1H, CH Ar), 5.38 – 5.30 (m, 2H, CH=CH), 4.26 (t, J = 7.2 Hz, 2H, CH_2-O), 3.87 (s, 3H, CH_3-OAr), 3.86 (s, 3H, CH_3-OAr), 2.88 (t, J = 7.2 Hz, 2H, CH_2-CH_2-O), 2.28 (t, J = 7.6 Hz, 2H, CH_2-C=O), 2.00 (q, J = 6.8 Hz, 4H, CH_2 allylic), 1.29 (m, 22H, CH_2 alkyl), 0.87 (t, J = 7.1 Hz, 3H, CH_3).

^{13}C NMR (126 MHz, $CDCl_3$) δ 173.9, 148.9, 147.8, 130.1, 129.8, 120.9, 112.2, 111.3, 65.0, 56.0, 55.9, 34.9, 34.5, 32.0, 29.9, 29.8, 29.7, 29.4, 29.3, 29.2, 29.2, 27.3, 27.3, 25.1, 22.8, 14.3.

(9*Z*,12*Z*)-3,4-dimethoxyphenethyl octadeca-9,12-dienoate (2)

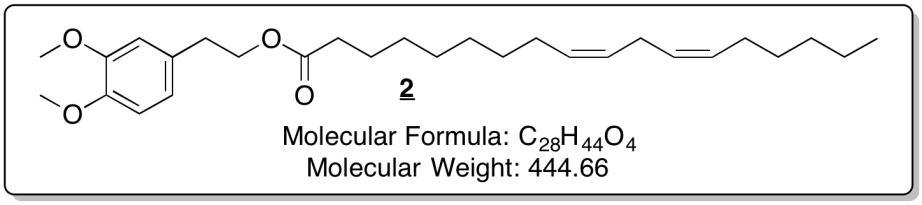

Dimethylated hydroxytyrosol (500 mg, 2.75 mmol) and LA (847 mg, 3.02 mmol) were dissolved in dry DCM (40 mL) under argon atmosphere. DCC (623 mg, 3.02 mmol) and DMAP (33 mL, 0.28 mmol) were added to the solution and the argon atmosphere was restored. Immediately, formation of turbidity and later white DCU precipitate was observed; reaction was further monitored by TLC (hexane/EtOAc 9:1, visualized by UV 254 nm and $KMnO_4$) and was allowed to stir overnight at room temperature.

After 18 hours, the reaction maintained at 4°C for 0.5 h to maximize the amount of precipitate, which was then removed by filtration on frit under reduced pressure and the filter residue was rinsed with a minimum of cold DCM. Filtrate was washed with water (2×40 mL) and brine (40 mL) to remove the protonated DMAP; aqueous phases were combined and extracted with excessive amount of DCM. Combined organic layers were dried with $MgSO_4$ and evaporated to yield 1.80 g of crude product.

Purification by column chromatography using 183 mL of SiO_2 and pentane/EtOAc (98:2 to 9:1) lead to 984 mg (80.1%) of compound **2** (colorless oil).

R_f (pentane/EtOAc 8:2) 0.74.

^{1}H NMR (500 MHz, $CDCl_3$) δ 6.80 (d, J = 8.1 Hz, 1H, CH Ar), 6.75 (dd, J = 8.1, 1.9 Hz, 1H, CH Ar), 6.73 (d, J = 1.8 Hz, 1H, CH Ar), 5.41 – 5.29 (m, 4H, CH=CH), 4.25 (t, J = 7.2 Hz, 2H, CH_2-O), 3.87 (s, 3H, CH_3-OAr), 3.86 (s, 3H, CH_3-OAr), 2.87 (t, J = 7.1 Hz, 2H, *CH_2*-CH_2-O), 2.76 (t, J = 6.6 Hz, 2H, CH_2 bis-allylic), 2.28 (t, J = 7.6 Hz, 2H, CH_2-C=O), 2.04 (q, J = 6.8 Hz, 4H, CH_2 allylic), 1.59 (quin, J = 8.0 Hz, 2H, *CH_2*-CH_2-C=O), 1.38 – 1.25 (m, 16 H, CH_2 alkyl), 0.88 (t, J = 6.9 Hz, 3H, CH_3).

^{13}C NMR (126 MHz, $CDCl_3$) δ 173.9, 148.9, 147.8, 130.3, 130.2, 128.2, 128.0, 120.9, 112.2, 111.3, 65.0, 56.0, 55.9, 34.9, 34.5, 31.7, 29.7, 29.5, 29.3, 29.2, 27.3, 27.3, 25.7, 25.1, 22.7, 14.2.

(9*Z*,12*Z*,15*Z*)-3,4-dimethoxyphenethyl octadeca-9,12,15-trienoate (3)

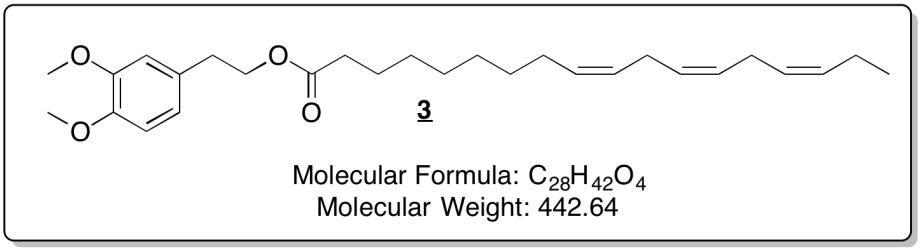

200 mg (1.10 mmol) of 2-(3,4-dimethoxyphenyl)ethanol and 336 mg (1.21 mmol) of α-linolenic acid (ALA) were dissolved in dry DCM (16 mL). DCC (249 mg, 1.21 mmol) and DMAP (13 mg, 0.11 mmol) were added and the reaction was allowed to stir in r.t. under argon while monitored by TLC (pentane/EtOAC 8:2, revealed by UV 254 nm and anisaldehyde). In reaction time 3.5 h, additional equivalents of DCC (168 mg, 0.60 mmol) and DMAP (7 mg, 0.06 mmol) were added to increase the conversion of the substrate. Reaction was terminated after 6 hours of stirring.

Reaction cooled down to 4 °C and kept at this temperature for 30 min to increase the amount of white DCU precipitate, which was filtered out on frit. Filtrate was diluted with additional 16 mL of DCM and extracted with H_2O (2×16 mL) and brine (16 mL). Subsequent collection of organic phases, drying them over $MgSO_4$, filtration and evaporation lead to 0.90 g of crude product.

Purification on silica gel column (80 mL of silica, pentane/EtOAc 93:7) yielded in 456 mg (94%) of compound **3** (colorless oil).

R_f (pentane/EtOAc 8:2) 0.7

^{1}H NMR (500 MHz, $CDCl_3$) δ 6.80 (d, J = 8.1 Hz, 1H, CH Ar), 6.76 (dd, J = 8.0, 2.0 Hz, 1H, CH Ar), 6.74 (d, J = 1.9 Hz, 1H, CH Ar), 5.42 – 5.28 (m, 6 H, CH=CH), 4.26 (t, J = 7.2 Hz, 2H, CH_2-O), 3.87 (s, 3H, CH_3-OAr), 3.86 (s, 3H, CH_3-OAr), 2.88 (t, J = 7.2 Hz, 2H, *CH_2*-CH_2-O), 2.83 – 2.78 (m, 4H, CH_2 bis-allylic), 2.28 (t, J = 7.2 Hz, 2H, CH_2-C=O), 2.11 – 2.02 (m, 4H, CH_2 allylic), 1.60 (quin, J = 7.2, 6.8 Hz, 2H, *CH_2*-CH_2-C=O), 1.38 – 1.24 (m, 8H, CH_2 alkyl), 0.97 (t, J = 7.5 Hz, 3H, CH_3).

^{13}C NMR (126 MHz, $CDCl_3$) δ 173.9, 149.0, 147.8, 132.1, 130.5, 130.4, 128.4, 128.4, 127.9, 127.2, 121.0, 112.2, 111.3, 65.0, 56.0, 55.9, 34.9, 34.5, 29.7, 29.3, 29.2, 27.3, 25.7, 25.1, 20.7, 14.4.

(9*Z*)-3,4-dihydroxyphenethyl octadec-9-enoate (4)

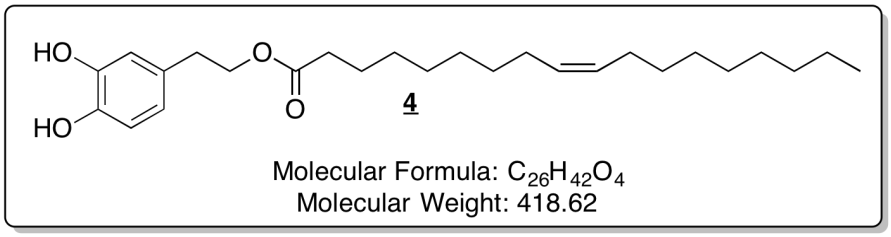

500 mg (1.12 mmol) of **1** were dissolved in dry DCM (9.3 mL) and 3.25 g (3.36 mmol) of *n*-Bu_4NI were added. The solution was cooled down to -78 °C with acetone/liquid nitrogen bath and BCl_3 (3.36 mL of 1M solution in DCM, 3.36 mmol) was carefully added drop by drop, via syringe. Temperature was then slowly brought to 0 °C and the reaction was stirred under argon for further 1 h, monitored by TLC (pentane/EtOAc 8:2, detection $KMnO_4$).

Reaction was quenched by an addition of 18 mL of iced water. The DCM was evaporated under reduced pressure and Et_2O (40 mL) was added to result a precipitate on the interphase which was eliminated by filtration on frit. Filtrate was diluted with additional 18 mL of water and extracted with Et_2O (3×80 mL). Organic phases were collected, dried over $MgSO_4$, filtered and evaporated.

The obtained crude product (0.90 g) was purified on silica column (70 mL of SiO_2, pentane/EtOAc 85:15) to yield 354 mg of colorless oil which was further purified by preparative HPLC (16 mL/min, H_2O/ACN, $t_{0'}$ 20:80, $t_{5'}$ 20:80, $t_{20'}$ 100:0, $t_{30'}$ 100:0, $t_{35'}$ 20:80, $t_{50'}$ 20:80, detection 220 nm). Finally, 248 mg (53%) of compound **4** (colorless oil) were obtained in high purity.

R_f (pentane/EtOAc 8:2) 0.3.

^{1}H NMR (500 MHz, $CDCl_3$) δ 6.78 (d, J = 8.0 Hz, 1H, CH Ar), 6.73 (d, J = 2.0 Hz, 1H, CH Ar), 6.62 (dd, J = 8.1, 2.1 Hz, 1H, CH Ar), 5.39 – 5.31 (m, 2H, CH=CH), 4.23 (t, J = 7.2 Hz, 2H, CH_2-O), 2.81 (t, J = 7.2 Hz, 2H, CH_2-CH_2-O), 2.29 (t, J = 15.1 Hz, 2H, CH_2-C=O), 2.01 (q, J = 7.0 Hz, 4H, CH_2 allylic), 1.59 (quin, J = 7.1 Hz, 2H, CH_2-CH_2-C=O), 1.38 – 1.20 (m, 20 H, CH_2 alkyl), 0.88 (t, J = 7.5 Hz, 3H, CH_3).

^{13}C NMR (126 MHz, $CDCl_3$) δ 174.8, 143.8, 130.5, 130.2, 129.9, 121.4, 115.9, 115.4, 65.3, 34.5, 29.8, 29.7, 29.5, 29.3, 29.2, 27.4, 27.3, 25.1, 22.8, 14.3.

UPLC (300 μL/min, H_2O/ACN, $t_{0'}$ 20:80, $t_{3'}$ 100:0, $t_{10'}$ 100:0, $t_{11'}$ 20:80, $t_{15'}$ 20:80, detection 280 nm): t_R 4.96 min, m/z 836 $[2M - H]^-$.

(9*Z*,12*Z*)-3,4-dihydroxyphenethyl octadeca-9,12-dienoate (5)

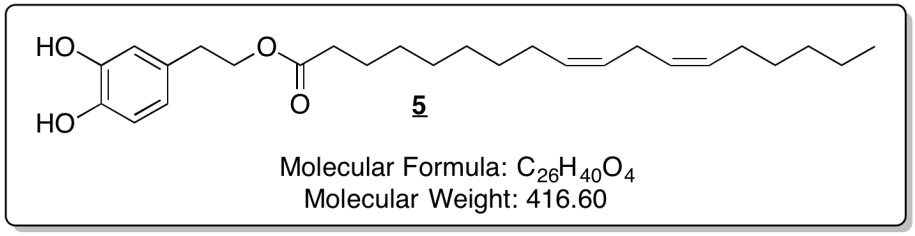

Protected hydroxytyrosol-LA **2** (150 mg, 0.34 mmol) was dissolved in 2.9 mL of dry DCM and *n*-Bu_4NI (987 mg, 1.02 mmol) was added. Afterwards, 1.02 mL of BCl_3 (1M solution in DCM, 1.02 mmol) were slowly added dropwise at -78 °C and the reaction was warmed up to 0 °C, stirring for further 1 h under argon. Monitoring was carried out by TLC (pentane/EtOAc 8:2, revealed by $KMnO_4$).

After 1 h, 7 mL of iced water were added to the reaction and the maximum amount of organic solvent was evaporated under reduced pressure. After addition of water (18 mL) and Et_2O to the aqueous residue, precipitate occurred on the interphase. It was filtered on frit and the filtrate was washed wit Et_2O (3×50 mL); combined organic phases were dried over $MgSO_4$, filtered and resulted in 0.30 g of raw material after evaporation.

This crude product was purified by silica gel column chromatography with 30 mL of silica and pentane/EtOAc (85:15) as eluent. Further purification of the obtained colorless oil (111 mg) by preparative HPLC (16 mL/min, H_2O/ACN, $t_{0'}$ 20:80, $t_{5'}$ 20:80, $t_{20'}$ 100:0, $t_{30'}$ 100:0, $t_{35'}$ 20:80, $t_{50'}$ 20:80, detection 220 nm) yielded in hydroxytyrosol-LA (colorless oil) **5** (78 mg, 55%).

R_f (pentane/EtOAc 8:2) 0.3.

^{1}H NMR (500 MHz, $CDCl_3$) δ 6.78 (d, J = 8.0 Hz, 1H, CH Ar), 6.73 (d, J = 2.0 Hz, 1 H, CH Ar), 6.63 (dd, J = 8.1, 2.0 Hz, 1H, CH Ar), 5.81 (s, 1H, OH-Ar), 5.64 (s, 1H, OH-Ar), 5.45 – 5.25 (m, 4H, CH=CH), 4.23 (t, J = 7.1 Hz, 2H, CH_2-O), 2.81 (t, J = 7.1 Hz, 2H, CH_2-CH_2-O), 2.77 (t, J = 6.7 Hz, 2H, CH_2 bis-alkyl), 2.28 (t, J = 7.5 Hz, 2H, CH_2-C=O), 2.04 (q, J = 7.2 Hz, 4H, CH_2 allylic), 1.58 (quin, J = 7.4 Hz, 2H, CH_2-CH_2-C=O), 1.46 – 1.16 (m, 14H, CH_2 alkyl), 0.88 (t, J = 7.0 Hz, 3H, CH_3).

^{13}C NMR (126 MHz, $CDCl_3$) δ 174.5, 143.8, 142.4, 130.7, 130.4, 130.2, 128.2, 128.0, 121.4, 116.0, 115.4, 65.2, 34.6, 34.5, 31.7, 29.7, 29.5, 29.3, 29.2, 29.2, 27.3, 27.3, 25.8, 25.1, 22.7, 14.2.

UPLC (300 μL/min, H_2O/ACN, $t_{0'}$ 20:80, $t_{3'}$ 100:0, $t_{10'}$ 100:0, $t_{11'}$ 20:80, $t_{15'}$ 20:80, detection 280 nm): t_R 4.20 min, m/z found 832 $[2M - H]^-$.

(9*Z*,12*Z*,15*Z*)-3,4-dihydroxyphenethyl octadeca-9,12,15-trienoate (6)

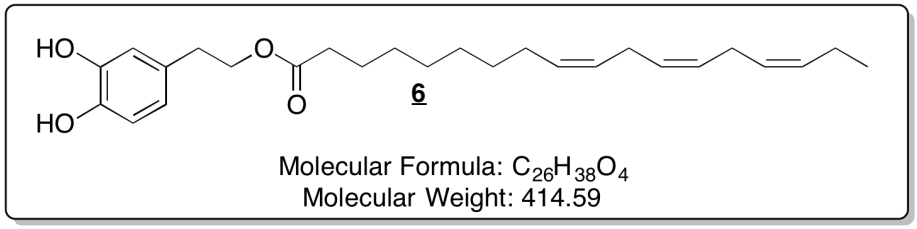

Compound **3** (170 mg, 0.38 mmol) was dissolved in dry DCM (3.2 mL) and *n*-Bu_4NI (929 mg, 0.96 mmol) were added. After bringing the temperature to -78 °C (acetone/liquid nitrogen), 1M BCl_3 in dry DCM (0.96 mL, 0.96 mmol) was slowly added into the reaction. After 1 h of stirring at 0 °C under argon, further *n*-Bu_4NI (186 mg, 0.19 mmol) was added and temperature was decreased back to -78 °C for further addition of BCl_3 (0.19 mL, 0.19 mmol). Course of the reaction was monitored by TLC (pentane/EtOAC 8:2, visualized by $KMnO_4$). Reaction was stirred at 0 °C under argon and it was terminated at 4.5 h of reaction time.

Iced water (7 mL) was poured directly into the organic media which was then evaporated to maximum. Addition of Et_2O to the aqueous solution led to the formation of a precipitate on the interphase, which was filtered on frit; filtrate was diluted with addition of 21 mL of water and was extracted with Et_2O (45 mL and 2×28 mL). Collection, drying over $MgSO_4$, filtration and evaporation of combined Et_2O layers led to 0.30 g of raw material.

This crude product was purified by silica gel column chromatography (25 mL of silica, pentane/EtOAc 85:15; 100 mg of colorless oil isolated) and preparative HPLC (16 mL/min, H_2O/ACN, $t_{0'}$ 20:80, $t_{5'}$ 20:80, $t_{20'}$ 100:0, $t_{30'}$ 100:0, $t_{35'}$ 20:80, $t_{50'}$ 20:80, detection 220 nm) and eventually, 70 mg (44%) of compound **6** were achieved.

R_f (pentane/EtOAc 8:2) 0.3.

^{1}H NMR (500 MHz, $CDCl_3$) δ 6.78 (d, J = 8.0 Hz, 1H, CH Ar), 6.73 (d, J = 1.6 Hz, 1H, CH Ar), 6.63 (dd, J = 8.0, 1.9 Hz, 1H, CH Ar), 5.43 – 5.28 (m, 6H, CH=CH), 4.23 (t, J = 7.1 Hz, 2H, CH_2-O), 2.85 – 2.77 (m, 6H, CH_2-CH_2-O, CH_2 bis-allylic), 2.28 (t, J = 7.5 Hz, 2H, CH_2-C=O), 2.11 – 2.01 (m, 4H, CH_2 allylic), 1.58 (quin, J = 7.4 Hz, 2H, CH_2-CH_2-C=O), 1.38 – 1.23 (m, 8H, CH_2 alkyl), 0.97 (t, J = 7.5 Hz, 3H, CH_3).

^{13}C NMR (126 MHz, $CDCl_3$) δ 174.4, 143.7, 142.3, 132.1, 130.8, 130.4, 128.4, 128.4, 127.9, 127.2, 121.4, 116.0, 115.4, 65.1, 34.6, 34.5, 29.7, 29.3, 29.2, 29.2, 27.3, 25.8, 25.7, 25.1, 20.7, 14.4.

UPLC (300 µL/min, H_2O/ACN, $t_{0'}$ 20:80, $t_{3'}$ 100:0, $t_{10'}$ 100:0, $t_{11'}$ 20:80, $t_{15'}$ 20:80, detection 280 nm): t_R 3.47 min, m/z 828 $[2M - H]^-$.

Synthesis of Resveratrol conjugates

(*E*)-4-(3,5-dihydroxystyryl)phenyl acetate (7)

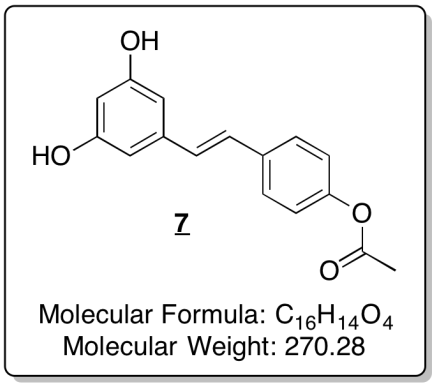

Resveratrol (2.88 g, 12.61 mmol) was dissolved in 2-methylbutan-2-ol (280 mL) in a 1L round bottomed flask. Vinyl acetate (72.4 mL, 756.7 mmol) and CALB (14.40 g) were added to the solution. The enzyme was weighed into a beaker without gloves to eliminate static electricity. The reaction was allowed to stir on a rotary evaporator under argon at 40 °C, protected from sunlight by aluminum foil while monitored by TLC (DCM/MeOH 95:5, visualized by UV 254 nm and anisaldehyde).

After 4.5 days, the enzyme was removed by filtration using a frit and was extensively washed with EtOAc (10×50 mL) and diethyl ether (2×50 mL). Filtrate was evaporated under reduced pressure resulting in 4.50 g of crude product.

The crude product was adsorbed on 4.5 mL of SiO_2 to form a solid deposit and purified by silica gel column chromatography using 450 mL of SiO_2 in total and DCM/MeOH (99:1 to 98:2) as mobile phase which yielded in 2.89 g (85%) of compound **7** as a white solid.

R_f (DCM/MeOH 95:5) 0.4.

^{1}H NMR (500 MHz, MeOD): δ 7.54 (d, J = 17.1 Hz, 2H, 2′-H, 6′-H), 7.07 (d, J = 17.4 Hz, 2H, 3′-H, 5′-H), 7.04 (d, J = 32.8 Hz, 1H, 8-H), 6.97 (d, J = 32.6 Hz, 1H, 7-H), 6.49 (d, J = 4.3 Hz, 2H, 2-H, 6-H), 6.20 (t, J = 4.3 Hz, 1H, 3-H), 2.28 (s, 3H, $CH_{3(OAc)}$).

^{13}C NMR (126 MHz, MeOD): δ 171.1, 159.7, 151.5, 140.6, 136.58, 130.24, 128.3, 128.3, 122.9, 106.1, 103.2, 20.9.

(*E*)-4-{3,5-bis[(triisopropylsilyl)oxy]styryl}phenyl acetate (8)

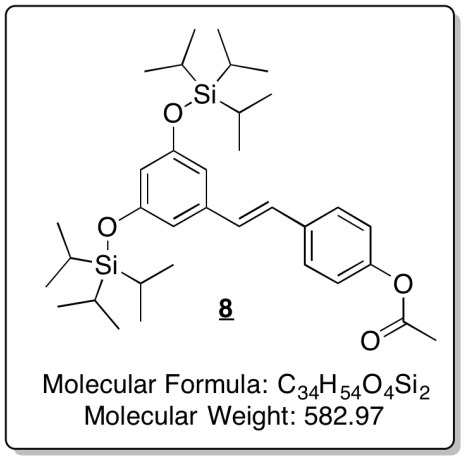

Protection of 4'-*O*-acetylresveratrol **7** was carried out in a 250 mL round bottomed flask where the compound (3.18 g, 11.78 mmol) was dissolved in dry THF (160 mL) under argon atmosphere. DIPEA (4.2 ml, 24.7 mmol) was added; after that, TIPS-OTf (6.7 ml, 24.7 mmol) was slowly added dropwise. Reaction was stirred at room temperature and it was monitored by TLC (pentane/EtOAc 7:3, visualized by UV 254 nm and anisaldehyde). After 4.5 h, another DIPEA (1.0 mL, 5.9 mmol) and TIPS-OTf were added carefully. The reaction was terminated after 7 h of overall time.

Solvent was evaporated under reduced pressure and the residue was dissolved in 200 mL of EtOAc. This solution underwent extraction with water (2×100 mL) and brine (100 mL) to eliminate the resulted ammonium salt. Organic phase was dried with $MgSO_4$ and evaporated to yield crude product (13.80 g).

Crude product was purified on silica gel column with 1380 mL of silica and pentane/EtOAc (99:1 to 7:3) as mobile phase to obtain 6.85 g of the compound **8** (colorless oil) containing 10% of TIPS-OH (90%).

R_f (pentane/EtOAc 9:1) 0.7

^{1}H NMR (500 MHz, $CDCl_3$): δ 7.50 (d, J = 17.3 Hz, 2H, 2′-H, 6′-H), 7.08 (d, J = 17.3 Hz, 2H, 3′-H, 5′-H), 6.97 (d, J = 32.5 Hz, 1H, 8-H), 6.92 (d, J = 32.5 Hz, 1H, 7-H), 6.64 (d, J = 4.3 Hz, 2H, 2-H, 6-H), 6.35 (t, J = 4.3 Hz, 1H, 3-H), 2.31 (s, 3H, $CH_{3(OAc)}$), 1.34 – 1.22 (m, 6 H, CH-Si), 1.11 (m, 36 H, $(CH_3)_2$CH).

^{13}C NMR (126 MHz, $CDCl_3$): δ 169.7, 157.3, 150.2, 139.0, 135.3, 129.3, 127.8, 127.7, 122.0, 111.6, 111.5, 21.4, 18.2, 12.9.

(*E*)-4-{3,5-bis[(triisopropylsilyl)oxy]styryl}phenol (9)

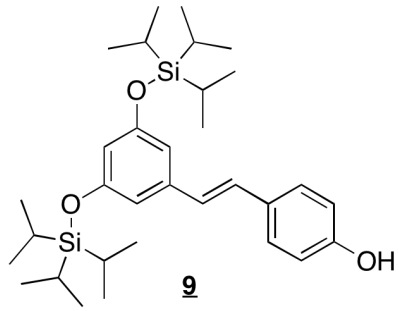

9

Molecular Formula: $C_{32}H_{52}O_3Si_2$
Molecular Weight: 540.94

Compound **8** (6.85 g of 90% **8**, 10.59 mmol) was dissolved in dry DCM (28 mL) and anhydrous MeOH (58 mL) in a 250 mL round bottomed flask. Sodium methoxide (191 mg, 3.53 mmol) was added and the reaction was stirred for 4.5 h under argon at room temperature while monitored by TLC (pentane/EtOAc 95:5, visualized by UV 254 nm and anisaldehyde). Then, further 0.3 eq. (191 mg, 3.53 mmol) of sodium methoxide was added to drive the reaction to completion. Reaction was terminated after 6.5 h of overall reaction time.

The reaction media was evaporated to gain crude product (7.80 g).

Purification of the crude product was carried out on silica gel column using 780 mL of silica and pentane/EtOAc 96:4 to 9:1 as mobile phase. Two fractions were isolated: 3.20 g of compound **9** containing 10% of TIPS-OH and 2.85 g of compound **9** obtained (99%; colorless oil).

R_f (pentane/EtOAc 95:5) 0.5.

^{1}H NMR (500 MHz, $CDCl_3$): δ 7.39 (d, J = 17.1 Hz, 2H, 2′-H, 6′-H), 6.94 (d, J = 32.5 Hz, 1H, 8-H), 6.84 – 6.80 (m, 3 H, 7-H, 3′-H, 5′-H), 6.62 (d, J = 4.3 Hz, 2H, 2-H, 6-H), 6.33 (t, J = 4.3 Hz, 1H, 4-H), 1.30 – 1.22 (m, 6 H, CH-Si), 1.11 (d, J = 14.5 Hz, 36 H, $(CH_3)_2$CH).

^{13}C NMR (126 MHz, MeOD): δ 158.5, 158.3, 141.3, 130.1, 129.9, 129.0, 126.5, 116.5, 112.1, 111.4, 18.4, 13.9.

(9*Z*,12*Z*)-4-{(*E*)-3,5-bis[(triisopropylsilyl)oxy]styryl}phenyl octadeca-9,12-dienoate (10)

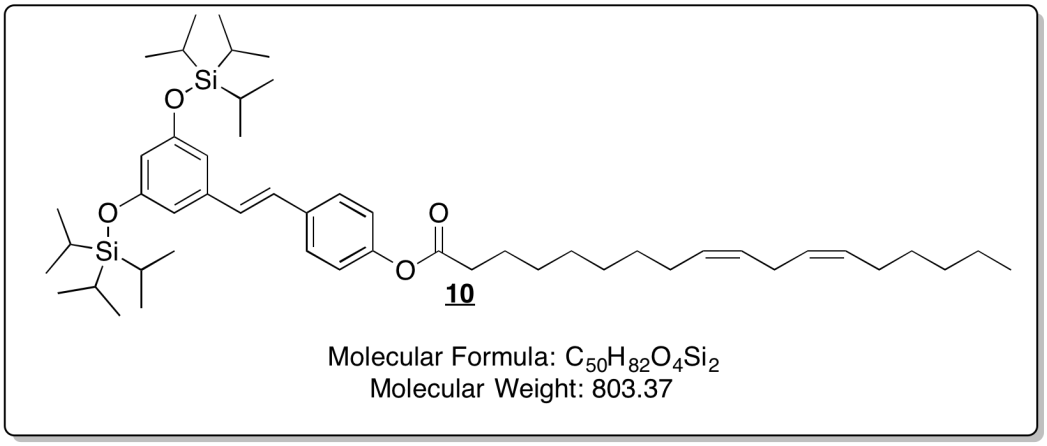

Molecular Formula: $C_{50}H_{82}O_4Si_2$
Molecular Weight: 803.37

Coupling between 90% compound **9** (1.00 g, 1.67 mmol) and LA (623 mg, 2,22 mmol) was performed in a 100 mL round bottomed flask. Compound 3 and solution of LA in dry DCM (40 mL) was added under argon. Next, DCC (573 mg, 2.78 mmol) and DMAP (113 mg, 0.93 mmol) were added and the solution was left to stir at room temperature under inert atmosphere and it was monitored by TLC (pentane/EtOAc 95:5, visualized by UV 254 nm and anisaldehyde/$KMnO_4$). Soon, the formation of white precipitate and progressive disappearance of the starting material were observed. The reaction was terminated after 3 hours.

Flask was put into the fridge (4 °C) for 30 min to maximize the amount of DCU crystals. White precipitate was then removed by filtration on frit, rinsed by a few drops of cold DCM. Filtrate was diluted by 40 mL of DCM and extracted twice with water (30 mL) and once with brine (30 mL); organic phase was re-extracted with 100 mL of DCM. Organic layers were collected, dried over $MgSO_4$ and evaporated; the resulted residue was recrystallized once more from DCM (10 mL) according to the former procedure. After evaporation of the filtrate, 2.00 g of crude product were gained. Purification by silica gel column chromatography (160 mL of silica, pentane/EtOAc 995:5 to 99:1) resulted in 1.10 g (82%) of compound **10** (colorless oil).

R_f (pentane/EtOAc 95:5) 0.7.

^{1}H NMR (500 MHz, CDCl3): δ 7.50 (d, J = 17.2 Hz, 2H, 2′-H, 6′-H), 7.06 (d, J = 17.3 Hz, 2H, 3′-H, 5′-H), 6.97 (d, J = 32.6 Hz, 1H, 8-H), 6.91 (d, J = 32.5 Hz, 1H, 7-H), 6.64 (d, J = 4.2 Hz, 2H, 2-H, 6-H), 6.35 (t, J = 4.3 Hz, 1H, 4-H), 5.42 – 5.34 (m, 4H, CH=CH), 2.78 (t, J = 12.9 Hz, 2H, CH_2 bis-allylic), 2.55 (t, J = 15.0, 2H, CH_2-C=O), 2.07 – 2.03

(m, 4H, CH_2 allylic), 1.79 – 1.72 (quin, *J* = 15.0, 2H, *CH_2*-CH_2-C=O), 1.46 – 1.22 (m, 20H, CH_2 alkyl + CH-Si), 1.11 (d, J = 7.3 Hz, 36 H, *$(CH_3)_2$*-CH), 0.89 (t, *J* = 13.9, 3H, CH_3).

^{13}C NMR (126 MHz, $CDCl_3$) δ 172.6, 157.4, 150.4, 139.1, 135.3, 130.6, 130.3, 129.3, 128.4, 128.2, 127.9, 127.7, 122.1, 111.7, 111.6, 77.6, 77.3, 77.1, 34.8, 29.9, 29.5, 29.4, 27.5, 26.0, 25.3, 18.3, 18.2, 14.4, 13.0.

(*E*)-4-{3,5-bis[(triisopropylsilyl)oxy]styryl}phenyl docosanoate (<u>11</u>)

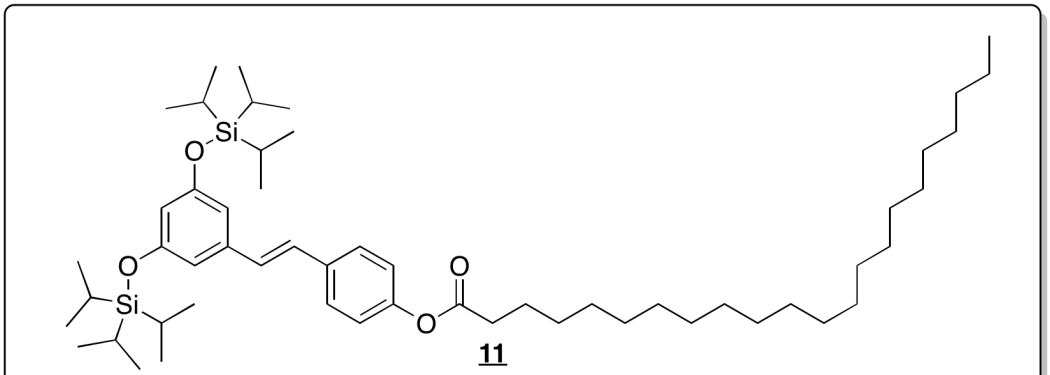

<u>11</u>

Molecular Formula: $C_{54}H_{94}O_4Si_2$
Molecular Weight: 863.51

Compound **<u>9</u>** (3.00 g, 5.55 mmol) and DA (2.27 g, 6.67 mmol) were partially dissolved in dry DCM (180 mL) and the required amount of dry DMF (55 mL) was added to solubilize the DA entirely. Afterwards, DCC (1.7 g, 8.33 mmol) and DMAP (339 mg, 2.78 mmol) were added and the reaction was stirred at room temperature under argon until the conversion was completed according to TLC (pentane/EtOAc 97:3, detected by UV 254 nm and anisaldehyde; reaction time 6 h). Reaction was put into the fridge (4 °C) to allow the formation of a small amount of precipitate, which was then filtered on frit. DCM (65 mL) was added to the filtrate and it was extracted with water (2×150 mL) and brine (150 mL). Organic layer was dried over MgSO4 and evaporated to gain a residue which was recrystallized from DCM; evaporation of the second filtrate resulted 8.00 g of crude product.

Purification on silica gel column (480 mL of SiO_2, pentane/EtOAc 99:1) yielded 6.63 g (76%) of **<u>11</u>** as a white waxy solid.

R_f (pentane/EtOAc 99:1) 0.4

^{1}H NMR (500 MHz, $CDCl_3$): δ 7.50 (d, *J* = 17.2 Hz, 2H, 2′-H, 6′-H), 7.06 (d, J = 17.3 Hz, 2H, 3′-H, 5′-H), 6.97 (d, *J* = 32.5 Hz, 1H, 8-H), 6.91 (d, *J* = 32.5 Hz, 1H, 7-H), 6.64 (d, *J* = 4.3 Hz, 2H, 2-H, 6-H), 6.35 (t, *J* = 4.3 Hz, 1H, 4-H), 2.55 (t, *J* = 15.0 Hz, 2H,

CH_2-C=O), 1.75 (quin, *J* = 15.1 Hz, 2H, *CH_2*-CH_2-C=O), 1.33-1.22 (m, 42H, CH_2 alkyl + CH-Si), 1.11 (d, *J* = 7.3 Hz, 36H, *$(CH_3)_2$*-CH), 0.88 (t, *J* = 7.1 Hz; 3H, CH_3).

^{13}C NMR (126 MHz, $CDCl_3$) δ 172.4, 157.2, 150.2, 138.9, 135.1, 129.1, 127.7, 127.5, 121.9, 111.5, 77.4 77.3, 77.1, 76.9, 34.6, 32.1, 29.8, 29.8, 29.7, 29.6, 29.5, 29.4, 29.2, 25.1, 22.8, 18.1, 17.7, 14.3, 13.1, 12.8.

(9*Z*,12*Z*)-4-[(*E*)-3,5-dihydroxystyryl]phenyl octadeca-9,12-dienoate (<u>12</u>)

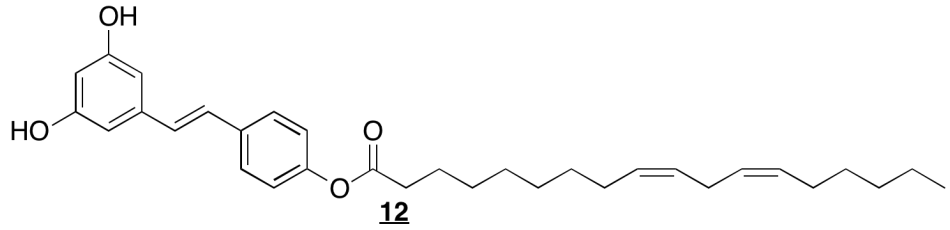

<u>12</u>

Molecular Formula: $C_{32}H_{42}O_4$
Molecular Weight: 490.68

Compound **<u>10</u>** (1.08 g, 1.35 mmol) was dissolved in dry THF (60 mL) in. Et_3N-3HF (1.32 mL, 8.08 mmol) was added via plastic syringe and the reaction was stirred at room temperature under argon. Further Et_3N-3HF (2×0.66 mL, 2×4.04 mmol) was added at four and six hours of reaction time. Reaction was terminated after another two hours (reaction time 8 h) when only a trace of starting material was visible. TLC monitoring was carried out using pentane/EtOAc (7:3 and 9:1) to observe the desired product formation and the disappearance of the starting material respectively; plates were visualized by UV 254 nm and anisaldehyde. Reaction media was evaporated and the residue was dissolved in EtOAc (120 mL); resulted solution underwent extraction with H_2O (3×60 mL) and brine (60 mL). Separated organic phase was dried over $MgSO_4$, filtered and evaporated to yield 1.0 g of crude product.

This product was purified by column chromatography using 120 mL of silica and pentane/EtOAc (7:3 to 6:4) as mobile phase to obtain **<u>12</u>** (546 mg, 83%) as a white waxy solid. (9*Z*,12*Z*)-4-{(*E*)-3-hydroxy-5[(triisopropylsilyl)oxy]styryl}phenyl octadeca-9,12-dienoate (mono-deprotected derivative; 115 mg, 13%) was also isolated.

R_f (pentane/EtOAc 7:3) 0.4

^{1}H NMR (500 MHz, $CDCl_3$) δ 7.43 (d, *J* = 8.5 Hz, 2H, 2′-H, 6′-H), 7.05 (d, *J* = 8.6 Hz, 2H, 3′-H, 5′-H), 6.90 (d, *J* = 16.3 Hz, 1H, 8-H), 6.81 (d, *J* = 16.3 Hz, 1H, 7-H), 6.47 (d, *J* = 2.2 Hz, 2H, 2-H, 6-H), 6.24 (t, *J* = 2.2 Hz, 1H, 4-H), 5.46 – 5.27 (m, 4H, CH=CH),

2.78 (t, J = 6.6 Hz, 2H, CH_2 bis-allylic), 2.58 (t, J = 7.6 Hz, 2H, CH-C=O), 2.06 (quin, J = 6.5 Hz, 4H, CH_2 allylic), 1.76 (quin, J = 7.5 Hz, 2H, CH_2-CH_2-C=O), 1.46 – 1.20 (m, 14 H), 0.89 (t, J = 6.8 Hz, 3H, CH_3).

^{13}C NMR (126 MHz, $CDCl_3$) δ 173.5, 157.0, 150.1, 139.7, 135.1, 130.4, 130.1, 128.4, 128.2, 128.0, 127.7, 121.8, 106.3, 102.6, 77.4, 77.2, 76.9, 34.6, 31.7, 29.7, 29.5, 29.3, 29.2, 27.3, 25.8, 25.0, 22.7, 14.2.

(*E*)-4-(3,5-dihydroxystyryl)phenyl docosanoate (<u>13</u>)

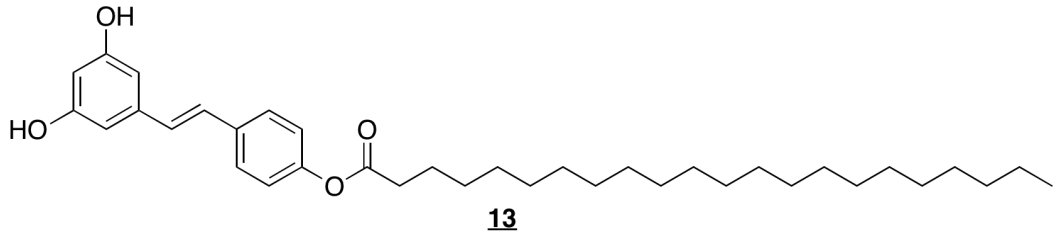

<u>13</u>

Molacular Formula: $C_{36}H_{54}O_4$
Molecular Weight: 550.82

Compound **<u>11</u>** (3.63 g, 4.20 mmol) was dissolved in dry THF (220 mL) under argon atmosphere. Addition of Et_3N-3HF was arranged via plastic syringe at reaction time 0 h (4.11 mL, 25.21 mmol), 3.5 h (2.06 mL, 12.61 mmol) and 6 h (2.06 mL, 12.61 mmol) while the reaction was allowed to stir at r. t. and was monitored by TLC (pentane/EtOAc 7:3 and 9:1, visualized by UV 254 nm and anisaldehyde).

After 8 hours, the THF was evaporated under reduced pressure and the residue was dissolved in 400 mL EtOAc and washed with H_2O (3×200 mL) and brine (200 mL). After drying and filtration of the organic layer, 2.70 g of raw material were obtained.

Crude product was adsorbed on 20 mL of silica subsequent silica gel column chromatography (200 mL of silica, pentane/EtOAc 7:3 to 0:1) resulted in 503 mg (17%) of (*E*)-4-(3-hydroxy-5-((triisopropylsilyl)oxy)styryl)phenyl docosanoate and 1.82 g (78.6%) of compound **<u>13</u>** as a white solid.

R_f (pentane EtOAc 7:3) 0.3

^{1}H NMR (500 MHz, $CDCl_3$/MeOD 10:1) δ 7.32 (d, J = 8.6 Hz, 2H, 2′-H, 6′-H), 6.87 (d, J = 8.5 Hz, 2H, 3′-H, 5′-H), 6.84 (d, J = 16.3 Hz, 1H, 8-H), 6.74 (d, J = 16.3 Hz, 1H, 7-H), 6.34 (d, J = 2.1 Hz, 2H, 2-H, 6-H), 6.08 (t, J = 2.1 Hz, 1H, 4-H), 2.39 (t, J = 7.5 Hz, 2H, CH_2-C=O), 1.57 (quin, J = 7.5 Hz, 2H, CH_2-CH_2-C=O), 1.25-1.06 (m, 36H, CH_2 alkyl), 0.69 (t, J = 6.6 Hz, 3H, CH_3).

^{13}C NMR (126 MHz, $CDCl_3$/MeOD 10:1) δ 172.8, 157.9, 149.8, 139.1, 135.0, 128.9, 127.3, 127.2, 121.6, 105.1, 102.1, 34.2, 31.7, 29.5, 29.4, 29.3, 29.2, 29.1, 28.9, 24.7, 22.5, 13.8.

UPLC (300 μL/min, H_2O/ACN, $t_{0'}$ 20:80, $t_{3'}$ 100:0, $t_{10'}$ 100:0, $t_{11'}$ 20:80, $t_{15'}$ 20:80, detection 300 nm): t_R 10.28 min.

Synthesis of phloroglucinol-DHA conjugate

Methyl 3-(2,4,6-trimethoxyphenyl)propanoate (14)

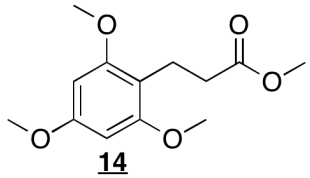

14

Molecular Formula: $C_{13}H_{18}O_5$
Molecular Weight: 254.28

1,3,5-Trimethoxybenzene (1.63 g, 9.70 mmol) and $AuCl_3$ (150 mg) were dissolved in DCE (33 mL). AgOTf (375 mg, 1.46 mmol) and methyl acrylate (1.31 mL, 14.55 mmol) were added and the reaction was brought to reflux (84 °C) and stirred under argon for 3 days. The course of the reaction was monitored by TLC (pentane/EtOAc 95:5, visualization by PMA).

After three days, the reaction was allowed to cool down to r.t. and the silver particles were filtered off through cotton. The filtrate was extracted with water (3×25 mL) and the aqueous phase was re-extracted with a corresponding amount of DCM. Organic layers were assembled, dried over $MgSO_4$, filtered and evaporated to obtain crude product (2.35 g).

Purification on a silica gel column (220 mL SiO_2, pentane/EtOAc 95:5 to 9:1) resulted in 1.57 g (64%) of compound **14** (white solid).

R_f (pentane/EtOAc 95:5) 0.7

^{1}H NMR (500 MHz, $CDCl_3$) δ 6.11 (s, 2H, CH Ar), 3.80 (s, 3H, CH_3-O-Ar), 3.78 (s, 6H, CH_3-O-Ar), 3.67 (s, 3H, CH_3-O-C=O), 2.92 – 2.86 (m, 2H, CH_2-CH_2-C=O), 2.48 – 2.42 (m, 2H, CH_2-C=O).

^{13}C NMR (126 MHz, $CDCl_3$) δ 174.4, 159.7, 158.9, 109.28, 90.4, 55.7, 55.4, 51.5, 33.8, 18.5.

Methyl 3-(2-hydroxy-4,6-dimethoxyphenyl)propanoate (15a)

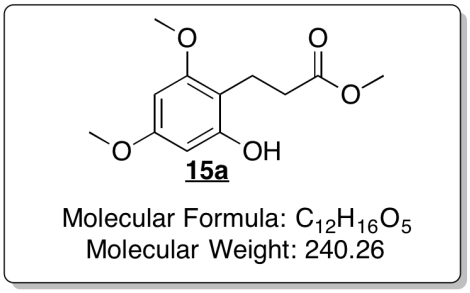

15a

Molecular Formula: $C_{12}H_{16}O_5$
Molecular Weight: 240.26

Compound **14** (500 mg, 1.97 mmol) was dissolved in dry DCM (12.5 mL). *n*-Bu_4NI (1.45 g, 3.94 mmol) was added and the reaction was cooled down to -30 °C with an acetone/liquid nitrogen bath. Next, BCl_3 1M in DCM (3.94 mL, 3.94 mmol) was added drop by drop. The reaction temperature was allowed to rise up to 0 °C and the reaction was stirred for 1 h, monitored by TLC (pentane/EtOAc 7:3, detected by anisaldehyde).

The reaction was terminated by slow addition of iced water (40 mL) into the reaction media. The organic solvent was evaporated and extraction with EtOAc (2×80 mL, 40 mL), collection of organic phases, drying over $MgSO_4$, filtration and evaporation lead to 1.50 g of crude product.

This crude product was adsorbed on silica to form a solid deposit and purified by silica gel column chromatography (150 mL of silica, pentane/EtOAc 9:1 to 85:15) to obtain 151 mg (32%) of compound **15a** as a yellowish, solid and 123 mg (26%) of product **15b** as a yellow crystal solid.

Rf (pentane/EtOAc 7:3) 0.5

^{1}H NMR (500 MHz, $CDCl_3$) δ 7.96 (s, 1H, OH Ar), 6.17 (d, J = 2.4 Hz, 1H, CH Ar), 6.06 (d, J = 2.4 Hz, 1H, CH Ar), 3.76 (s, 3H, CH_3-O-Ar), 3.76 (s, 3H, CH_3-O-Ar), 3.68 (s, 3H, CH_3-O-C=O), 2.82 – 2.78 (m, 2H, CH_2-CH_2-C=O), 2.69 – 2.65 (m, 2H, CH_2-C=O).

^{13}C NMR (126 MHz, $CDCl_3$) δ 177.8, 159.9, 159.2, 156.1, 108.3, 94.8, 91.5, 55.5, 55.38, 52.5, 33.8, 17.7.

Methyl 3-(4-hydroxy-2,6-dimethoxyphenyl)propanoate (15b)

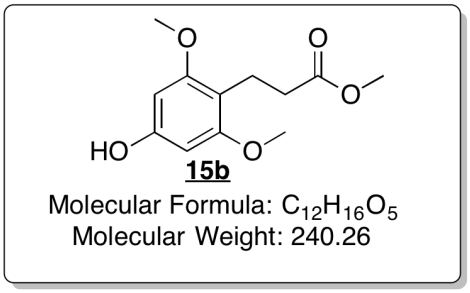

15b

Molecular Formula: $C_{12}H_{16}O_5$
Molecular Weight: 240.26

R_f (pentane/EtOAc 7:3) 0.3

^{1}H NMR (500 MHz, $CDCl_3$) δ 6.04 (s, 2H, CH Ar), 3.75 (s, 6H, CH_3-O-Ar), 3.67 (s, 3H, CH_3-O-C=O), 2.90 – 2.85 (m, 2H, CH_2-CH_2-C=O), 2.47 – 2.42 (m, 2H, CH_2-C=O).

Methyl 3-(2-isopropoxy-4,6-dimethoxyphenyl)propanoate (16a)

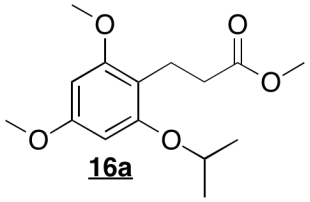

16a

Molecular Formula: $C_{15}H_{22}O_5$
Molecular Weight: 282.34

Compound **15a** (109 mg, 0.45 mmol) was dissolved in dry DMF (6 mL) under argon atmosphere. K_2CO_3 (313 mg, 2.27 mmol), KI (376 mg, 2.27 mmol) and *i*Pr-Br (211 μL, 2.27 mmol) the reaction was brought to 80 °C. After 15 h of stirring and monitoring by TLC (pentane/EtOAC 8:2, visualization by anisaldehyde), the temperature was raised to 100 °C and the reaction was stirred for another 7 hours.

After bringing it back to r.t., 20 mL of EtOAc were added and the DMF was extracted with water (3×10 mL). Organic layers were collected, dried over $MgSO_4$, filtered and evaporated.

Raw material (160 mg) was purified on silica gel column (16 mL of silica, pentane/EtOAc 97:3 to 96:4) to obtain compound 47 mg (37%) of **16a** as a colorless oil.

R_f (pentane/EtOAc 8:2) 0.4

^{1}H NMR (500 MHz, $CDCl_3$) δ 6.11 (d, *J* = 2.2 Hz, 1H, CH Ar), 6.09 (d, *J* = 2.2 Hz, 1H, CH Ar), 4.49 (sept, *J* = 6.0 Hz, 1H, *CH*-$(CH_3)_2$), 3.78 (s, 3H, CH_3-O-Ar), 3.78 (s, 3H, CH_3-O-Ar), 3.67 (s, 3H, CH_3-O-C=O), 2.91 – 2.86 (m, 2H, *CH_2*-CH_2-C=O), 2.47 – 2.43 (m, 2H, CH_2-C=O), 1.31 (d, *J* = 6.1 Hz, 6H, *$(CH_3)_2$*-CH).

3-(2-isopropoxy-4,6-dimethoxyphenyl)propan-1-ol (<u>17</u>)

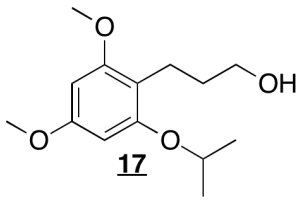

<u>17</u>

Molecular Formula: $C_{14}H_{22}O_4$
Molecular Weight: 254.33

Compound **<u>16a</u>** (47 mg, 0.17 mmol) was dissolved in dry Et_2O (1 mL) at 0 °C and Li[AlH_4] 1M in Et_2O (170 μL, 0.17 mmol) was added via syringe. Reaction was stirred for 3 hours under argon atmosphere while monitored by TLC (pentane/EtOAc 9:1, revealed with anisaldehyde).

Then, Et_2O (5 mL) and saturated Rochelle's salt (sodium-potassium tartrate) aqueous solution (10 mL) were added to the reaction. Phases were separated and residues of product were extracted from the aqueous phase with Et_2O (2×10 mL). Combined organic layers were dried over $MgSO_4$, filtered and evaporated to achieve compound **<u>17</u>** as a colorless oil (42 mg, 98%).

R_f (pentane/EtOAc 9:1) 0.2

^{1}H NMR (500 MHz, $CDCl_3$) δ 6.14 (d, *J* = 2.3 Hz, 1H, CH Ar), 6.12 (d, *J* = 2.3 Hz, 1H, CH Ar), 4.53 (sept, *J* = 6.0 Hz, 1H, *CH*-$(CH_3)_2$), 3.80 (s, 3H, CH_3-O-Ar), 3.79 (s, 3H, CH_3-O-Ar), 3.45 (q, *J* = 6.1 Hz, 2H, CH_2-OH), 2.70 (t, *J* = 6.4 Hz, 2H, CH_2-Ar), 2.60 (t, *J* = 6.7 Hz, 1H, OH), 1.73 (quin, *J* = 6.1 Hz, 2H, *CH_2*-CH_2-OH), 1.34 (d, *J* = 6.1 Hz, 6H, *$(CH_3)_2$*-CH).

5-Isopropoxybenzene-1,3-diol (<u>18</u>)

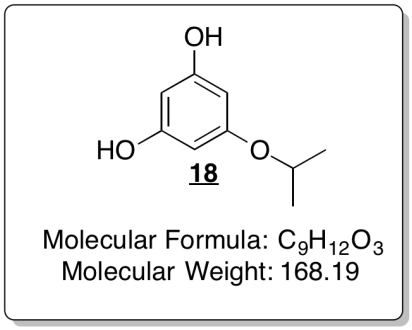

Phloroglucinol (2.00 g, 15.87 mmol) was dissolved in dioxane (20 mL) and 5 mL of propan-2-ol saturated by HCl (43 g/143 g) were added via plastic syringe, under argon. Temperature was raised to 70 °C and the reaction was stirred for 5 hours whereas further *i*Pr-OH/HCl (g) was added at 2 h (5 mL) and 3.5 h (5 mL) of the reaction time (additions were done at r.t.). Monitoring was carried out by TLC (DCM/MeOH 95:5, revealed by anisaldehyde) and visually, a change of color from yellow to red solution was observed. After 5 hours, the reaction media was evaporated and the crude product (4.3 g) was purified on silica gel column (300 mL SiO_2, DCM/MeOH 98:2) to result compound **<u>18</u>** (748 mg, 28%).

R_f (DCM/MeOH 95:5) 0.4

^{1}H NMR (500 MHz, $CDCl_3$) δ 5.98 (d, J = 2.1 Hz, 2H, CH Ar), 5.93 (t, J = 2.1 Hz, 1H, CH Ar), 5.04 (s, 2H, OH Ar), 4.46 (sept, J = 6.1 Hz, 1H, *CH*-$(CH_3)_2$), 1.31 (d, J = 6.1 Hz, 6H, *$(CH_3)_2$*-CH).

^{13}C NMR (126 MHz, $CDCl_3$) δ 161.6, 159.8, 94.6, 92.9, 70.0, 55.4, 22.2.

2,4-Dihydroxy-6-isopropoxybenzaldehyde (<u>19a</u>)

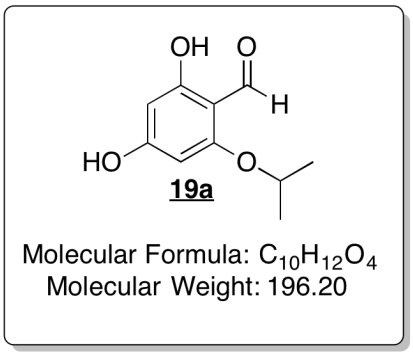

Compound **<u>18</u>** (200 mg, 1.19 mmol) was dissolved in dry Et_2O. $Zn(CN)_2$ (140 mg, 1.19 mmol) and $ZnCl_2$ (32 mg, 0.24 mmol) were added and HCl (g) was bubbled through the solution via a system of separatory traps for 1 h (color of the solution changed from

yellowish to bright red). Afterwards, the reaction tube was clogged and the reaction was stirred overnight at r.t. After 16 h, the reaction media was evaporated and the residue was re-dissolved in H_2O (5 mL) and was heated under reflux for 5 min. Resulted red oily precipitate was filtered and the aqueous filtrate was extracted with EtOAc (3×10 mL). Organic layers were collected, dried over $MgSO_4$, filtered, evaporated and combined with the formerly filtered precipitate.

This crude material (0.20 g) was purified by silica gel column chromatography (20 mL of silica, pentane/EtOAc 9:1) to obtain 147 mg (63%) of a whitish solid – mixture of compound **19a** and **19b** 8:2. This product was recrystallized from hot toluene (3.5 mL) and filtered to finally gain compound **19a** (68 mg, 29%) as a yellow, needle-like crystalline solid.

R_f (pentane/EtOAc 6:4) 0.5

^{1}H NMR (500 MHz, MeOD) δ 10.00 (d, J = 0.4 Hz, 1H, CH=O), 5.94 (dd, J = 2.1, 0.5 Hz, 1H, CH Ar), 5.82 (dd, J = 2.1, 0.4 Hz, 1H, CH Ar), 4.65 (sept, J = 6.0 Hz, 1H, *CH*-$(CH_3)_2$), 1.37 (d, J = 6.1 Hz, 6H, *$(CH_3)_2$*-CH).

^{13}C NMR (126 MHz, $CDCl_3$) δ 191.9, 167.2, 165.6, 162.9, 105.9, 94.9, 92.4, 71.0, 21.7.

Methyl 3-(2,4-dihydroxy-6-isopropoxyphenyl)acrylate (20a)

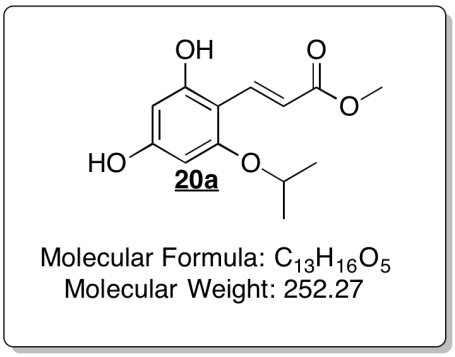

Compound **19a** (100 mg 93%, 0.47 mmol) was dissolved in dry DCM (3.5 mL) under argon atmosphere. Methyl (triphenylphosphoranylidene)acetate (256 mg, 0.76 mmol) was added and the reaction was stirred overnight at room temperature, under argon, monitored by TLC (pentane/EtOAc 6:4, visualized by UV 254 nm).

After 22 h, the reaction media was evaporated to gain 360 mg of crude product.

This product was adsorbed on silica to form a solid deposit and purified on silica gel column with 200 mL of (pentane/EtOAc 9:1to 6:4) and the resulting 60 mg of product were again adsorbed on silica re-purified on silica gel column (6 mL of silica, pentane/EtOAc 9:1) to finally result 66 mg (51%) of compound **20a** as an originally white

solid, providing violet solution in MeOH and EtOAc, gradually changing color to dark red/violet.

R_f (pentane/EtOAc 6:4) 0.3

^{1}H NMR (500 MHz, MeOD) δ 8.10 (d, *J* = 16.2 Hz, 1H, *CH*=CH-C=O), 6.75 (d, *J* = 16.2 Hz, 1H, CH-C=O), 5.98 (d, *J* = 2.2 Hz, 1H, CH Ar), 5.95 (d, *J* = 2.1 Hz, 1H, CH Ar), 4.90 (s, 2H, OH Ar), 4.57 (sept, *J* = 6.1 Hz, 1H, *CH*(CH_3)$_2$), 3.73 (s, 3H, CH_3-O), 1.36 (d, *J* = 6.1 Hz, 6H, *(CH$_3$)$_2$*-CH).

^{13}C NMR (126 MHz, MeOD) δ 172.0, 162.4, 161.5, 161.3, 138.9, 138.8, 115.4, 105.6, 96.2, 94.0, 71.9, 51.7, 22.4.

LIST OF ABBREVIATIONS

2D	Two-dimensional
A2E	*N*-Retinylidene-*N*-retinyle thanol-amine
ALA	α-Linolenic acid
AMD	Age-related macular degeneration
AREDS	Age-related eye disease study
ARPE-19	Human retinal pigment epithelium cell lines
ATP	Adenosine triphosphate
A*t*R	All-trans-retinal
Bu	Butyl
CALB	Candida antarctica lipase, Novozyme 435
CNRS	National Centre for Scientific Research
CoA	Coenzyme A
DA	Docosanoic acid
DCC	*N,N*-Dicyclohexylcarbo-diimide
DCE	Dichloroethane
DCM	Dichloromethane
DCU	*N,N*′-Dicyclohexylurea
DHA	Docosahexaenoic acid
DIPEA	*N,N*-Diisopropylethyl-amine
DMAP	4-Dimethylaminopyridine
DNA	Deoxyribonucleic acid
ENSCM	École Nationale Supérieure de Chimie
EPA	Eicosapentaenoic acid
EpRE	Electrophile response element
Eq.	Equivalent
EVOO	Extra virgin olive oil
FA	Fatty acids
HDL	high-density lipoprotein
HPLC	High-performance liquid chromatography
IBMM	Institute of biomolecules Max Mousseron
iPr	Isopropyl
iPr-OH/HCl	Propan-2-ol saturated with HCl (g)
Keap1	Kelch-like ECH-associated protein 1
LA	Linoleic acid
LDL	low-density lipoprotein
MS	Mass spectrometry
MUFA	Mono-unsaturated fatty acid
NMR	Nuclear magnetic resonance
Nrf2	Nuclear factor erythroid 2-related factor 2
OA	Oleic acid
PEP	Phosphoenolpyruvic acid
PMA	Phosphomolybdic acid
PUFA	Poly-unsaturated fatty acid
r.t.	Room temperature (20-25 °C)

RCS	Reactive carbonyl species
ROS	Reactive oxygen species
SFA	Saturated fatty acid
Tf	Trifluoromethylsulfonyl
THF	Tetrahydrofuran
TIC	Total ion count
TIPS	Triisopropylsilyl
TLC	Thin-layer chromatography
UMR	Joint research unit
UPLC	ultra-performance liquid chromatography
UV	Ultra violet
VEGF	vascular endothelilal growth factor

LITERATURE

1. Crauste, C., et al., *Synthesis and Evaluation of Polyunsaturated Fatty Acid- Phenol Conjugates as Anti-Carbonyl-Stress Lipophenols.* Eur J Org Chem, 2014. **2014**(21): p. 4548-4561
2. European Pharmacopoeia, *European pharmacopoeia*. 2007, Strasbourg: Council Of Europe.
3. Estruch, R., et al., *Effects of a Mediterranean-style diet on cardiovascular risk factors: a randomized trial.* Ann Intern Med, 2006. **145**(1): p. 1-11.
4. Guasch-Ferre, M., et al., *Olive oil intake and risk of cardiovascular disease and mortality in the PREDIMED Study.* BMC Med, 2014. **12**(78): p. 1-11
5. Oliveras-Lopez, M.J., et al., *Extra virgin olive oil (EVOO) consumption and antioxidant status in healthy institutionalized elderly humans.* Arch Gerontol Geriatr, 2013. **57**(2): p. 234-42.
6. Lee, T.C., et al., *The impact of polyunsaturated fatty acid-based dietary supplements on disease biomarkers in a metabolic syndrome/diabetes population.* Lipids Health Dis, 2014. **13**(196)
7. Gomes, P.M., et al., *Supplementation of alpha-linolenic acid improves serum adiponectin levels and insulin sensitivity in patients with type 2 diabetes.* Nutrition, 2015. **31**(6): p. 853-7.
8. de Bock, M., et al., *Olive (Olea europaea L.) leaf polyphenols improve insulin sensitivity in middle-aged overweight men: a randomized, placebo-controlled, crossover trial.* PLoS One, 2013. **8**(3): p. e57622.
9. Hernaez, A., et al., *Olive Oil Polyphenols Decrease LDL Concentrations and LDL Atherogenicity in Men in a Randomized Controlled Trial.* J Nutr, 2015. **145**(8): p. 1692-7.
10. Gharby, S., et al., *Chemical characterization and oxidative stability of two monovarietal virgin olive oils (Moroccan Picholine and Arbequina) grown in Morocco.* JMES, 2013. **4**(6): p. 935-942.
11. Haddada, F.M., et al., *Fatty Acid, Triacylglycerol, and Phytosterol Composition in Six Tunisian Olive Varieties.* J Agr Food Chem, 2007. **55**(26): p. 10941–10946
12. Temime, S.B., et al., *Changes in olive oil quality of Chétoui variety according to origin of plantation.* J Food Lipids, 2006. **13**(1): p. 88-99.

13. Dabbou, S., et al., *Characterisation of virgin olive oils from European olive cultivars introduced in Tunisia.* Eur J Lipid Sci Tech, 2009. **111**(4): p. 392–401
14. Haslam, E. and Y. Cai, *Plant polyphenols (vegetable tannins): gallic acid metabolism.* Nat Prod Rep, 1994. **11**(1): p. 41-66.
15. Tripoli, E., et al., *The phenolic compounds of olive oil: structure, biological activity and beneficial effects on human health.* Nutr Res Rev, 2005. **18**(1): p. 98- 112.
16. Esti, M., L. Cinquanta, and E. La Notte, *Phenolic Compounds in Different Olive Varieties.* J Agric Food Chem, 1998. **46**(1): p. 32-35.
17. Krichene, D., et al., *Phenolic compounds, tocopherols and other minor components in virgin olive oils of some tunisian varieties.* J Food Biochem, 2007. **31**(2): p. 179-194.
18. Dabbou, S., et al., *Cultivar and growing area effects on minor compounds of olive oil from autochthonous and European introduced cultivars in Tunisia.* J Sci Food Agr, 2009. **89**(8): p. 1314-1325
19. Dabbou, S., et al., *Comparison of the chemical composition and the organoleptic profile of virgin olive oil from two wild and two cultivated Tunisian Olea europaea.* Chem Biodivers, 2011. **8**(1): p. 189-202.
20. Bonanome, A., et al., *Effect of dietary monounsaturated and polyunsaturated fatty acids on the susceptibility of plasma low density lipoproteins to oxidative modification.* Arterioscler Thromb, 1992. **12**(4): p. 529-33.
21. Moreno, J.J. and M.T. Mitjavila, *The degree of unsaturation of dietary fatty acids and the development of atherosclerosis (review).* J Nutr Biochem, 2003. **14**(4): p. 182-195.
22. Visioli, F., et al., *Low density lipoprotein oxidation is inhibited in vitro by olive oil constituents.* Atherosclerosis, 1995. **117**(1): p. 25-32.
23. Masella, R., et al., *Antioxidant activity of 3,4-DHPEA-EA and protocatechuic acid: a comparative assessment with other olive oil biophenols.* Redox Rep, 1999. **4**(3): p. 113-21.
24. Petroni, A., et al., *Inhibition of platelet aggregation and eicosanoid production by phenolic components of olive oil.* Thromb Res, 1995. **78**(2): p. 151-60.

25. Calabriso, N., et al., *Extra virgin olive oil rich in polyphenols modulates VEGF-induced angiogenic responses by preventing NADPH oxidase activity and expression.* J Nutr Biochem, 2016. **28**: p. 19-29.
26. Brooks, P.R. and M.C. Wirtz, *Boron trichloride/tetra-n-butylammonium iodide: A mild, selective combination reagent for the.* J Org Chem, 1999. **64**(26): p. 9719-9721.
27. Pany, S., A. Majhi, and J. Das, *PKC activation by resveratrol derivatives with unsaturated aliphatic chain.* PLoS One, 2012. **7**(12): p. e52888.
28. Buschini, E., et al., *Recent developments in the management of dry age-related macular degeneration.* Clin Ophthalmol, 2015. **9**: p. 563-74.
29. Khandhadia, S. and A. Lotery, *Oxidation and age-related macular degeneration: insights from molecular biology.* ERMM, 2010. **12**: p. e34.
30. Sparrow, J.R., K. Nakanishi, and C.A. Parish, *The lipofuscin fluorophore A2E mediates blue light-induced damage to retinal pigmented epithelial cells.* Invest Ophth Vis Sci, 2000. **41**(7): p. 1981-1989.
31. Cideciyan, A.V., et al., *Mutations in ABCA4 result in accumulation of lipofuscin before slowing of the retinoid cycle: a reappraisal of the human disease sequence.* Hum Mol Genet, 2004. **13**(5): p. 525-534.
32. Zhu, Q., et al., *Natural polyphenols as direct trapping agents of lipid peroxidation-derived acrolein and 4-hydroxy-trans-2-nonenal.* Chem Res Toxicol, 2009. **22**(10): p. 1721-7.
33. Kim, M.M. and S.K. Kim, *Effect of phloroglucinol on oxidative stress and inflammation.* Food Chem Toxicol, 2010. **48**(10): p. 2925-33.
34. Bazinet, R.P. and S. Layé, *Polyunsaturated fatty acids and their metabolites in brain function and disease.* Nat Rev Neurosci, 2014. **15**(12): p. 771-785.
35. Guesnet, P. and J.-M. Alessandri, *Docosahexaenoic acid (DHA) and the developing central nervous system (CNS) – Implications for dietary recommendations.* Biochimie, 2011. **93**(1): p. 7-12.
36. Suh, M., et al., *Relationship between dietary supply of long-chain fatty acids and membrane composition of long- and very long chain essential fatty acids in developing rat photoreceptors.* Lipids (USA), 1996(1): p. 61-64.

37. MacDonald, I.M., et al., *Effect of docosahexaenoic acid supplementation on retinal function in a patient with autosomal dominant Stargardt-like retinal dystrophy.* Br J Ophthalmol, 2004. **88**(2): p. 305-306.
38. Halliwell, B., *Free radicals, antioxidants, and human disease: curiosity, cause, or consequence?* The Lancet. **344**(8924): p. 721-724.
39. Gutteridge, J.M., *Lipid peroxidation and antioxidants as biomarkers of tissue damage.* Clin Chem, 1995. **41**(12 Pt 2): p. 1819-28.
40. Betteridge, D.J., *What is oxidative stress?* Metabolism, 2000. **49**(2 Suppl 1): p. 3-8.
41. Nimse, S.B. and D. Pal, *Free radicals, natural antioxidants, and their reaction mechanisms.* RSC Advances, 2015. **5**(35): p. 27986-28006.
42. Thornalley, P.J., A. Langborg, and H.S. Minhas, *Formation of glyoxal, methylglyoxal and 3-deoxyglucosone in the glycation of proteins by glucose.* Biochem J, 1999. **344**(1): p. 109-116.
43. Tatone, C., et al., *Evidence that carbonyl stress by methylglyoxal exposure induces DNA damage and spindle aberrations, affects mitochondrial integrity in mammalian oocytes and contributes to oocyte ageing.* Hum Reprod (Oxford, England), 2011. **26**(7): p. 1843-1859.
44. Sparrow, J.R., et al., *The bisretinoids of retinal pigment epithelium.* Prog Retin Eye Res, 2012. **31**(2): p. 121-35.
45. Mata, N.L., J. Weng, and G.H. Travis, *Biosynthesis of a major lipofuscin fluorophore in mice and humans with ABCR-mediated retinal and macular degeneration.* Proc Natl Acad Sci U S A, 2000. **97**(13): p. 7154-9.
46. Westerfeld, C. and S. Mukai, *Stargardt's disease and the ABCR gene.* Semin Ophthalmol, 2008. **23**(1): p. 59-65.
47. Chen, Y., et al., *Mechanism of all-trans-retinal toxicity with implications for stargardt disease and age-related macular degeneration.* J Biol Chem, 2012. **287**(7): p. 5059-5069.
48. *Lutein + zeaxanthin and omega-3 fatty acids for age-related macular degeneration: the Age-Related Eye Disease Study 2 (AREDS2) randomized clinical trial.* JAMA, 2013. **309**(19): p. 2005-2015.

49. Chew, E.Y., et al., *Secondary analyses of the effects of lutein/zeaxanthin on age-related macular degeneration progression: AREDS2 report No. 3.* JAMA Ophthalmol, 2014. **132**(2): p. 142-149.
50. Merle, B., et al., *Dietary omega-3 fatty acids and the risk for age-related maculopathy: the Alienor Study.* Invest Ophthalmol Vis Sci, 2011. **52**(8): p. 6004-6011.
51. Georgiou, T., et al., *Pilot study for treating dry age-related macular degeneration (AMD) with high-dose omega-3 fatty acids.* PharmaNutrition, 2014. **2**(1): p. 8-11.
52. Velilla, S., et al., *Smoking and age-related macular degeneration: review and update.* J Ophthalmol, 2013. **2013**: p. 1-11
53. Cheung, L.K. and A. Eaton, *Age-related macular degeneration.* Pharmacotherapy, 2013. **33**(8): p. 838-855.
54. Catchpole, I., et al., *Systemic administration of Abeta mAb reduces retinal deposition of Abeta and activated complement C3 in age-related macular degeneration mouse model.* PLoS One, 2013. **8**(6): p. e65518.
55. Butovsky, O., et al., *Identification of a unique TGF-beta-dependent molecular and functional signature in microglia.* Nat Neurosci, 2014. **17**(1): p. 131-143.
56. Ramawat, K.G. and J.M. Merillon, *Phenolic compounds: Introduction*, in *Natural products*. 2013, Springer-Verlag Berlin Heidelberg. p. 1544-1580.
57. Pandey, K.B. and S.I. Rizvi, *Plant polyphenols as dietary antioxidants in human health and disease.* Oxid Med Cell Longev, 2009. **2**(5): p. 270-278.
58. Olthof, M.R., P.C. Hollman, and M.B. Katan, *Chlorogenic acid and caffeic acid are absorbed in humans.* J Nutr, 2001. **131**(1): p. 66-71.
59. Vercauteren, J., *Plan, schémas, formules et illustrations de cours de pharmacognosie*. 2016.
60. Hollman, P.C., et al., *Relative bioavailability of the antioxidant flavonoid quercetin from various foods in man.* FEBS Letters, 1997. **418**(1-2): p. 152-156.
61. Ader, P., et al., *Cinnamate uptake by rat small intestine: transport kinetics and transepithelial transfer.* Exp Physiol, 1996. **81**(6): p. 943-955.
62. Kurlbaum, M. and P. Hogger, *Plasma protein binding of polyphenols from maritime pine bark extract (USP).* J Pharm Biomed Anal, 2011. **54**(1): p. 127-32.

63. Manach, C., et al., *Polyphenols: food sources and bioavailability.* Am J Clin Nutr, 2004. **79**(5): p. 727-47.
64. Verstraeten, S.V., et al., *Flavan-3-ols and procyanidins protect liposomes against lipid oxidation and disruption of the bilayer structure.* Free Radical Bio Med, 2003. **34**(1): p. 84-92.
65. Vitrac, X., et al., *Distribution of [14C]-trans-resveratrol, a cancer chemopreventive polyphenol, in mouse tissues after oral administration.* Life Sci, 2003. **72**: p. 2219-2233.
66. Donovan, J.L., et al., *Catechin is metabolized by both the small intestine and liver of rats.* J Nutr, 2001. **131**(6): p. 1753-1757.
67. Walle, U.K., A. Galijatovic, and T. Walle, *Molecular and Cellular Pharmacology: Transport of the flavonoid chrysin and its conjugated metabolites by the human intestinal cell line Caco-2.* Biochem Pharmacol, 1999. **58**: p. 431-438.
68. Rice-Evans, C.A., et al., *The relative antioxidant activities of plant-derived polyphenolic flavonoids.* Free Radic Res, 1995. **22**(4): p. 375-83.
69. Rice-Evans, C.A., N.J. Miller, and G. Paganga, *Structure-antioxidant activity relationships of flavonoids and phenolic acids.* Free Radical Bio Med, 1996. **20**(7): p. 933-956.
70. Letenneur, L., et al., *Flavonoid intake and cognitive decline over a 10-year period.* Am J Epidemiol, 2007. **165**(12): p. 1364-1371.
71. Payne, A.J., et al., *Antioxidant Drug Therapy Approaches for Neuroprotection in Chronic Diseases of the Retina.* Int J of Mol Sci, 2014. **15**(2): p. 1865-1886.
72. Sykiotis, G.P. and D. Bohmann, *Stress-activated cap'n'collar transcription factors in aging and human disease.* Sci Signal, 2010. **3**(112).
73. Forman, H.J., K.J. Davies, and F. Ursini, *How do nutritional antioxidants really work: nucleophilic tone and para-hormesis versus free radical scavenging in vivo.* Free Radical Bio Med, 2014. **66**: p. 24-35.
74. Lo, C.-Y., et al., *Trapping reactions of reactive carbonyl species with tea polyphenols in simulated physiological conditions.* Mol Nutr Food Res, 2006. **50**(12): p. 1118-1128.
75. Chih-Yu, L., H. Wen-Tuan, and C. Xiu-Yu, *Efficiency of Trapping Methylglyoxal by Phenols and Phenolic Acids.* J Food Sci, 2011. **76**(3): p. H90-H96.

76. Bin, D.U., et al., *Antioxidant Activity of Resveratrol from Wine Grape Pomace.* Nat Prod Res, 2008. **20**(5): p. 899-902.
77. Gülçin, İ., *Antioxidant properties of resveratrol: A structure–activity insight.* Innov Food Sci Emerg, 2010. **11**: p. 210-218.
78. Vlachogianni, I.C., et al., *In vitro assessment of antioxidant activity of tyrosol, resveratrol and their acetylated derivatives.* Food Chem, 2015. **177**: p. 165-173.
79. Nicolosi, G., C. Spatafora, and C. Tringali, *Chemo-enzymatic preparation of resveratrol derivatives.* J Mol Catal. B, Enzymatic, 2002. **16**: p. 223-229.
80. Toshiyuki, S., et al., *Local and chemical distribution of phlorotannins in brown algae.* J Appl Phycol, 2004. **16**(4): p. 291-296.
81. Roscoe, H.E., *A Treatise on Chemistry*. 1891: Macmillan & Company.
82. Lohrie, M. and W. Knoche, *Dissociation and keto-enol tautomerism of phloroglucinol and its anions in aqueous solution.* J Am Chem Soc, 1993. **115**(3): p. 919-924
83. Dyker, G., et al., *Gold(III) Chloride-Catalyzed Addition Reactions of Electron- Rich Arenes to Methyl Vinyl Ketone.* Adv Synth Catal, 2003. **345**(11): p. 1247-1252
84. Shi, Z. and C. He, *Efficient Functionalization of Aromatic C−H Bonds Catalyzed by Gold(III) under Mild and Solvent-Free Conditions.* J Org Chem, 2004. **69**(11): p. 3669-3671.
85. Das, J., S. Pany, and A. Majhi, *Chemical modifications of resveratrol for improved protein kinase C alpha activity.* Bioorgan Med Chem, 2011. **19**: p. 5321-5333.
86. Chiba, K., T. Arakawa, and M. Tada, *Electrochemical synthesis of euglobal-G1, -G2, -G3, -G4, -T1 and -IIc.* J Chem Soc, 1998(17): p. 2939-2942
87. Gia, O., et al., *4'-Methyl derivatives of 5-MOP and 5-MOA: synthesis, photoreactivity, and photobiological activity.* J Med Chem, 1996. **39**(22): p. 4489-4496.
88. Zheng, C., et al., *Ortho-dearomatization of phenols creating all-carbon spiro-bicycles.* Org Lett, 2013. **15**(16): p. 4046-4049.